Molecular basis for the therapeutic uses of botulinum toxin for chronic pain

Thesis submitted for the degree

of

Doctor of Philosophy

by

Jianghui Meng, B.Sc., M.Sc.

Supervised by

Prof. Oliver Dolly

International Centre for Neurotherapeutics

Dublin City University

Ireland

July 2008

Declaration

I hereby certify that this material, which I now submit for assessment on the programme of study leading to the award of Doctor of Philosophy, is entirely my own work and has not been taken from the work of others save and to the extent that such work has been cited and acknowledged within the text of my work.

Signed: ID No: 53155955

Jianghui Meng Date:

Dedications

I would like to express my deep and sincere gratitude to my supervisor, Professor J. Oliver Dolly, Head of the International Centre for Neurotherapeutics and who is funded by a research professorship from SFI, for recruiting and guiding me to conduct this research. His wide knowledge and insightful comments have been of great value for me. I am very grateful to his detailed review, constructive criticism and excellent advice during preparation of the papers and this thesis. I deeply appreciate the days and nights he spent with me in writing and discussion papers.

Also I thank Allergan Inc. for providing a research contract for this research programme.

I want to especially thank Dr Gary Lawrence and Dr Macdara Bodeker who helped with the thesis revision and made valuable comments. Also, I am greatful to my collagues for useful discussion, inspiration, friendship or practical help.

Finally, I dedicate this thesis to my dear mom, dad, brother-Jiangwei and my son-Owen, who I always owe debt for unforgettable busy time and, especially, my husband-Jiafu, who shares with me the bad and the good times with his unstinting help, support and forbearance. Without their inexhaustible supply of encouragement, understanding and assistance it would have been impossible for me to finish this work.

Publications and presentations

Papers

1. Jianghui Meng, Jiafu Wang, Gary W. Lawrence, J. Oliver Dolly. Synaptobrevin I mediates exocytosis of CGRP from sensory neurons and inhibition by botulinum toxins reflects their anti-nociceptive potential. *J. Cell Sci.* 2007 120, 2864-74.

3. Jiafu Wang, Jianghui Meng, Gary W. Lawrence, Tom H.Zurawski, Astrid Sasse, Macdara O. Bodeker, Marcella A. Gilmore, Ester Fernández-Salas, Joseph Francis, Lance E. Steward, K. Roger Aoki, J. Oliver Dolly. Novel chimeras of botulinum neurotoxin A and E unveil contributions from the binding, translocation and protease domains to their functional characteristics. *J. Biol. Chem.* 2008 283, 16993-17002.

2. Cheong SC, Wang Y, Meng JH, Hill R, Sweeney K, Kirn D, Lemoine NR, Halldén G. E1A-expressing adenoviral E3B mutants act synergistically with chemotherapeutics in immunocompetent tumor models. *Cancer Gene Ther* 2008; 15(1):40-50.

4. Jianghui Meng, Jiafu Wang, Mark Pickering, Astrid Sasse, Keith Murphy, K. Roger Aoki, Gary W. Lawrence and J. Oliver Dolly. Capsaicin-evoked CGRP release from nociceptive neurons is resistant to botulinum neurotoxin A due to sustained increased $[Ca^{2+}]_i$ but can be inhibited by a re-targeted A/E chimera. (Manuscript is being prepared).

Book chapter

J. Oliver Dolly, MD, Jianghui Meng, Jiafu Wang, Gary W. Lawrence, Macdara O. Bodeker, Tom H. Zurawski, Astrid Sasse. 'Multiple steps in the blockage of exocytosis by botulinum neurotoxins' Botulinum Toxin: Therapeutic Clinical Practice and Science. Elsevier (2007), Ch 1, (in press)

Abstracts

J. Oliver Dolly, MD, Jianghui Meng, Jiafu Wang, Tom H. Zurawski, Astrid Sasse, Lance E. Steward, Ester Fernández-Salas, Joseph Francis, Marcella A. Gilmore, K. Roger Aoki, and Gary W. Lawrence. Multiple steps in the blockade of exocytosis by

botulinum neurotoxins. International Conference on Neurotoxins, Nov 29, 2006-Dec 2, 2006.

Presentation

Jianghui Meng, Jiafu Wang, Gary W. Lawrence and J. Oliver Dolly. CGRP release from sensory neurons occurs by SNARE-dependent exocytosis and is unique in requiring synaptobrevin I: inhibition by botulinum neurotoxins reflects their anti-nociceptive potential. Irish Neuroscience Group Meeting, Nov 24-25, 2006.

Abbreviations

AChE, acetylcholinesterase

Ara-C, cytosine-β-D-arabinofuranoside

BCA kit, bicinchoninic acid protein assay kit

BoNT/A, B, C1, D, E, F and G, botulinum neurotoxin serotype

BOTOX, botulinum toxin A-haemagglutinin complex

BR2, bradykinin type 2 receptor

BR-HBS, basal release HEPES buffered saline

$[Ca^{2+}]_i$, intracellular calcium concentration

CGNs, cerebellar granule neurons

CGRP, calcitonin gene-related peptide

Chimera AB, chimeric toxin containing LC and translocation domains of BoNT/A and binding domain of BoNT/B

Chimera BA, chimeric toxin containing LC and translocation domains of BoNT/B and binding domain of BoNT/A

Chimera EA, chimeric toxin containing LC and translocation domains of BoNT/E and binding domain of BoNT/A

CLR, calcitonin receptor-like receptor

CMF-HBSS, Ca^{2+}- Mg^{2+}- free Hanks' balanced salt solution

DAPI, 4', 6'-diamidino-2-phenylindole

DC, di-chain

DIV, days *in vitro*

DRGs, dorsal root ganglion neurons

DTT, dithiothreitol

ECL, enhanced chemiluminescence

EDTA, ethylenediaminetetraacetic acid

EIA, enzyme immuno-assay

Fab, antigen-binding fragment

Fc, constant fragment

GPCR, G-protein coupled receptor

Gαs, G-protein α subunit

HC, heavy chain

$H_{C,}$ binding domain

H_N, translocation domain

IB_4, isolectin B_4

kDa, kilodalton

LC, light chain

LCH_N, light chain and translocation domains

LDCVs, large dense-core vesicles

LDS, lithium dodecyl sulfate

Mabs, monoclonal antibodies

Mr, relative molecular mass

NF-200, neurofilament 200 kDa

NGF, nerve growth factor

NO, nitric oxide

NPY, neuropeptide Y

O.D, optical density

P5, postnatal day 5

PGE2, prostaglandin E2

PMSF, Phenylmethylsulfonyl Fluoride

PVDF, Polyvinylidene Fluoride

RAMP, receptor activity-modifying protein

SA-HRP, streptavidin-horseradish peroxidase

Sbr, synaptobrevin, also known VAMP

SC, single chain

SCSVs, small clear synaptic vesicles

SDS-PAGE, sodium dodecyl sulfate polyacrylamide gel electrophoresis

ShRNA, short hairpin RNA

SNAP-25, synaptosomal-associated protein with *Mr* = 25 k

SNARE, soluble NSF (N-ethylmaleimide sensitive factor) attachment protein receptor

SP, substance P

SV2, synaptic vesicle protein 2

SV2-L4, the forth loop of synaptic vesicle protein 2

TFA, trifloroacetic acid

TGNs, trigeminal ganglion neurons

TMB, 3,3',5,5'-tetramethylbenzidine

TO mice, Tyler’s Ordinary mice

TU, transduction units

VAMP, vesicle-associated membrane protein

VIP, vasoactive intestinal peptide

VR1, vanilloid receptor type 1

Table of Contents

List of Figures

Chapter 1

Chapter 2

Chapter 3

Chapter 4

Chapter 5

List of Tables

Chapter 1

Chapter 2

Chapter 3

Abstract

Calcitonin gene-related peptide (CGRP), a potent vasodilator that mediates inflammatory pain, was found to co-occur in rat trigeminal ganglia neurons (TGNs) with 3 exocytotic soluble NSF (N-ethylmaleimide sensitive factor) attachment protein receptors (SNAREs) [synaptosomal-associated protein with *Mr* = 25 k (SNAP-25), syntaxin I, synaptobrevin (Sbr) isoforms] and synaptotagmin. Ca^{2+}-dependent CGRP release evoked with K^+-depolarisation was higher than that evoked by capsaicin or bradykinin from neurons containing the vanilloid receptor 1 and/or bradykinin receptor 2. Botulinum neurotoxin (BoNT) type A cleaved SNAP-25 and inhibited release triggered by K^+ > bradykinin >> capsaicin. Unlike BoNT/D, /B did not affect exocytosis although rat TGNs possess its receptor, synaptotagmin I/II, and Sbr II/III got proteolysed (I is resistant in rat) but, in mouse, /B additionally cleaved Sbr I and blocked release. Knock-down of Sbr I expression substantially reduced CGRP exocytosis. These novel findings implicate Sbr I in CGRP exocytosis together with SNAP-25. An in-depth study was performed on the feeble inhibition by /A of capsaicin-elicited CGRP release, as it stimulates C-fibres — a prime target for attenuating nociception; their inactivation was sought using the superior membrane-translocating properties of BoNT/E which cleaves 26 residues from SNAP-25 rather than the 9 by /A. Chimera EA was engineered to exploit the light chain and translocation domain from /E, together with the acceptor binding from /A to overcome the inability of /E to interact with TGNs. Purified /EA bound synaptic vesicle protein 2 type C *in vitro* and entered the neurons because capsaicin-evoked exocytosis of CGRP was inhibited. Unlike /A, the longer truncation of SNAP-25 by /EA diminished its participation in stable SNARE complexes, unlike $SNAP\text{-}25_A$. Prolonged elevation of $[Ca^{2+}]_i$ by capsaicin, as revealed by $^{45}Ca^{2+}$ uptake and Fluo 4-AM imaging, gives a persistent trigger for CGRP release from /A-treated cells. The successful targeted delivery of EA into nociceptive neurons and the consequential blockade of CGRP release, even when evoked by sustained elevation of $[Ca^{2+}]_i$, highlight the versatility of this novel chimera.

1.0 General introduction

1.1 Botulinum neurotoxins

1.1.1 Origin

Clostridum botulinum is a gram-postive, anaerobic, spore-forming and rod-shaped bacterium which produces botulinum neurotoxin (BoNT). These are the most potent toxins known, causing flaccid neuromuscular paralysis. In 1817, the German physician Justinus Kerner described a paralytic condition caused by eating sausages, and such food-borne paralysis was named "botulism" (Latin for a 'sausage-related condition'). The bacteria are commonly found in soil, and were first recognized and isolated in 1895-1896 by Emile van Ermengem from home cured ham that had been implicated in a botulism outbreak (Ermengem, 1897). In 1944, Edward Schantz successfully cultured *Clostridium botulinum* and isolated botulinum toxin (Schantz, 1994), and, in 1949, Burgen's group discovered that the toxin blocks neuromuscular transmission (Burgen, 1949). Since then, seven serologically distinct but structurally similar BoNTs serotypes have been idenfied (Dolly and Lawrence, 2007; Montecucco and Schiavo, 1994; Pellizzari et al., 1999; Popoff et al., 2001) and named A-G, according to the order of their discovery. Serotypes A, B, E and F are responsible for the majority of human botulism; BoNT/C and /D are causative agents for animal and avian botulism (Tsukamoto et al., 2005) and were discovered in birds and in cattle, respectively (Coffield et al., 1997; Davletov et al., 2005). Serotype G was isolated from soil. BoNTs usually occur in complexes with non-toxic proteins named haemagglutinins plus non-toxic non-haemagglutinin (NTNH). These associated non-toxic proteins stablize the toxin at low pH and dissociate at neutral pH, protecting toxin moiety from proteolytic attack during exposure to the gastrointestinal environment [reviewed by (Humeau et al., 2000)]. When BoNT-contaminated food reaches the small intestine, the toxin crosses the interstinal wall and enters the bloodstream (Simpson, 2004). Type A toxin has been the most widely studied and successfully used for therapeutic purposes to date. Type B is commercially available but higher doses are required (Davletov et al., 2005; Foran et al., 2003; Jankovic, 2004).

1.1.2 Mechanism of action

These neurotoxins potently and preferentially inhibit the release of acetycholine from peripheral motor nerves causing flaccid neuromuscular paralysis typical of botulism (Dolly and Lawrence, 2007; Montecucco and Schiavo, 1994; Pellizzari et al., 1999;

Popoff et al., 2001). Intracellular administration of BoNTs blocks Ca^{+}-regulated exocytosis of all transmitters, both from small clear synaptic vesicles (SCSVs) and large dense-core vesicles (LDCVs) (Bergquist et al., 2002; Foran et al., 1995; Foran et al., 2003; Keller and Neale, 2001; McInnes and Dolly, 1990). Each BoNT is synthesized as a relatively inactive single-chain protein with a molecular weight of ~150 kDa and becomes activated upon proteolytic cleavage by bacterial endogeneous proteases or by trypsin *in vitro* to yield the binding/translocating heavy chain (HC) and enzymatic light chain (LC), linked through a disulphide bond and non-convalent interactions. The 3D crystal structures for BoNT/A and /B have been determined (Lacy et al., 1998; Swaminathan and Eswaramoorthy, 2000) (Fig. 1.1).

BoNTs have 3 individual domains (each with a molecular mass of ~50 kDa): (1) a catalytic LC domain (a zinc-dependent endopeptidase); (2) a translocation domain (H_N); (3) a binding domain (H_C) composed of two subdomains: C terminal binding domain (H_{CC}) and N terminal binding (H_{CN}) (Fig. 1.1), which binding to gangliosides and high-affinity protein acceptors (Chai et al., 2006; Jin et al., 2006). A multi-step mechanism of action for BoNT at the motor terminal was proposed (Black and Dolly, 1986; Dolly et al., 1984; Dolly et al., 1994; Humeau et al., 2000; Schiavo et al., 2000; Simpson, 1979). These steps include: binding to ecto-acceptors on cholinergic nerve terminals; acceptor-mediated internalization and membrane translocation of LC; after gaining access into the neuronal cytosol, the metalloprotease activities of the LCs selectively proteolyse and disable soluble NSF (N-ethylmaleimide sensitive factor) attachment protein receptor (SNAREs) which mediate vesicular transmitter release. So far, synaptic vesicle protein 2 (SV2) has been identified as a high affinity binding component for BoNT/A. SV2 is an integral membrane glycoprotein, occuring in three well-characterized isoforms, SV2A, SV2B, and SV2C. SV2A is more widely distributed in the nervous system, whereas SV2C is only observed in a small number of neurons in a few brain areas (Bajjalieh et al., 1994; Bajjalieh et al., 1993; Janz et al., 1998; Janz and Sudhof, 1999). Isoforms of another synaptic protein, synaptotagmin I/II were found to be the putative protein acceptors for /B and /G (see later) (Dong et al., 2003; Dong et al., 2006; Rummel et al., 2004). After binding, the toxins are internalized by acceptor-mediated endocytosis (Fig. 1.2 A). An intact di-chain (DC) is needed for translocation of LC to the cytosol where it cleaves one or two of three essential proteins involved in the Ca^{2+}-regulated exocytosis machinery (Fig. 1.2 B).

SNAP-25 (synaptosomal associated protein with *Mr* = 25k) that predominantly resides on the plasma membrane is cleaved by BoNT/A, /C1 and /E, all at distinct sites; syntaxin IA/IB is also cleaved by BoNT/C1. BoNT/B, /D, /F and /G act on synaptobrevin (Sbr) [also known as vesicle-associated membrane protein (VAMP)] isoforms I, II and III; Sbr I in rat is unusual in being resistant to type B cleavage due to a mutation at the fission site (Foran et al., 2003; Humeau et al., 2000; Yamasaki et al., 1994) (Table 1.1). In neuronal exocytosis, syntaxin and sbr are anchored in plasma and synaptic vesicle membranes, respectively, by their C-terminal domains, whereas SNAP-25 is tethered to the plasma membrane via several cysteine-linked palmitoyl chains. The core SNARE complex is a four-α-helix bundle, where one α-helix is contributed each by syntaxin-1 and sbr and two α-helices by SNAP-25 (Sutton et al., 1998). Synaptotagmin is a Ca^{2+} sensor and is involved in early synaptic vesicle docking to the presynaptic membrane via interaction with SNAP-25. Its N-terminal domain resides in the luman of synaptic vesicle and its C-terminal cytoplasmic region binds to Ca^{2+} (Fig. 1.3) (Littleton et al., 2001). Upon binding to Ca^{2+}, it then facilates the late steps of Ca^{2+}-evoked synaptic vesicle fusion with the presynaptic membrane [reviewed by (Humeau et al., 2000)]. Truncation of the exocytotic machinery SNARE proteins by BoNTs pertubs the formation of SNARE complex and inhibits exocytosis (see Chapter 5).

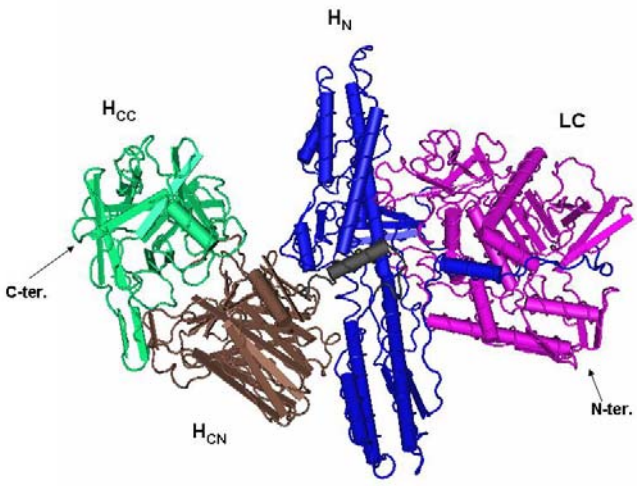

Fig. 1.1 Structure of BoNT/A. *Backbone trace of BoNT/A: LC in pink, the H_N in blue, N-terminal (H_{CN}, in brown) and C-terminal (H_{CC}, in green) binding domains are shown. The picture was generated using Cn3D4.1 software from published structure database (GenBank accession No: 3BTA) (Lacy et al., 1998).*

Table 1.1 BoNTs and the substrates they cleave

Serotype	Intracellular target protein	Cleavage sites in rat
/A	SNAP-25	EANQ^{197}RATK
/B	Sbr I, II*	GASQ^{76}FETS (rat Sbr I is resistant:GASVFESS)
/C1	SNAP-25 Syntaxin IA/ IB	ANQR^{198}ATKM DTKK^{254}AVKY/ DTKK^{253}AVKY
/D	Sbr I, II*	RDQK^{61}LSELD for I and II
/E	SNAP-25	QIDR^{180}IMEK
/F	Sbr I, II*	ERDQ^{60}KLSE for I ERDQ^{58}KLSE for II
/G	Sbr I, II*	ETSA^{83}AKLK for I ETSA^{81}AKLK for II

**Rat and mouse Sbr III is also cleaved by BoNT/B, D, F, G*

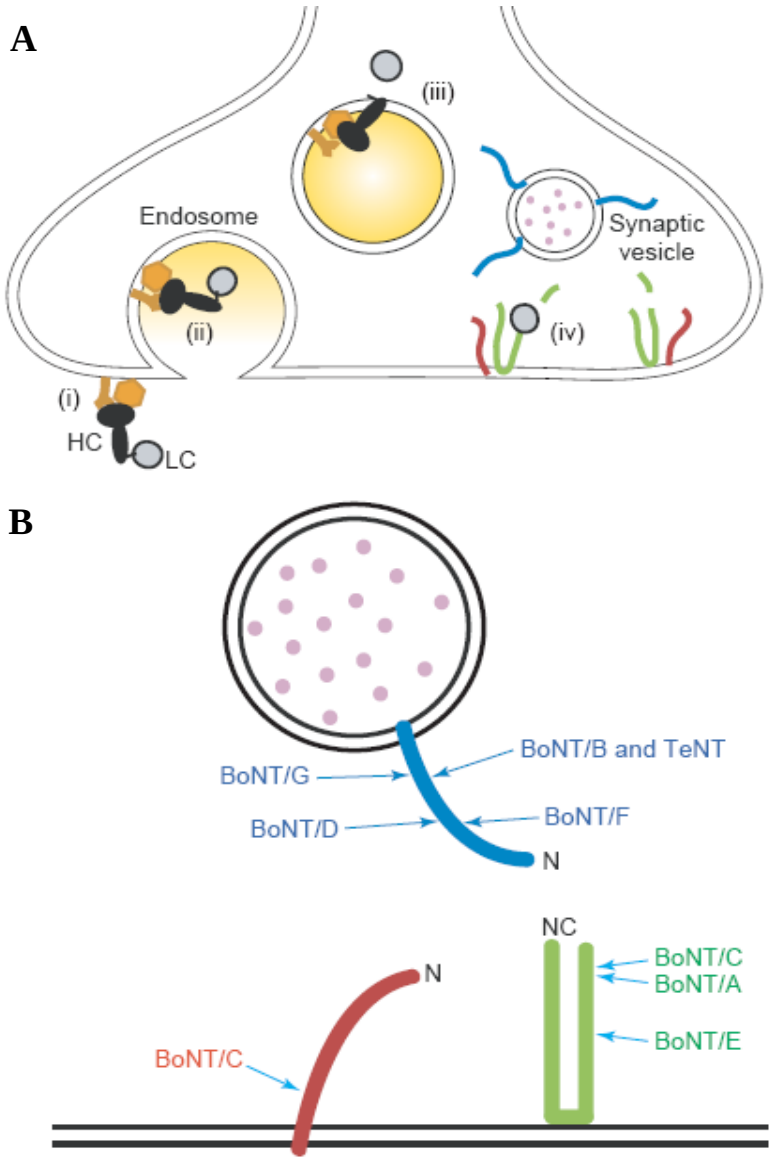

Fig. 1.2 Inhibitory action of BoNTs on transmitter release. *(A) Four steps are involved in the intoxication: (i) the toxin heavy chain (HC, black) mediates cell-surface binding with ganglioside and glycoprotein receptors (orange); (ii) acceptors-mediated internalization; (iii) translocation of light chain LC (gray) to the cytosol and (iv) cleavage of their repective SNARE substrates; sbr (blue), syntaxin 1 (red) and SNAP-25 (green) (B) The relative cleavage sites of each BoNT on its substrate are shown [pictures are reproduced from (Brungerb, 2005)].*

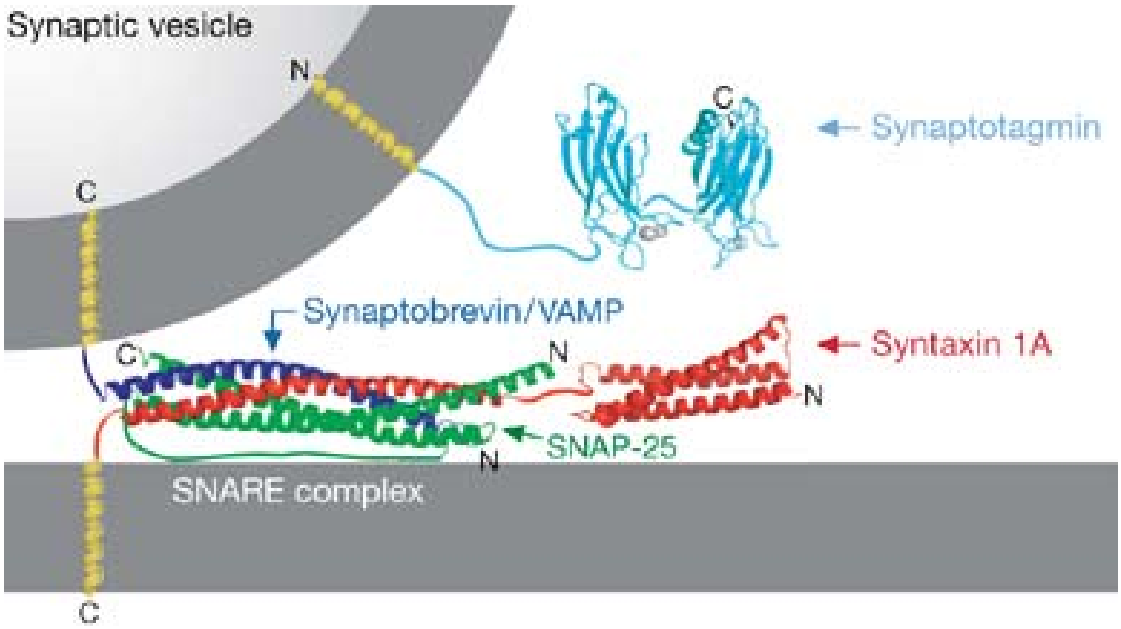

Fig. 1.3 SNARE complex and synaptotagmin driven exocytosis. *The core SNARE complex is formed by four α-helices constituted by each from sbr, syntaxin and two from SNAP-25; synaptotagmin is a* Ca^{2+} *sensor and regulates SNARE zipping and vesicle fusion. Synaptotagmin has an N-terminal transmembrane region and two C-terminal C2 domains - C2A and C2B which bind to* Ca^{2+}*. Picture is adapted from (Munson, 2007).*

1.2 Potential anti-nociceptive uses of BoNTs

1.2.1 Pain pathways and evidence for pain relief by BoNTs

The symptoms of botulism suggest that BoNTs act preferentially on peripheral cholinergic motor nerve endings, a notion supported by many experimental findings; thus, the most common clinical application of these toxins is for the treatment of overactive muscles (voluntary and involuntary) or glands innervated by such neurons (Ward and Barnes, 2007). However, some patients treated for cholinergic over-activity disorders noted a concomitant relief of pain symptoms that was difficult to reconcile with a purely cholinergic block (Binder et al., 2000). Pain of various kinds (nociceptive, neuropathic, inflammatory) pose major medical challenges, with 21% of the worldwide adult population suffering from persistent pain (WHO report 2004). The experience of pain is due to the combined activity of distinct systems that transmit and modulate pain. The pain pathway is bi-directional and consists of ascending and descending pathways. The ascending pathways transmit information from peripheral nociceptors to higher levels of the central nervous system (Bloedel and McCreery, 1975). Transmission of pain signals from the periphery to the cortex involves signal processing within the spinal cord, brain stem, and forebrain (Levy et al., 2004). The descending pathway travel along the asending route and transfer information from central structures to neurons, including the dorsal horn of the spinal cord and sensory nuclei of the brainstem (i.e. trigeminal nuclei). The descending pathway allows the brain to modulate pain sensation so that the brain can either amplify or inhibit incoming pain signals through desending modulatory pathways (Bloedel and McCreery, 1975; Hole and Berge, 1981). Recent clinical investigations have indicated that myofacial pain, migraine and certain types of headache seem to respond to local injection of botulinum toxin A-haemagglutinin complex (BoTOX) (Gupta, 2005). Additionally, the preparation can reduce capsaicin-induced pain [however this still remains controversial (see overview in Chapter 5)], and secondary hyperalgesia in a human experimental model of trigeminal sensitisation (Gazerani et al., 2006).

Release of substance P (SP), a neuropeptide involved in neurogenic inflammation, is inhibited by various BoNT serotypes in cultured neurons from embryonic rat dorsal root ganglia (DRGs) (Welch et al., 2000). Exocytosis of glutamate, another

neurotransmitter involved in nociception in the periphery and in the dorsal horn of the spinal cord, was also shown be suppressed in rat paw challenged with formalin (Cui et al., 2004). Some studies suggested that the mechanism of pain relief by BoNTs is due to peripheral desensitisation, which indirectly prevents central neuron sensitisation. Notablly, study examines the time course of muscle relaxation and pain relief in spastic and nonspastic muscle conditions, where the analgesic property has generally been attributed to muscular relaxation, the pain reduction by BoNT/A happens before muscle relaxation and even last longer than the muscle relaxation (Aoki, 2005; Freund and Schwartz, 2003).

1.2.2 Pathophysiology of migraine and evidence of involvement of neuropeptides

The pathogenesis of migraine headache involves three major constituents: the cranial blood vessels, the trigeminal innervation of these vessels, and the reflex connection of the trigeminovascular system in the cranial parasympathetic outflow; so far, there is no *in vivo* model systems that mimic all aspects of the migraine attack (Goadsby et al., 2002; Mehrotra et al., 2008). In support of particular roles for vasoactive neuropeptides such as calcitonin gene-related peptide (CGRP) and SP, antagonists for these peptides or their receptors were shown to reduce pain. CGRP antagonists, such as CGRP8-37, attenuated pain upon injection into the dorsal horn (Bird et al., 2006); another antagonist of the α type CGRP receptor (BIBN4096BS) reduces vasodilation (Salvatore et al., 2008). Infusion of CGRP produced a migraine-like headache (Olesen and Lipton, 2004) and baseline CGRP levels were increased in migraineurs (Fusayasu et al., 2007). Inhibition of CGRP release or antagonism of CGRP receptors could be a viable therapeutic target for the pharmacological treatment of migraine (Edvinsson, 2004; Mehrotra et al., 2008). However, the short-lived effect of these antagonists is disadvantagous for use in therapy; the half-life for the two aforementioned antagonists is only hundreds of minutes (Edvinsson, 2007; Salvatore et al., 2008). With BOTOX® being found to be effective in the treatment of chronic pain, especially chronic headaches, it offers several advantages of being safe, tolerable and effective in prevention of migraines resistant to other drugs (Blumenfeld, 2003; Farinelli et al., 2006; Menezes et al., 2007; Suzuki et al., 2007). One injection works for three months, rather than patients taking pills every day and frequently becoming intolerant or refractory.

To better understand release mechanisms of pain mediators and, thereby, exploit the advantages of using toxin therapy to attenuate pain symptoms (e.g. migraine), there is an urgent need for studies on the interaction between BoNTs and pain-sensing neurons.

1.3 Peripheral sensory neurons: pain mediators and trigger factors

A number of sensory nerve types are involved in propagating pain (Woolf, 2004; Woolf and Ma, 2007). Activation of the trigeminal nerve is involved in migraine and cluster headache which are very prevalent (~16% of adults).

1.3.1 Trigeminal ganglion neurons (TGNs)

Stimulation of the trigeminal nerve, the largest of the cranial nerves, triggers release of CGRP and SP from sensory neurons in trigeminal ganglia (TG), a migraine pain relay centre. Release of CGRP and SP induces vasodilation and mast cell degranulation; this further increases the levels of inflammatory agents which, in turn, enhance the synthesis and release of these peptides (Durham and Cady, 2004). Cell bodies of the trigeminal nerve reside in the trigeminal ganglion, which is located on the cerebral surface of the sphenoid bone in the middle cranial fossa. As its name suggests, it has three major branches: ophthalmic, maxillary and mandibular, and contains the cells of origin of most of the sensory fibers of the trigeminal nerve. The 3 branches provide most of nociceptive input from the cerebrovasculature and craniofacial region. Nociceptors are free nerve endings enriched with receptors sensitive to mechanical stress, extreme heat or cold, and noxious chemicals. Fig.1.4 shows the structure of trigeminal ganglion and surroundings. The central processes enter the brain at the level of the pons, conveying pain and temperature, descend into the brain stem and comprise the SPINAL TRACT V.

According to the size of neurons and type of transmitters released, sensory neurons are divided into several groups: fast-conducting, myelinated A-β fibres mediate the synaptic release of transmitters such as excitatory amino acids from small clear synaptic vesicles (SCSVs) which cause cortical spreading depression, neuronal hyper-excitability and central sensitization; on the other hand, the slow transfer of signals via the A-δ and unmyelinated C fibres elicit the secretion of CGRP, SP, neurokinin A (Silberstein and Aoki, 2003). Isolectin B_4 (IB_4), an alpha-D-galactose-binding lectin isolated from *Griffonia (Bandeiraea) simplicifolia*, has been used to label primary sensory afferent terminals of small-diameter TGNs *in vivo*. C-fibers can be divided into

two groups based on growth factor dependency and IB_4 binding. IB_4-negative nociceptors have been proposed to contribute to inflammatory pain, and IB_4-positive neurons are sensitized to VR1 ligands during inflammation and, thus, IB_4-positive C-fiber neurons may contribute to inflammatory hyperalgesia (Breese et al., 2005).

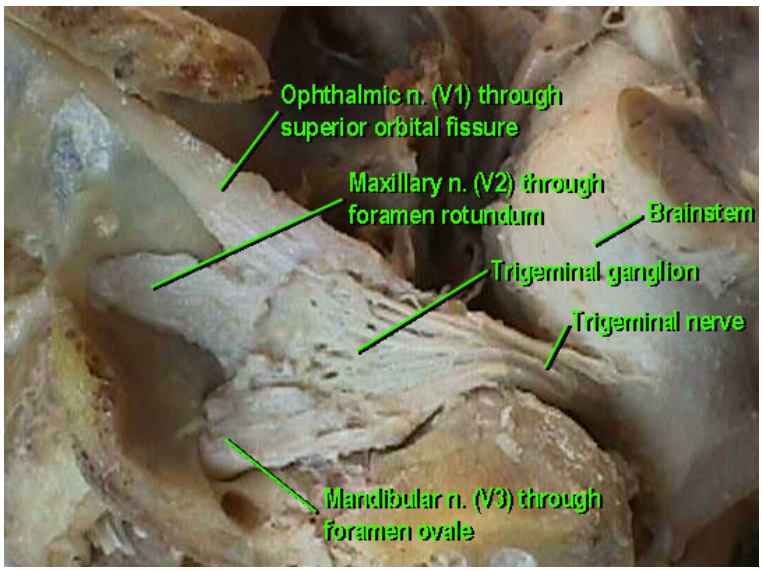

Fig. 1.4 Trigeminal ganglion dissection guidance

Picture reproduced from http://medinfo.ufl.edu/year1/trigem/anatomy.html

1.3.2 CGRP, SP and their receptors

CGRP is a 37-amino acid neuropeptide produced by tissue-specific alternative processing of the primary RNA transcripts of the calcitonin gene; it has two isoforms: α CGRP (or CGRP-I) and β CGRP (or CGRP-II). α and β differ by one amino acid in rats and three residues in humans (Poyner et al., 2002) (Table 1.2). α CGRP is present in sensory neurons whereas β CGRP mainly occurs in the enteric nervous system. The level of CGRP in the cerebrospinal fluid becomes elevated significantly during the painful phase of migraine (Goadsby and Edvinsson, 1993). Also, release of CGRP in the periphery is a reliable marker for neurogenic inflammation; the time course of CGRP plasma levels parallels headache intensity and successful treatment of such attacks abort both the associated pain and CGRP release (Goadsby and Edvinsson, 1993).

In the migraine pathophysiology, release of CGRP may be through several putative pathways of vascular hyper-reactivity: NO (nitric oxide) released from endothelial cells

not only has its own vascular effects but up-regulates CGRP gene expression in rat trigeminal ganglia (Fig. 1.5). While the primary dysfunction in brain causes CGRP-dependent vasodilation; cortical spreading depression (CSD) could be the initial trigger for CGRP release due to activation of the trigeminovascular system (Doods et al., 2007).

There are two types of CGRP receptors identified so far: CGRP1 and CGRP2; isofrom 1 shows preference for binding to the CGRP antagonist: CGRP8-37. CGRP receptors are hetero-dimers comprising GPCR (G-protein coupled receptor), CLR (calcitonin receptor-like receptor), an accessory protein, RAMP1 (receptor activity-modifying protein 1), and a receptor component protein (RCP) (Fig. 1.6); CGRP receptors are distributed on the postsynaptic and presynaptic membranes. CGRP initially released from trigeminal ganglion causes subsequent release of inflammatory cytokines from mast cells which, in turn, induce more CGRP release by activation of a positive feed back loop (Durham and Russo, 2003). Binding of CGRP to its receptor causes activation of multiple signalling pathways (Fig. 1.7).

SP is a 11-amino acid peptide (H-Arg-Pro-Lys-Pro-Gln-Gln-Phe-Phe-Gly-Leu-Met-NH_2), and is a member the tachykinin family that also includes neurokinin A (NK-A), neurokinin B (NK-B), neuropeptide K (NP-K), and neuropeptide-γ (NP-γ). SP is derived from tissue-specific alternative splicing of the pre-protachykinin I gene and is produced almost exclusively in neuronal tissues.

The SP receptor is a neurokinin A receptor which also belongs to the tachykinin receptor sub-family of GPCR; its activation leads to the mobilization of intracellular Ca^{2+} and elevation of cAMP levels (Mitsuhashi et al., 1992), and induces changes in the subsequent signalling as described for CGRP (Fig. 1.7).

CGRP and SP are released from peripheral nerve terminals in response to an inflammatory stimulus, such as local application of capsaicin or bradykinin (see 1.3.3). *In situ*, nearly 80% of SP-positive trigeminal (and other sensory) ganglion neurons contain CGRP, which indicates both peptides are largely co-expressed; However, CGRP is also found in some C-fibers nociceptors that lack SP. Both peptides serve as the major mediators of inflammatory pain, and notably, they are released from LDCVs at sites away from the active zones where most SCSVs exocytosis occurs (Kummer,

1992). This more diffuse type of secretion affords communication with neighbouring cells over wide areas. Accordingly, CGRP and SP cause dilation of intracranial blood vessels and transmit nociceptive signals from this vasculature to the central nervous system though CGRP was significantly more potent than SP as a cerebrovascular dilator (McCulloch et al., 1986).

Table 1.2 Peptide sequences of α and β isoforms of CGRP in rat and human

h α CGRP	A C D T A T C V T H R L A G L L S R S G G V V K N N F V P T N V G S K A F
h β CGRP	A C N T A T C V T H R L A G L L S R S G G M V K S N F V P T N V G S K A F
r α CGRP	S C N T A T C V T H R L A G L L S R S G G V V K D N F V P T N V G S E A F
r β CGRP	S C N T A T C V T H R L A G L L S R S G G V V K D N F V P T N V G S K A F

Non-conserved amino acids between the two isoforms of each species are underlied. h, human; r, rat.

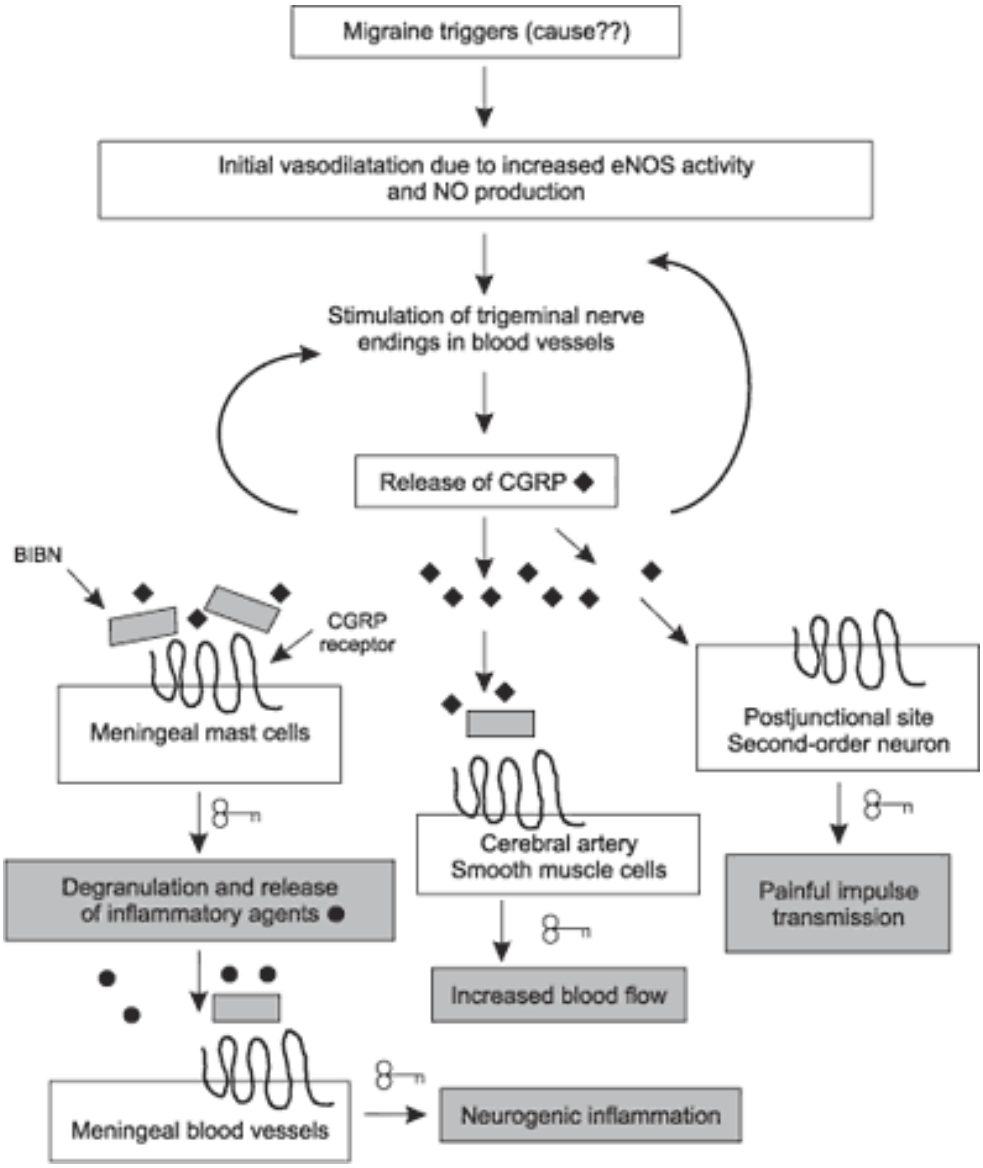

Fig. 1.5 CGRP and SP are potent vasodilators in nociception of migraine and other inflammatory based pain. *While triggers for migraine pathophysiology are currently unknown, endothelial NO (nitric oxide) is responsible for the initial vasodilation. NO production coincides with CGRP release from trigeminal ganglia implicating CGRP as a trigger of migraine through two possible mechanisms; one possibility is that released CGRP binds to mast cell via its receptor causing mast cell degranulation and subsequent release of other inflammatory agents. Alternatively, CGRP may bind the smooth muscle of cerebral artery causing its relaxation and increased blood flow. Additionally, CGRP binds the secondary hypothalamus neurons causing painful impulse transmission. Binding of CGRP to its receptor is blocked by an antagonist of the α type CGRP receptor* (BIBN) *Picture is reproduced from (Kapoor, 2004).*

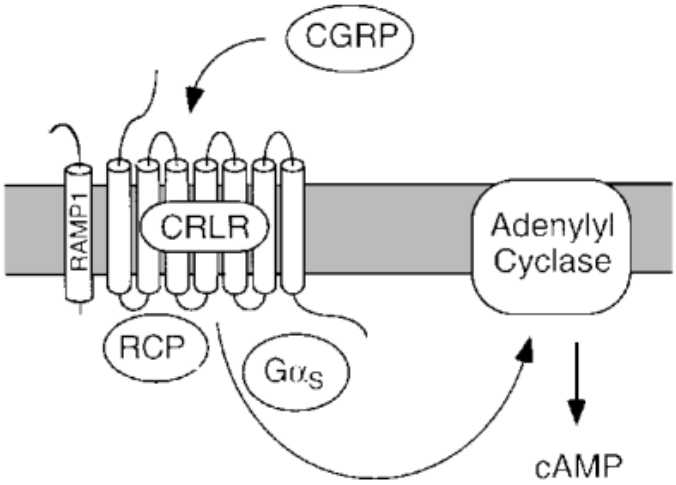

Fig. 1.6 The CGRP receptor. *This is a complex proposed to comprise a ligand-binding protein (CRLR) which is an accessory protein for trafficking and pharmacology, a receptor activity-modifying protein 1 (RAMP1), and receptor component protein (RCP) which is a member of a multi-protein complex required for GPCR signal transduction. CGRP receptor is a G-protein coupled receptor, its subunit ($G\alpha_S$, G-protein a subunit) activates the adenylyl cyclase and then converts ATP to cyclic-AMP (cAMP), followed by activation of multiple signalling pathways, as shown in Fig. 1.7. Picture is reproduced from (Prado et al., 2002).*

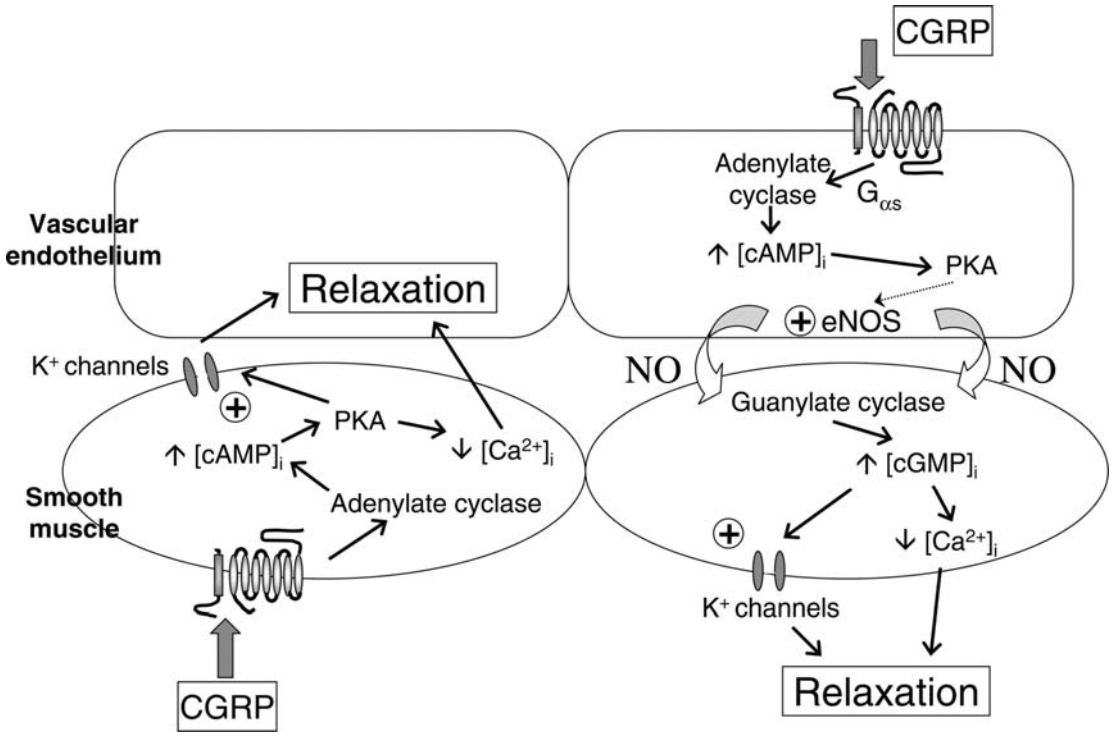

Fig. 1.7 Model for CGRP receptor function and its activation of signalling pathways. *Left panel shows endothelium-independent vasodilatation in response to CGRP. Activation of CGRP receptors on smooth muscle cells is coupled to production of cAMP by adenylate cyclase. cAMP then binds to the regulatory subunits of PKA leading to dissociation of the associated catalytic subunits and phosphorylation of numerous substrates, opening K^+ channels and activating Ca^{2+} sequestration mechanisms causing smooth muscle relaxation. Right panel shows endothelium-dependent vasodilation response to CGRP. It interacts with receptors on endothelial cells and stimulates production of NO. This is mediated via cAMP accumulation, although a direct effect of PKA on endothelial NO synthase (eNOS) is yet to be fully characterized. Diffusion of NO into adjacent smooth muscle cells, activates guanylate cyclase, leading to muscle relaxation. [Picture is adapted from (Brain and Grant, 2004)].*

.

1.3.3 Capsaicin and bradykinin

There are subpopulations of nociceptive neurons in TG that are selectively stimulated by capsaicin and/or bradykinin. Capsaicin (chemical structure of carbon backbone and functional groups are shown in Fig. 1.8 A) from chilli peppers is well known as a C-fibre specific activator that causes an inward currents and produces pain by acting on the vanilloid receptor type 1 (VR1, also known as TRPV1), a nonselective cation channel that prefers Ca^{2+} over Na^{+} and an integrator of inflammatory pain pathways, which is located mainly on the C-fibres (Caterina et al., 1997; Tominaga et al., 1998). VR1 positive neurons are recognised as nociceptive neurons because they are activated by three different stimuli — capsaicin, heat (>43°C) or protons (acidification) — that are known to cause pain *in vivo* (Caterina et al., 1997; Tominaga et al., 1998) (Fig. 1.8 B). Recently, researchers proposed a VR1 pore dilation model. A time- and concentration-dependent change in ionic (i.e. Ca^{2+}) permeability following prolonged exposure to capsaicin was found with VR1 channels. The prolonged exposure increases the permeability of the VR1 channel pore (Bautista and Julius, 2008; Chung, 2008). Capsaicin-responsive nerves may be stimulated to release pre-stored pro-inflammatory neuropeptides. The neuropeptides released from VR1-positive nerves such as CGRP and SP cause mast cells degranulation, thereby, liberating histamine which, in turn, stimulates VR1 positive nerves to release more CGRP and SP (Szallasi and Blumberg, 1999) (Fig. 1.8 C).

Bradykinin (Arg-Pro-Pro-Gly-Phe-Ser-Pro-Phe-Arg), another nociceptive neuronal marker, activates sensory neurons by acting on the G-protein-coupled bradykinin type 2 receptor (BR2), causing elevation of $[Ca^{2+}]_i$ and inducing transmitter release (Chuang et al., 2001), which in turn, cause acute sensation of pain (Steranka et al., 1988).

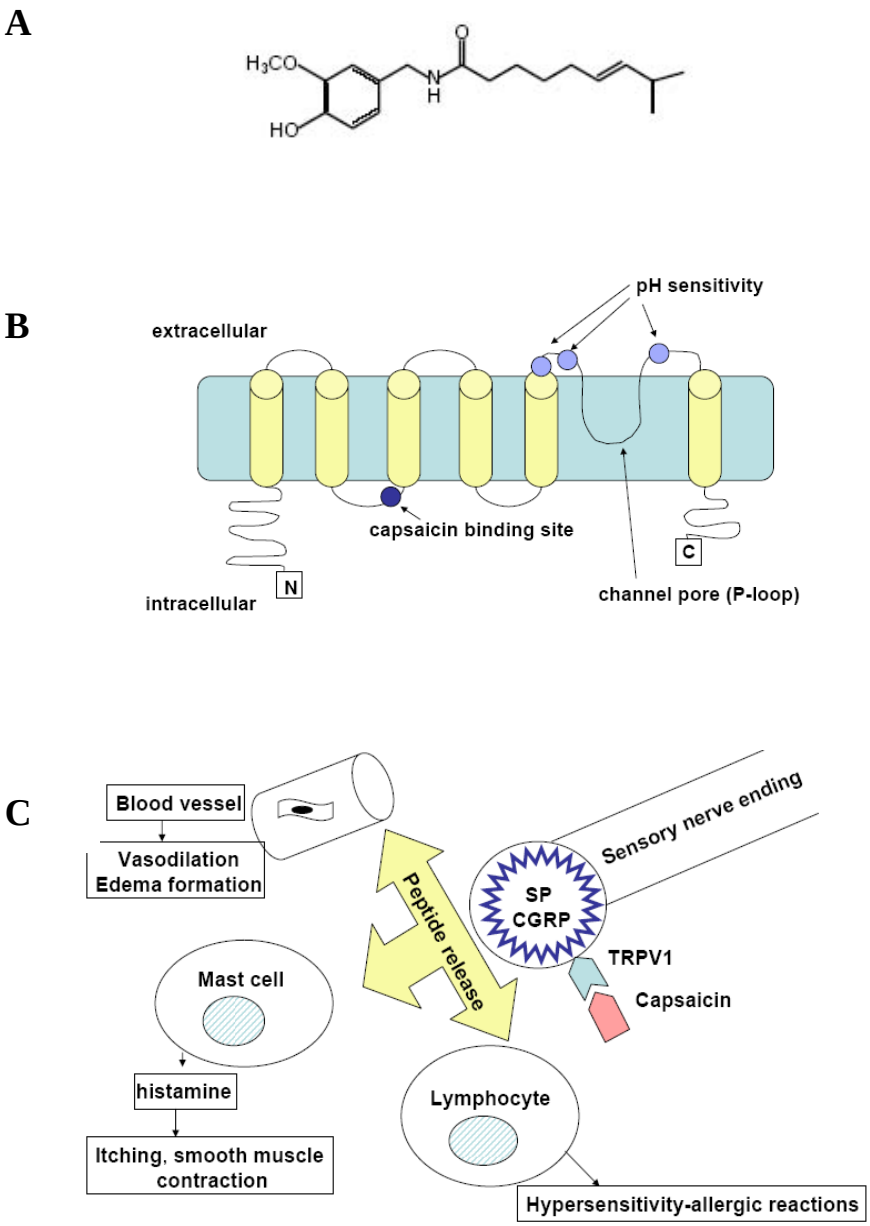

Fig. 1.8 Capsaicin chemical structure and its receptor VR1. *(A) Capsaicin structure; (B) VR1 has six transmembrane (TM) domains and a short, pore-forming hydrophobic stretch between the fifth and sixth TM domains (Cortright and Szallasi, 2004; Ferrer-Montiel et al., 2004); the channel pore has selectivity:* $Ca^{2+} > Mg^{2+} > K^{+} \approx Na^{+}$*; initial open state of VR1 shows low permeability to large cations. Polonged exposure to agonists increases the pore size, leading to enhanced permeability of the channel to large cations [reviewed by (Bautista and Julius, 2008)]. (C) Schematic illustration of the role of peripheral vanilloid-sensitive nerve endings in evoking neurogenic inflammatory and allergic-hypersensitivity reactions (Szallasi and Blumberg, 1999).*

1.4 Project aims and objectives

For the purpose of deciphering a molecular basis for the anti-nociceptive effects of BoNTs, an *in vitro* model was needed. Two types of sensory neurons, TGNs and DRGs, were chosen because these can be easily dissected, cultured and both are important in pain-transduction; also, TGNs are especially well known as a migraine pain-relay centre (see section 1.3.1).

The first objective, after successfully establishing these sensory neuronal systems *in vitro*, was to examine the location of their nociceptive neuronal markers (VR1, BR2 and IB_4 binding) in relation to pain-related peptides (i.e. CGRP or SP), by conventional or confocal microscopy in either phase-contrast or fluorescent mode. It was then necessary to demonstrate not only the presence of the core exocytotic machinery i.e. SNAREs (SNAP-25 and syntaxin or Sbr isoforms), and their associated proteins (synaptotagmin variants) but their co-occurence or co-localization with pain-related peptides. This should be achieved by separation of vesicles from these cultured sensory neurons allowing investigation of pain signalling pathways through immuno-analysis of their peptide content, SNAREs or related proteins. The presence of these BoNT substrates would imply the potential ability of various BoNTs in inhibiting the release of pain peptides.

The application of robust enzyme immuno-assays would allow the quantification of Ca^{2+}-dependent release of pain-peptides from these sensory neurons upon stimulation with various secretagogues (i.e. capsaicin or bradykinin with or without Ca^{2+}) or by membrane depolarisation (via manipulation of the external $[K^+]$ in the presence or absence of Ca^{2+}). Dependence of these exocytotic events on SNARE function should be ascertained by designing experiments utilising the 5 serotypes of natural BoNT (/A, /B, /C, /D, /E), all of which cleave their respective intracellular SNAREs at distinct sites. Blockade of the release of pain-mediators upon BoNT intoxication would not only demonstrate the role of SNAREs but allow the identification of particular SNARE isoforms.

A major objective of this project was to address the potential role of Sbr I in CGRP release. As no toxin can cleave Sbr I selectively, it was necessary to employ gene knock-down experiments using shRNA expressed by lentiviral particles, previously demonstrated to easily infect non-dividing cells. Characterisation of the intact SNARE complexes and resolution of the activity of truncated-SNAREs in mediating exocytosis was a crucial objective of this work. Experiments employing immuno-precipitation,

vesicle immuno-isolation and 2-dimensional gel electrophorisis techniques allowed the characterisation of particular SNARE complexes. Because CGRP resides in LDCVs, the presence of isoforms of SNARE was largely unknown, the use of a particular variant by various neurons should raise functional implications for other cells previously unrecognised (i.e. Sbr II was shown to occur predominantly in SCSVs whereas Sbr I was found to be required for mediating CGRP release, see Chapter 4).

Another experimental strategy of this work was to employ chimeric technology whereby various hybrid BoNTs were created by inter-changing binding domains between various serotypes. This approach would allow the introduction of different BoNT proteases into neurons previously insensitive to that particular serotype (i.e. chimeric EA toxin was engineered by substitution the binding domain of BoNT/E, which is unable to bind to neurons due to lack of its acceptor, by its counterpart from BoNT/A which can bind, see Chapter 5). Elucidation of the functionality of these chimeras and comparison with the parental toxins in different sensory models (each with dissimilar sensitivities to various BoNTs) should yield insights into, firstly, the functional domains of BoNT and, secondly, steps of transmitter release which previously could not be perturbed by their parental toxins in sensory systems (i.e. perticipation of SNAP-25 truncated by toxins in the formation of SDS-resistant SNARE complex). Only /A- but not chimera EA-truncated SNAP-25 was found to occur in the complex; and Ca^{2+}-reversibility of inhibition of exocytosis was found to be much greater after treatment with BoNT/A than chimera EA, see Chapter 5).

More in-depth studies were carried out in order to investigate the relationships between capsaicin-induced $[Ca^{2+}]_i$ elevation and CGRP release rate; the observed prolonged elevation of $[Ca^{2+}]_i$ elicited by capsaicin, revealed by $^{45}Ca^{2+}$ uptake and confocal imaging using Fluo 4-AM, could overcome BoNT/A inhibition. Most importantly, these chimeric toxins could also have improved pharmacological outcomes over their parents.

2.0 Materials and Methods

2.1 Materials

Suppliers' addresses are listed in the Appendix.

2.1.1 Cell culture and related reagents

Leibowitz's L15, Dulbecco's modified Eagle's Medium (DMEM) and Ham's F12 culture media, foetal bovine serum, Ca^{2+}- and Mg^{2+}-free Hanks' balanced salt solution (CMF-HBSS), Dulbecco's phosphate buffered saline (lacking Mg^{2+} and Ca^{2+}), antibiotics and mouse nerve growth factor (NGF-2.5S or 7S) and GlutMax I were purchased from GibcoBRL. Dispase II, collagenase I and DNase I were supplied by Roche Inc. Basal Eagle's Medium, Cytosine-β-D-arabinofuranoside (Ara-C), capsaicin, bradykinin, protease inhibitor cocktail, poly-L-lysine and laminin were bought from Sigma.

2.1.2 Antibodies

Table 2.1 List of antibodies

Primary antibodies and catalogue numbers	Monoclonal (Mab) or polyclonal, raised in species indicated and Immunogen epitope	Vendor	Dilution	
			*IF	*WB
SNAP-25 Cat. No. SMI81	Mab, binding to the amino-terminal of the C-terminal peptide	Sternberger Monoclonals, Inc.	1:500	1:1000
SNAP-23 Cat. No. 111 202	Rabbit, synthetic peptide DRIDIANARAKKLIDS (aa 196-211 in human)	Synaptic Systems	1:1000	1:1000
Syntaxin I Cat. No. S0664	Mab	Sigma	1:500	1:2000
Syntaxin II Cat. No. 110 022	Rabbit, cytoplasmic domain of rat syntaxin 2 (aa 1 - 265).	Synaptic Systems	1:1000	1:1000
Syntaxin III Cat. No. 110 032	Rabbit, cytoplasmic domain of rat syntaxin 3 (aa 1 - 260).	Synaptic Systems	1:1000	1:1000
Sbr I Cat. No. 104 002	Rabbit, synthetic peptide SAPAQPPAEGTEG (aa 2 - 14 in rat synaptobrevin 1)	Synaptic Systems	1:1000	1:1000
Sbr II Cat. No. 104 202	Rabbit, synthetic peptide SATAATVPPAAPAGEG (aa 2 - 17 in rat synaptobrevin 2)	Synaptic Systems	1:1000	1:1000

Sbr II (Cl69.1) Cat. No.104 211	Mab, synthetic peptide SATAATVPPAAPAGEG (aa 2 - 17 in rat synaptobrevin 2)	Synaptic Systems	1:1000	1:1000
Sbr I/II/III (anti-HV62)	Guinea pig, a synthetic peptide corresponding to residues 33–94 of. human synaptobrevin-2	Self-generated (Foran et al., 2003)		1:400
Synaptotag-min I/II Cat. No. SC-12466	Goat, an internal region of Synaptotagmin I	Santa Cruz Biotechnology	1:100	
Syt-Ecto (Cl604.2) Cat. No. 105 311C 3	Mab, synthetic peptide (aa 1 - 19 of rat synaptotagmin 1)	Synaptic Systems	1:100	
SV2A Cat. No. 119 002	Rabbit, synthetic peptide EEGFRDRAAFIRGAKD (aa 2 - 17 in human)	Synaptic Systems	1:1000	1:1000
SV2B Cat. No. 119 102	Rabbit, synthetic peptide DDYRYRDNYEGYAPN D (aa 2 - 17 in rat)	Synaptic Systems	1:1000	1:1000
SV2C Cat. No. SC-11944	Goat, N-terminus of SV2C of rat origin	Santa Cruz Biotechnology	1:100	1:10000
CGRP Cat. No. C8198	Rabbit, synthetic CGRP (rat)	Sigma	1:500	
CGRP (CD8) Cat. No. C9487	Mab, synthetic peptide of C-terminal αCGRP (rat)	Sigma	1:500	
SP Cat. No. AB14184	Mab, Synthetic peptide: RPRPQQFFGLM, corresponding to amino acids 1-11 of Human Substance P.	Abcam	1:1000	
VR1 Cat. No. RA10110	Rabbit, RASLDSEESESPPQENS C	Neuromics	1:1000	
VR1 Cat. No. AB10295	Guinea pig, synthetic peptide: YTGSLKPEDAEVFKDS MVPGEK, corresponding to C terminal amino acids 817-838 of Rat Vanilloid Receptor 1.	Chemicon	1:1000	
BR2 Cat. No. RDI-BRDYKRabm	Mab, peptide 350-364 C terminal of human B2 Bradykinin Receptor	RDI Division of Fitzgerald Industries Intl	1:500	
NF-200 Cat. No. N-0142	Mab, the carboxyterminal tail segment of	Sigma	1:500	

	enzymatically dephosphorylated pig neurofilament H-subunit			
BoNT/A	Rabbit	Allergan. Inc.		1:5000
LC/E	Rabbit	Allergan. Inc.		1:15000

**IF, immunofluorescence staining; WB, Western blotting*

Rabbit non-immune IgG was bought from Sigma; anti-species secondary antibodies fluorescently-labelled or conjugated to horseradish peroxidase were obtained from Invitrogen or Jackson Immuno-Research, respectively.

2.1.3 Natural BoNTs

Homogeneous, fully-active di-chain BoNT/A was obtained from Dr. B. DasGupta (Department of Food Microbiology and Toxicology, University of Wisconsin-Madison, 53706, USA.). Metabiologics Inc. supplied BoNT/B which contained some single chain; it was converted (> 95%) to the di-chain form by nicking with Trypzean (200 µg of toxin and 2 µg of enzyme in 0.2 ml 50 mM HEPES/50 mM NaCl, pH 7.4) at 27°C for 40 minutes, followed by addition of 20 µg of soyabean trypsin inhibitor. BoNT/C1 and /D were obtained from Metabiologics Inc. A highly purified single chain (SC) of natural BoNT/E from Metabiologics Inc was nicked to the DC form (>95%) with Trypzean (8µg/mg BoNT) for 40 minutes at 27ºC.

2.1.4 Animals

Wistar rats were bought from Bioresources Unit of Trinity College; Tyler's Ordinary (TO) mice and Sprague Dawley rats were bred in an approved Bioresources Unit at Dublin City University (DCU).

2.1.5 EIA assay reagents

CGRP and SP enzyme immuno-assay (EIA) kit were bought from SPI-BIO. The EIA kit for rat vasoactive intestinal peptide (VIP) (EK-064-16) and neuropeptide Y (NPY) (EK-049-03) were purchased from PHOENIX PHARMACEUTICALS, INC. The serotonin EIA kit (17-EA602-96) was obtained from ALPCO DIAGNOSTICS.

2.1.6 ShRNA reagents for knock down of Sbr I gene expression

ShRNA lentiviral transduction particles were bought from Sigma Aldrich.

2.1.7 Other reagents

Enhanced chemiluminescence (ECL) reagents were from Amersham or Millipore. Bicinchoninic acid (BCA) protein assay kit was bought from Pierce. Precast Bis-Tris gels, 20 x MOPs running buffer were purchased from Invitrogen. Trypzean, trypsin inhibitor, protein A agarose, 6'-diamidino-2-phenylindole (DAPI), isolectin B_4-FITC and Coomassie Brilliant Blue G 250, trifloroacetic acid (TFA), and acetic acid were supplied by Sigma. Thrombin was bought from Novagen. Dolethal was prescribed by the Biosources Unit of Trinity College. Fluo 4-AM was purchased from Molecular Probes (Invitrogen). Gangliosides mixture contained ~18% GM_1, 55% GD_{1a}, 15% GD_{1b}, 10% GT_{1b} and 2% other gangliosides extracted from bovine gray matter, and an aminopeptidase N inhibitor were supplied by Calbiochem.

2.2 Procedures for isolation and culture of neurons

2.2.1 Animals, anesthesia and dissection setup

Postnatal day 5 (P5) Wistar or P3-5 Sprague Dawley rats or P5 TO mice were deeply-anesthetized with intraperitoneal injection of Dolethal (50 mg/kg body wt). Heads were wiped with 70% ethanol, decapitated, and kept on ice until surgery. Dissection of TGs, DRGs and CGNs were performed inside an open-front laminar hood; working surface and all instruments including fine forceps, spring scissors, fine iris scissors were cleaned and sterilized by 70% ethanol to reduce the likehood of contamination. All dissection procedures were performed in the Bioresources Unit at Dublin City University (DCU).

2.2.2 TGs dissection, dissociation and culture

The procedures of (Eckert et al., 1997) were used with a number of modifications. The location of TGs is shown in Fig. 1.4 and 2.1. After removal of skin from the skull, the brain and both optic nerves were removed to expose the TGs. The three main branches were cut and the connective tissue removed to release the TGs.

The tissue was placed in ice-cold L15 medium, washed twice in ice-cold sterile Ca^{2+} and Ca^{2+}- Mg^{2+}- free Hanks' balanced salt solution (CMF-HBSS) before centrifugation at 170 g for 1 minute. After chopping into small pieces and passing through L15 medium precoated 10 ml Falcon pippetes, the tissue was incubated at 37°C for 30

minutes with shaking in 1:1 mixture of CMF-HBSS containing 2.4 U/ml dispase II and 1 mg/ml collagenase I. The suspension was then gently triturated through L15 medium precoated 10 ml serological pipetts until cloudy, before adding 1 mg/ml DNase I for 15 minutes. Following centrifugation at 170 g for 5 minutes, the pellet was resuspended and washed three times in culture medium [Ham's F12 solution or DMEM containing 10% (v/v) heat-inactivated foetal bovine serum, 100 U/ml penicillin, and 100 µg/ml streptomycin]. Cells were seeded at ~$3x10^6$ cells/well onto poly-L-lysine (0.1 mg/ml) and laminin (20 µg/ml) coated 24-well plates in F12 supplemented with 2.5 or 7s NGF (50 ng/ml) and maintained in a CO_2 incubator at 37°C. After 24 hours and every other day thereafter, the culture supernatant was replaced with medium containing an anti-mitotic agent, Ara-C (10µM).

2.2.3 DRGs: dissection and culture of their neurons

DRGs were dissected from P5 rats or mice. The locations of DRGs are shown in Fig. 2.2. After opening the spine, the spinal cord was exposed and pushed back; ganglia were snipped, lifted and freed after cutting the connections.

DRGs were washed, dissociated as for TGNs (above) and cultured at density 10^6/well in 24-well plate in DMEM containing 10% (v/v) foetal bovine serum, 100 U/ml penicillin, 100 µg/ml streptomycin and 50 ng/ml 2.5s NGF. Ara-C (10 µM) was added from day 1 to 5 in culture; medium was exchanged every other day.

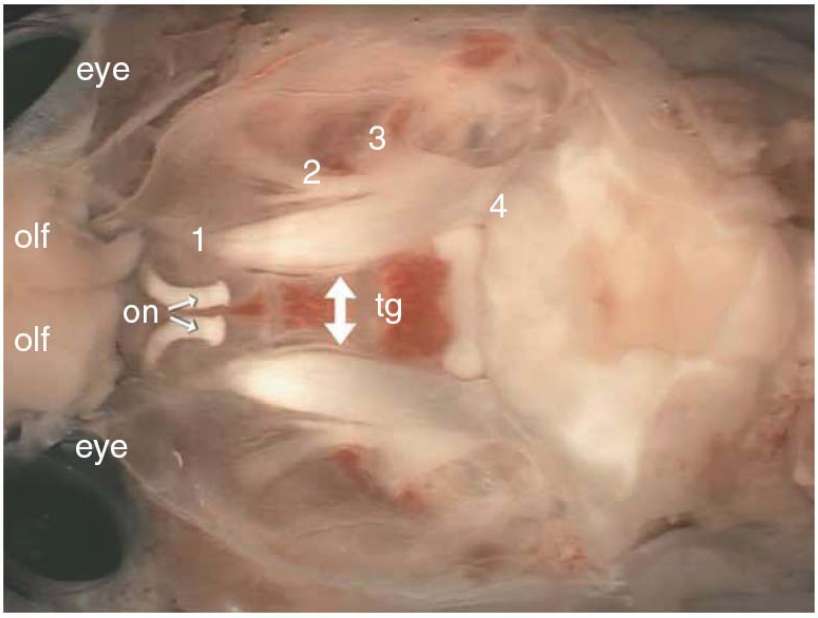

Fig. 2.1 Location of trigeminal ganglia (tg, double arrow) in rat cranial cavity: on, optic nerves; olf, olfactory bulb. *The three trigeminal branches are labelled at the location to be severed for removal of the ganglia: 1, ophthalmic; 2, maxillary; 3, mandibular; 4, fifth cranial nerve. Picture adaped from (Malin et al., 2007).*

Fig. 2.2. Location of DRGs. *The location of the ganglia are pointed with arrows. Pairs of DRGs reside at cervical, thoracic, lumbar and sacral vertebral levels. Picture adapted from (Malin et al., 2007).*

2.2.4 Culturing of cerebellar granule neurons (CGNs)

Procedures for isolation and culturing CGNs were adapted from (Foran et al., 2003). Briefly, cerebella were removed from 5-8 day-old rats and enzymetically digested using 1:1 mixture of trypsin-EDTA in Dulbecco's phosphate buffered saline (lacking Mg^{2+} and Ca^{2+}) (7.5 ml each) for 20 min at 37°C. Cells were collected by centrifugation at 170 g for 5 minutes and resuspended in culture medium at 1×10^6/ml in basal Eagle's medium containing 10 mM HEPES-NaOH, pH 7.3, 19.6 mM KCl, 9.4 mM D-glucose, 0.7 mM $CaCl_2$, 0.4 mM $MgSO_4$, and 0.25 mM NaH_2PO_4; 1x N2 supplement, 1 mM GlutMax I (contains the dipeptide L-alanyl-L-glutamine which is only removed from the medium by cell metabolism; there is no build-up of toxic metabolites due to spontaneous breakdown); 60 U/ml penicillin, 60 µg/ml streptomycin, and 2% (v/v) horse dialyzed serum were subsequently added. Cells were seeded at density ~$5x10^6$ in 24 well plates onto poly-L-lysine (0.1 mg/ml)-coated 24-well plates and Ara-C (40µM) was added after culturing for 20-24 hours. Neurons were maintained by replacement every 7-10 days with freshly-prepared medium.

2.3 Cytochemical staining and microscopic recording of images

TGNs cultured on poly-L-lysine and laminin coated coverslips were washed three times with Dulbecco's phosphate buffer saline (lacking $Mg^{2+}$and Ca^{2+}) then fixed for 20 minutes with 3.7% paraformaldehyde at room temperature in the latter buffer. The cells were then washed with PBS three times, followed by permeabilization for 5 minutes with 0.2% Triton X-100 in PBS before blocking with 1% bovine serum albumin (BSA) in PBS for 1 hour. Primary antibodies were applied in the same solution and left overnight at 4ºC; after extensive washing, fluorescently-conjugated secondary antibodies were added for 1 hour at room temperature. Fluorescent labelling of IB_4–binding cells was performed as detailed by (Stucky et al., 2002). Briefly, rat cultured TGNs were fixed by 3.7% paraformaldehyde in CMF-PBS for 20 minutes, followed by rinsing 3 times with PBS. Staining was performed with 4 µg/ml FITC-IB_4, in 0.1 M phosphate buffer (contains 84 ml 0.2 M Na_2HPO_4 mix with 216 ml 0.2 M NaH_2PO_4 and add H_20 to 600 ml, pH 7.2), 0.1 mM $CaCl_2$, 0.1 mM $MgCl_2$, 0.1 mM $MnCl_2$ for 1 hour at room temperature. In some cases, counter-staining of nuclei was carried out with DAPI (1 µg/ml in water) added before the final wash.

Immuno-fluorescent pictures were taken with an inverted confocal (Leica Dmire 2) or an Olympus IX71 microscope equipped with a CCD camera. Images were analysed

using Leica confocal software and Image-Pro Plus 5.1, respectively. The omission of primary antibody from the fluorescence staining gave the background for secondary antibody; the signal intensity above this was taken as positive reactivity.

2.4 Quantitation of neurotransmitters release and/or total cellular content

2.4.1 Basal and stimulated release

At 7 days in vitro (DIV), medium was gently aspirated from the TGNs or DRGs, 0.5 ml of basal release buffer (BR-HBS, mM; 22.5 HEPES, 135 NaCl, 3.5 KCl, 1 $MgCl_2$, 2.5 $CaCl_2$, 3.3 glucose, and 0.1% BSA, pH 7.4) was added into each well, followed by 30 minutes incubation at 37°C. The solution bathing the cells was briefly centrifuged at 4°C and the supernatants stored at -20°C until subjected to EIA. Ca^{2+}-dependent release stimulated with 60 mM KCl in HBS (isotonically balanced with NaCl) or various concentrations of KCl (isotonically balanced with NaCl) as indicated in figure legends was performed in the same way. For stimulation with capsaicin or bradykinin, stocks (10 mM) were prepared in ethanol or dimethyl sulphoxide, respectively, and further diluted in BR-HBS to reach the required concentrations. In some cases, the final concentration of vehicle was kept at 0.1%; this was also included in BR-HBS when measuring basal efflux. Quantitation of Ca^{2+}-independent basal release and that evoked by K^+, capsaicin or bradykinin was carried out as above except for Ca^{2+} being replaced by 2 mM EGTA. The values obtained for each were subtracted from the requisite totals to yield the Ca^{2+}-dependent components; the latter figure minus the basal value yielded the Ca^{2+}-dependent evoked release; expression of the evoked release relative to that for basal efflux gave the increment for each stimulus. Intracellular total content per well was determined on randomly selected wells for each culture preparation. Briefly, 500 µl of 2 M acetic acid/ 0.1% TFA were added into each well, cells are scraped off and lysed by freeze/thaw three times followed by high-speed vacuum evaporation. Before EIA assay, 500 µl of EIA buffer was added to resuspend the dried pellets; samples from each well were kept in -20°C prior to assay of neuropeptides. When EIA assay was performed (see below), no degradation of peptide was observed because addition of the aminopeptidase N inhibitor (1 mM final concentration) did not make any difference.

2.4.2 Enzyme immuno-assay (EIA) of neuropeptides

2.4.2.1 CGRP

This EIA was based on a double-antibody sandwich technique that permits measurement of CGRP within the range of 1-500 pg/ml. The wells of the 96-well plates supplied with the kits were coated with a Mab specific for CGRP. This antibody binds any CGRP introduced in the wells (samples or standards supplied with the kits). An acetylcholinesterase (AChE)-Fab conjugate (anti-CGRP AChE tracer) which binds selectively to a different epitope on the CGRP molecule was also added to the wells. This allowed the two antibodies to form a sandwich by binding on different parts of the CGRP molecule, which remained immobilised on the plate; the excess reagents are washed away. The concentration of the CGRP was then determined by measuring the enzymatic acitivity of the AChE using Ellman's reagent, which contains acetylthiocholine as the substrate. The final product of the enzymatic reaction, 5-thio-2-nitrobenzoic acid, is bright yellow and can be read at 405-420 nm. The intensity of the yellow colour, which was determined spectrophotometrically, is proportional to the amount of the CGRP present in the well.

For determining the amounts of CGRP released, 0.1 ml of sample or standard was added to 96-well plates followed by 0.1 ml of CGRP tracer solution, and incubated at 4ºC overnight. After plates were washed with buffer supplied in the kits for 5 times, Ellman's reagent was added and incubated in the dark at room temperature until the mixture turned yellow (at least 30 minutes). Plates were read photometrically at 405 nm using a Techan microplate reader. For data analysis, a standard curve (linear curve fit) was generated for each assay (Fig. 2.3) and a best-fit line through the points drawn using Excel software; this was used to determine the concentration of CGRP in test samples. The accuracy of estimation of concentration for unknown samples depends on the absorbance falling within the desired range of standard curve. Samples with absorbance values beyond standard curve points need to be further diluted or concentrated before the assay is performed.

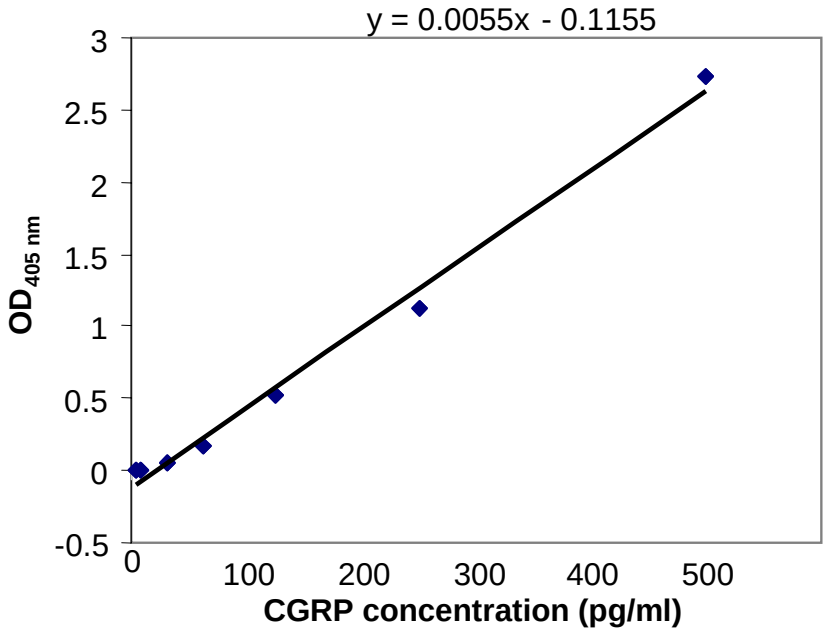

Fig. 2.3 A representative CGRP standard curve. *This was generated by Excel software using linear regression. The blank reading was substracted from the sample or standard value and plotted in y-axis. Known concentrations of CGRP standards were plotted in x-axis. An equation was displayed above the chart and the peptide with unknown concentration in samples can be determined by extrapolation to it.*

2.4.2.2 SP

SP EIA assay was based on the competition between SP and a SP-AChE tracer for a limited number of SP-specific binding sites in a rabbit antiserum. Because the concentration of the SP-tracer is held constant while the concentration of SP varies, the amount of SP-tracer that was able to bind to the rabbit antiserum would be inversely proportional to the concentration of SP in the well. This rabbit antiserum-SP (either free or tracer) complex was bound via a mouse monoclonal anti-rabbit IgG that had been previously attached to the well. The plate was washed to remove any unbound reagents, and then Ellman's reagent (which contains the substrate for AChE) was added to the well. The yellow product of this enzymatic reaction was read as for CGRP (see above). The intensity of this color was proportional to the amount of SP tracer bound to the well, which was inversely proportional to the quantity of free SP present during the incubation.

A sample or standard (0.05 ml) was added into each well followed by 0.1 ml SP-tracer, and plates were incubated at 4ºC overnight. After washing 5 times with washing buffer, Ellman's reagent was added into plates followed by incubation for 1~2 hours at room temperature. A representative SP standard curve is shown in Fig. 2.4, and the unknown concentration was determined from it by identifying the %B/B0, which is the (OD_{405} of sample or standard- OD_{405} of non-specific bound) / (OD_{405} of maximum bound- OD_{405} of non-specific bound); maximum bound is the reading value form assay when sample or standard was not added; non-specific binding (NSB) was obtained by omitting sample or standard and antibody from the assay (NSB also is called non-immunological binding of the tracer to the well; even in the absence of specific antiserum, a very small amount of tracer still binds to the well). The sample concentrations were extrapolated from the known y-axis value using the standard curve. A new standard curve was generated for every assay.

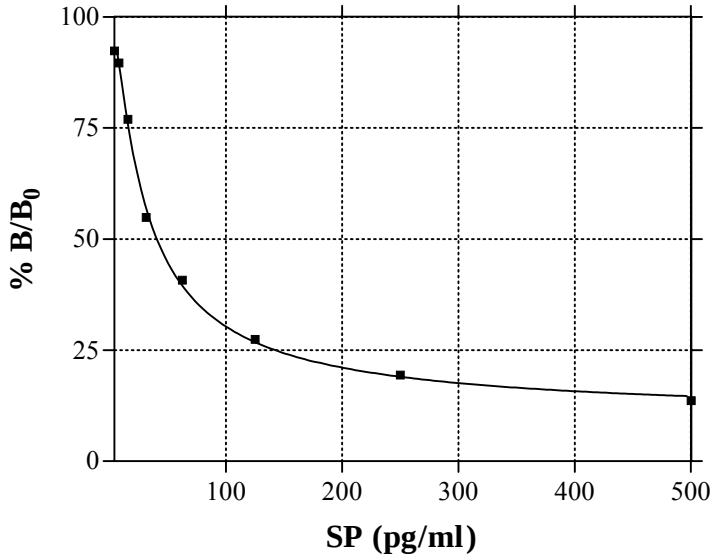

Fig. 2.4 A representative SP standard curve. *This was generated by Prism software 4.0 using nonlinear regression curve fit in two site binding (hyperbola) equation.* *%B/B0 is the % sample or standard bound/maximum bound. Known concentrations of SP standards were plotted in x-axis. Unknown concentrations of samples were extrapolated using the software based on standard curve created for each assay.*

2.4.2.3 NPY

Aliquots from the same samples assayed for CGRP or SP were also used to quantify the content of NPY present. The immuno-plate in this kit is pre-coated with secondary antibody and the non-specific binding sites are blocked. The secondary antibody binds to the Fc fragment of the primary antibody whose Fab fragment was competitively bound by both biotinylated peptide and peptide standard or samples. The biotinylated peptide interacted with streptavidin-horseradish peroxidase (SA-HRP) which catalyzes the 3,3',5,5'-tetramethylbenzidine (TMB) substrate solution composed of TMB and hydrogen peroxide producing a blue colored solution. The enzyme-substrate reaction is stopped by hydrogen chloride, turning the solution yellow which was read at 450 nm. The intensity of the yellow is directly proportional to the amount of biotinylated peptide-SA-HRP complex but inversely proportional to the quantity of the peptide in standard solutions or samples. A standard curve of a peptide with known concentration can be established accordingly. The peptide with unknown concentration in samples is determined by extrapolation from this standard curve. Very low cross-reactivity with SP or vasoactive intestinal peptide (VIP) is seen with this kit.

2.4.2.4 VIP

Aliquots of samples subjected to the above assays were also used to assess VIP present.

Procedures were similar as that for NPY assay:

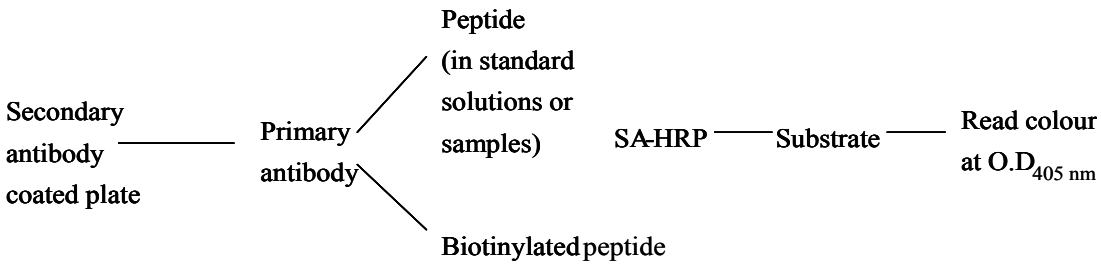

This kit showed very low cross-reactivity to NPY, SP, galanin, or secretin according to the information from the supplier.

2.4.2.5 Serotonin

Samples and standards were acylated and applied to a microtiter plate which was precoated with un-acylated serotonin. Serotonin antiserum was applied. Acylated serotonin and solid phase-bound serotonin compete for a fixed number of antiserum

binding sites. When the system reaches equilibrium, free antigen and free antigen-antiserum complexes are removed by washing. The antibody bound to the solid phase serotonin is detected by anti-rabbit/peroxidase. The substrate TMB/peroxidase reaction product is read at 450 nm. The amount of antibody bound to the solid phase serotonin is inversely proportional to the serotonin concentration of the sample. The sensitivity for CSF and platelet-free plasma samples is 0.3 ng/ml, and the kit displays very low reactivity with tryptamine or melatonin.

2.5 Crude fractionation of CGRP- and SP-containing large dense-core vesicles (LDCVs) from rat TGs

TGs were dissected from around 35 5-day-old Wistar rats and homogenized using a motor-driven Teflon dounce homogenizer in 10 ml of homogenization buffer [0.32 M sucrose, 1 mM EDTA, 4 mM HEPES, pH 7.2, and a cocktail of protease inhibitors which is a mixture of protease inhibitors with broad specificity for the inhibition of serine, cysteine, aspartic proteases and aminopeptidases, and it contains 4-(2-aminoethyl) benzenesulfonyl fluoride, pepstatinA, E-64, bestatin, leupeptin, and aprotinin without any metal chelators. Lysate was passaged through a 25G needle. Nuclei, unbroken cells, and large cell debris were removed by low speed centrifugation at 1,200 g for 15 minutes. Microsomes were pelleted by centrifuging the resultant supernatant at 100,000 g for 2 hours. Pellets were resuspended and hypo-osmoticly lysed for 45 minutes on ice in resuspension buffer (40 mM sucrose, 1 mM EDTA, 4 mM HEPES, pH 7.2. and 1:100 (v:v) protease inhibitors from sigma). Continuous gradients were formed using 10% and 50% sucrose (w/v) in 1 mM EDTA, 4 mM HEPES, pH 7.2 with a gradient mixer. The resuspended pellet was then layered above this continuous gradient. After centrifugation at 95,000 g for 18 hours at 4°C, fractions (600 µl) were collected from the bottom working towards the top; protein concentrations were measured with a BCA kit (see 2.14). Aliquots of each fracion were solubilised in an equal volume of 4 M acetic acid/0.2% TFA followed by 3 cycles of freeze/thaw before the solvent was evaporated using speed-vacuum. The dried pellets were dissolved in EIA buffer before assay for CGRP or SP concentration by EIA.

2.6 Immuno-absorption of vesicles from TGNs

Cultured TGNs from a pair of 24-well plates were washed and treated as above (in 2.5), modified from (Berg et al., 2000). After the resultant supernatant was subjected to centrifugation at 100,000 g for 2 hours, and the resultant pellets resuspended in ice-cold hypotonic lysis buffer (40 mM sucrose, 1 mM EDTA, 4 mM HEPES, pH 7.2 and 1:100 (v:v) protease inhibitors from Sigma) for 45 minutes to osmoticly lyse microsomes and librate vesicles, then vesicles were sedimented (100,000 g for 2 hours) then resuspended in homogenisation buffer without applying to continuous gradient centrifugation. Aliquots of the suspension (~144 µg protein determined by BCA assay) were incubated overnight at 4°C with rabbit antibodies (10 µg) specific for Sbr I or II (these antibodies recognise N-terminal cytoplasmic domain), or rabbit non-immune control IgG, all coupled to protein A agarose; the beads were washed 5 times with homogenisation buffer. Equal aliquots (0.5 ml) were sedimented and pellets dissolved in 2 x LDS sample buffer for SDS-PAGE, or in 2 M acetic acid/0.1%TFA for EIA; the solvents were removed from the latter by vacuum drying and the residues dissolved in EIA buffer for CGRP quantitation.

2.7 Co-immunoprecipitation of SNAREs from detergent solubilised TGNs

The pellets of PBS-washed TGNs were dissolved in 1 ml of extraction buffer [(mM): KCl, 140; EDTA, 2; HEPES-KOH pH 7.3, 20; and 1% (v/v) triton X-100]. After extraction for 1 hour at 4°C and centrifugation for 3 minutes at 700 *g* to remove unlysed cells and large debris, the supernatant was incubated overnight at 4°C with 10 µg of rabbit IgG against Sbr I or II, or syntaxin II or III coupled to protein A agarose beads. After sedimentation, the beads were washed 5 times in extraction buffer and proteins eluted using 2xLDS-PAGE sample buffer. A control sample was treated similarly except rabbit non-immune IgG was used. SNAREs were detected by SDS-PAGE and Western blotting, as described later.

2.8 Treatment of neurons with BoNTs: monitoring of effects on CGRP release, SNARE cleavage, and exo-endocytotic activities

2.8.1 Toxin incubation, release of neurotransmitters, cell lysis, SDS-PAGE and immunoblotting

After 7 DIV, fresh medium alone or that containing natural BoNT/A, /B, /C1, /D, /E or engineered chimeric toxin was added to the TGNs at 37°C for times indicated in figure legends, at the concentrations specified. After removal of the unbound toxin and subsequent washing with 2 x 1 ml of toxin-free BR-HBS buffer, Ca^{2+}-dependent basal release of CGRP or SP and that evoked by 60 mM K^+, 1 μM capsacin or 0.1 μM bradykinin were measured, as described previously. Non-toxin treated samples were processed similarly. In each case, stimulated release was calculated as in 2.4.1. Expression of the resultant values for BoNT-treated samples relative to those for the controls gave the % of CGRP or SP release remaining. After the release assay, the cells in each well were lysed in 0.2 ml of 2 x LDS sample buffer, heated for 5 minutes at 95°C and separated by SDS-PAGE using 12% precast Bis-Tris gels (Foran et al., 2003). Specific antibodies were used for the Western blotting analysis.

2.8.2 Quantitation of substrate cleavage

After ECL development, digital images were obtained using the G BOX Chemi-16 gel documentation system; intensities of each lane were quantified with Image J software. For determination of the fraction of each SNARE cleaved, the ratios calculated for intact substrate and the requisite internal standard (i.e. a SNARE not susceptible to the toxin in use, to normalize any variation between wells) for BoNT-treated samples were expressed relative to those for non-toxin treated controls. Data were calculated and graphs generated by Excel and Prism 4.0 software; each point represents the mean ± s.e.m or mean ± s.d., as indicated in figure legends from several independent experiments.

2.8.3 Ecto-Syt I binding and uptake into TGNs

For assay of synaptic vesicle exocytosis and recycling, rat TGNs were cultured for 7 DIV on poly-L-lysine and laminin coated coverslips, and incubated with 100 nM BoNT/A or chimera EA in culture medium for 24 hours. Toxins were washed away and cells exposed to Ecto-Syt Abs (1:100) for 15 minutes in the basal buffer, or 60 mM K^+ or 1 μM capsaicin stimulation buffer (as described previously for CGRP release assays). After washing three times with basal buffer, cells on coverslips were fixed for 20 minutes with 3.7% paraformaldehyde in Ca^{2+}- and Mg^{2+}-free PBS at room temperature and fluorescent images were recorded using an Olympus IX71 inverted

microscope fitted with epifluorescence. Images were captured with a CCD camera and processed using Image Pro-Plus version 5.1 (Media Cybernetics).

2.9 Measurement of intracellular [Ca^{2+}] and Ca^{2+} uptake into TGNs

Coverslips containing TGNs were loaded with 3 μM Fluo 4-AM in basal release buffer at room temperature for 20 minutes, mounted on a custom-built low-volume (350 μl) chamber attached to an Axioskop 2 FS MOT/LSM Pascal confocal microscope (Zeiss). An argon laser was used to excite Fluo 4-AM at 488 nm. Serial images were taken of Ca^{2+} fluorescent signals at 10 sec. intervals while the superfusate was switched after ~2 minutes from BR-HBS to stimulation buffer: 60 mM K^+ or 1 μM capsaicin. The intensity of fluorescence at 505~530 nm (f) was analysed off-line on a cell-by-cell basis, and expressed relative to the baseline fluorescence (f_0) measured for each cell in BR-HBS. Mean f/f_0 ratios ± SEM were plotted; n values are given in figure legends (Fig. 5.11).

Cultured TGNs were incubated with 24 μCi/ml $^{45}Ca^{2+}$ in BR-HBS containing 0.1% ethanol, l μM capsaicin or 60 mM K^+ at room temperature for the times indicated in the figure. The incubation was stopped by 6 washes in 1 ml BR-HBS buffer, the samples solubilised in 200 μl of 0.1% SDS and counted in Beckman CP scintillation spectrometer. Ca^{2+} uptake was calculated from a standard curve of the amount of $^{45}Ca^{2+}$ against counts/minute.

2.10 Knock-down of Sbr I gene expression in cultured TGNs using small hairpin RNA (shRNA)

ShRNA (small hairpin RNA) lentiviral particles for knock down of Sbr I gene expression were used; these are transduction-ready viral particles with ~1.5×10^7 transduction units (TU)/ml. The shRNA target set contains five clones specific for different regions of mouse Sbr I mRNA (Table 2.2). 20 μl (3×10^5 TU) of each clone of shRNA viral particles were added to 200 μl culture medium and applied to ~10^5 cells/well of mouse cultured TGNs at 7 DIV; 200 μl fresh culture medium was added the next day and every other day thereafter. Neurons which were not treated by viral particles were used as negative controls. Infected cells were kept in culture for 8-10 days before monitoring of basal and stimulated release of CGRP detailed in 2.4.1. Immediately thereafter, cells were solubilized in 2xLDS sample buffer prior to analysis

of level of each SNARE protein by SDS-PAGE and Western blotting, with specific antibodies for SNAP-25 (SMI-81), syntaxin I (HPC-1), Sbr I (rabbit IgG) or Sbr II (rabbit IgG).

Table 2.2 ShRNA target set for knock-down of mouse Sbr I

Clone no.	ShRNA TRC No.	Sequence
5	TRCN0000110585	CCGGCGGGAATTATTTCCTGGGTTTCTCGAGAAACCCAGG AAATAATTCCCGTTTTTG Region: 3'UTR
4	TRCN0000110586	CCGGGCCATCATCGTGGTAGTGATTCTCGAGAATCACTAC CACGATGATGGCTTTTTG Region: CDS
3	TRCN0000110587	CCGGCGTGGTAGTGATTGTAATCTACTCGAGTAGATTACA ATCACTACCACGTTTTTG Region: CDS
2	TRCN0000110588	CCGGGCTGGGAGCTATCTGTGCCATCTCGAGATGGCACAG ATAGCTCCCAGCTTTTTG Region: CDS
1	TRCN0000110589	CCGGCATGACCAGTAACAGGCGGTTCTCGAGAACCGCCTG TTACTGGTCATGTTTTTG Region: CDS

3'UTR, 3' untranslated region; CDS, coding sequence; TRC, the RNAi consortium

2.11 Generation of a novel BoNT chimera EA which binds to the BoNT/A acceptor SV2C-L4 *in vitro*.

2.11.1 Designing a construct for BoNT chimera EA by recombinant substitution of the H_C domain of BoNT/E with its counterpart from BoNT/A

In order to re-target BoNT/E proteolytic LC into TGNs insensitive to BoNT/E, I designed a new EA chimera. The LC and H_N gene fragments from BoNT/E (LC-H_N/E) were fused to the H_C of /A (H_C/A) to generate chimera EA transgene (LC-H_N/E-H_C/A).

2.11.2 Creation of chimera EA: construction, expression and purification followed by nicking with Trypzean

The chimera EA transgene was cloned into a prokaryotic expression vector and expressed in *E. coli* BL21 (DE3) strain. Its detailed construction, expression and purification were performed by Dr. Wang J and are described in (Wang et al., 2008). Nicking of this chimeric toxin between LC and HC was achieved by incubation with Trypzean (8 μg/mg BoNT) for 1 hour at 25°C and monitored by SDS-PAGE, followed by Coomassie protein staining and Western blotting, using rabbit antibodies against BoNT/A and LC/E.

2.11.3 GST-SV2C-L4 pull-down assay for toxin-acceptor interaction

A cDNA portion encoding the intra-luminal for toxin-acceptor interaction SV2C loop 4 (SV2C-L4, amino acids 454-579) was PCR amplified from pCMV SV2C plasmid (a gift from T. Südhof, Houston, Texas), cloned into pGEX-2T and expressed in BL21 (DE3) *E. coli* by Dr. Astrid Sasse.

For pull down assay, GST-SV2C-L4 (~100μg) was immobilised onto 100 μl of glutathione–Sepharose-4B matrix and incubated with BoNT/A, /E, or EA chimera (100 nM each) in a total volume of 100 μl of binding buffer (50 mM Tris, 150 mM NaCl, 0.5% triton X-100, pH 7.6) in the presence of 0.6mg/ml gangliosides mixtures for 4 hours at 4°C. Beads were collected by centrifugation and washed five times, each wash for 15 minutes at 4ºC with 1 ml of binding buffer. Bound proteins were eluted by 2x LDS-sample buffer, and less than 5% of bound protein was subjected to electrophoresis on 4-12% precast Bis-Tris gels. Toxins were detected by Western blotting with IgGs against LC/E or BoNT/A. Input GST-SV2C-L4 protein was detected with goat anti-SV2C antibody.

2.12 Production of BoNT chimeras AB (LC-H_N/A-H_C/B) and BA (LC-H_N/B-H_C/A)

I designed BoNT chimeras AB and BA by recombinant substitution of the H_C domain in /A and /B with their counterpart from the other serotype. The construction, expression and purification were performed by Dr Wang J (our unpublished data). Nicking of chimera AB toxin between LC and HC was achieved by incubation with Trypzean (3 μg/mg BoNT) for 1 hour at 25°C, followed by addition of soyabean trypsin inhibitor (30 μg/mg BoNT). Chimera BA which contains an engineered thrombin cleavage site in the loop region was efficiently and precisely nicked by thrombin (1 U/mg toxin) for 1 hour at 22°C, followed by addition of PMSF to a final concentration of 1 mM.

2.13 SDS-PAGE, protein staining, Western blotting and 2-dimensional (2-D) gel electrophorisis

2.13.1 SDS-PAGE

Proteins were loaded onto 12% or 4-12% precast Bis-Tris gel and electrophoresis run at 180 volts using MOPs running buffer (1 liter: 250 mM MOPS, 250 mM Tris, 5 mM EDTA, 0.1% SDS) until proteins were separated according to their molecular weights, indicated by pre-stained protein markers. Proteins were then fixed and stained as detailed in 2.13.2 or 2.13.3, or electrophoretically transferred to a Immobilon™ PVDF membrane for immunoblot assay as described in 2.13.4.

.

2.13.2 Sypro-ruby staining of protein gels

Gels were rinsed with distilled water and fixed in 10% methanol/7% acetic acid (v/v) for 30 minutes with shaking at room temperature. After rinsing the gels with distilled water, 10 ml of Sypro-ruby staining solution was added to the gel-trays which were covered by foil to protect from light. The staining was carried overnight with shaking at room temperature. After rinsing with distilled water and destaining with 10% methanol/7% acetic acid for 30 minutes, the gels were visualized under UV and stained bands were recorded using the gel-documentation system (described above).

2.13.3 Coomassie Blue staining

Protein gels prepared as in 2.13.1 were placed in 0.25 % (w/v) of Coomassie brilliant blue G 250 in 10% acetic acid (v/v) and 45 % methanol for 2-4 hours with gentle rocking to distribute the dye evenly over the gel. Gels were destained using 30% methanol/10% acetic acid until protein bands became distinct.

2.13.4 Western blotting

A piece of PVDF membrane with a rated pore size of 0.45 µm (Millipore) was wet for about 30 second in methanol followed by rinsing with ddH_2O twice, before soaking in transfer buffer (1L: 25 mM Tris-base, 190 mM glycine, 100 ml methanol and 900 ml H_2O) for 15 mins; then, assemble "sandwich" for transblot: (+) Sponge - filter paper - membrane - protein gels (prepared as in 2.13.1) - filter paper - sponge (-). Then put assembled "sandwich" in a transfer tank (TE62, Hoefer. Inc.) filled with transferring

buffer as above and transfer for 2~3 hours at 45 volts at 4°C; When finished, immerse membrane in blocking buffer (1L: 5 ml 2 M Tris-bis, 30 ml 5 M NaCl, 1 ml Tween 20, 7.6, 5% skimmed milk w/v) and block for 1 hour at room temperature. Then incubate with primary antibody diluted in blocking buffer for 1 hour at room temperature. After washing 3 x 10 min with 0.1 % Tween 20 in PBS, anti-species secondary antibodies conjugated to horseradish peroxidase (diluted in blocking buffer) were incubated for 1 hour; following washing 3 x 10 min with 0.1 % Tween 20 in PBS, proteins were detected by ECL reagent which contains a luminol substrate of horseradish peroxidase and can be converted to a light releasing substance. Images were recorded using G BOX Chemi-16 gel documentation system and intensities quantified with Image J software.

2.13.5 2-dimensional (2-D) gel electrophorisis

An established 2D SDS-PAGE method (Lawrence and Dolly, 2002) was used to investigate whether cleaved SNAP-25 products form SDS-resistant SNARE complexes during Ca^{2+}-triggered exocytosis in rat cultured TGNs treated with BoNT/A or chimera EA. After stimulating cells with 1 μM capsaicin for 30 minutes at 37°C, the buffer was removed and cells solubilised in LDS-sample buffer without boiling. Proteins were separated by SDS-PAGE on 4-12% precast Bis-Tris gel. Each sample lane was cut into strips reflecting different distances of migration through the gel, chopped into small pieces and boiled for 10 minutes in LDS-sample buffer; after being left overnight at room temperature, the samples were boiled again for 5 minutes before loading the extracted proteins onto a second 12% precast Bis-Tris gel. SNAREs released from complexes after boiling were detected in the second gel by Western blotting with specific antibodies, their position indicating the migration distance through the first gel (i.e. *Mr* of the SDS-resistant SNARE complex).

2.14 Protein concentration assay by BCA protein assay kit

The BCA protein assay combines the well-known reduction of Cu^{2+} to Cu^{+} by protein in an alkaline medium with the highly sensitive and selective colorimetric detection of the cuprous cation (Cu^{+}) by bicinchoninic acid. The first step is the chelation of copper by protein in an alkaline solution to form a blue colored complex. In this step, known as the biuret reaction, peptides containing three or more amino acid residues form a light blue colored chelate complex with cupric ions in an alkaline environment (pH 8.0).

Proteins will react to produce a light blue to violet complex that absorbs light at 540 nm. The intensity of the color produced is proportional to the number of peptide bonds participating in the reaction. In the second step of the color development reaction, BCA, a highly sensitive and selective colorimetric detection reagent reacts with the cuprous cation (Cu^{+}) that was formed in step 1. The purple-colored reaction product is formed by the chelation of two molecules of BCA with one cuprous ion. The BCA/copper complex is water-soluble and exhibits a strong linear absorbance at 562 nm with increasing protein concentrations. Briefly, 25 µl of sample from each fraction or BSA standard were applied to a 96 microplate; 200 µl mixture of reagent A and B (50:1) supplied in the kit were added to each well. The plate was mixed thoroughly and incubated for 30 minutes at 37°C before absorbance at 562 nm was read. Concentrations were calculated from the linear range of the standard curve.

2.15 Statistical analysis

Data were calculated and graphs generated by GraphPad Prism 4.0; each point represents the means ± S.E.M. or ± S.D. as indicated in Figure legends; student's unpaired t-test was used to evaluate significance of changes.

3.0 TGNs are a suitable model for investigating anti-nociceptive potential of BoNTs

3.1 Overview

This chapter describes the culturing of TGNs and demonstrates their expression of sensory neuron markers and the release of pain-peptides in response to K^+-depolarisation or known pain stimuli. These cells were then used to establish a basis for the putative anti-nociceptive effects of BoNT/A and to evaluate the roles of particular SNARE isoforms in regulated CGRP exocytosis (Chapter 4). Based on insights gleaned with natural BoNTs, novel BoNT chimeras were generated recombinantly with the goal of eventually creating new variants with improved anti-nociceptive potential (Chapter 5).

3.2 Results

3.2.1 Dissection of TGs and culture of their neurons

Neonatal rats or mice were used as a source of TGs because sensory neurons usually appear at embryonic day E10-13 for mouse, and E9-14 for rat. At P3-5, mouse and rat TGs are bigger than in the embryonic stage, relatively ease to dissect and readily susceptible to enzymatic dissociation. The dissociated TGNs were seeded onto poly-L-lysine and laminin precoated 24-well plates and cultured in F12 or DMEM medium supplemented with nerve growth factors (NGF 2.5s or 7s), as detailed in the Chapter 2. Sensory neurons obtained from neonatal rats require neuronal trophic factors, especially NGF to support differentiation, maintain phenotype and induce synthesis of transmitters (Malin et al., 2007). Immediately after plating cells, neuronal cell bodies were round, smooth, and phase-bright and usually less than 50% of total cell count. Within 2 hours of plating, most of neuronal cells attach to the coated surface. Neurites were discernable the next day. Non-neuronal cells attached more firmly to the culture surface, and divided quickly to occupy the growth area; thus, it was necessary to remove them as soon as possible. Therefore, Ara-C, a pyrimidine anti-metabolite that inhibits DNA synthesis, was added on day 2-5 to kill proliferating cells; fluorodeoxyuridine and uridine also proved effective. By day 5, most of the non-neuronal cells had died and cell debris could be removed by several changes of the culture medium. Morphological and histochemistrical experiments, neurotransmitters release assays, and treatment with toxins were performed at 5-7 DIV.

3.2.2 Morphological and histochemical features of the cultured neurons

3.2.2.1 Phase contrast microscopy of rat and mouse TGNs

Phase contrast micrographs revealed that rat (Fig. 3.1 A, B) and mouse (Fig. 3.1 C) neuronal cells are easily distinguished by large, round, phase-bright cell bodies with extended fine fibres (Fig. 3.1). At 1 DIV, satellite cells show spindle-liked cell soma shape and relative broader fibres; Astrocytes usually have polygonal or star shape with short fibres (Fig. 3.1 A). TGNs possessed bipolar or multi-polar neurite extensions; some had a pseudo-unipolar shape. There was no distinct difference in the neuronal morphology between rat and mouse (Fig. 3.1 B, C). At 7 DIV neuronal cells are enriched comparing with 1 DIV (Fig. 3.1 B, C). Just like TGNs *in vivo*, the cultured neurons seemed to be roughly made up of two populations representing small and large neurons.

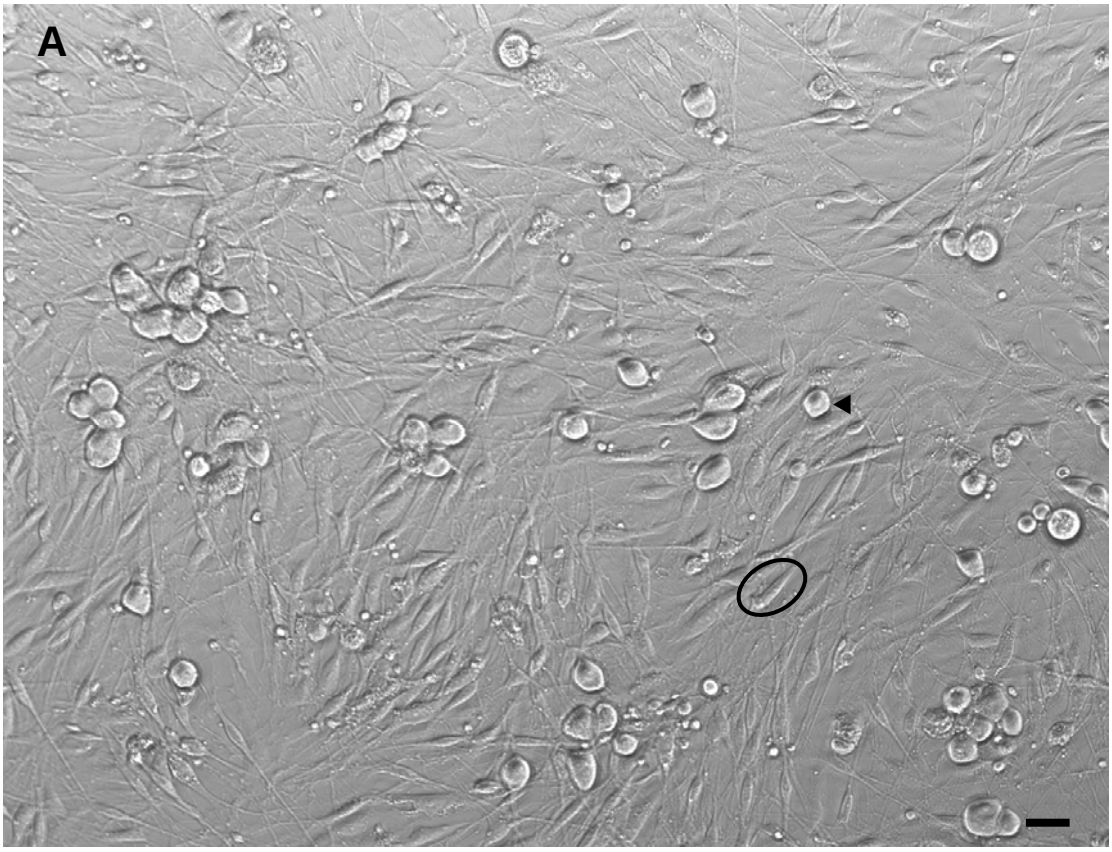
A

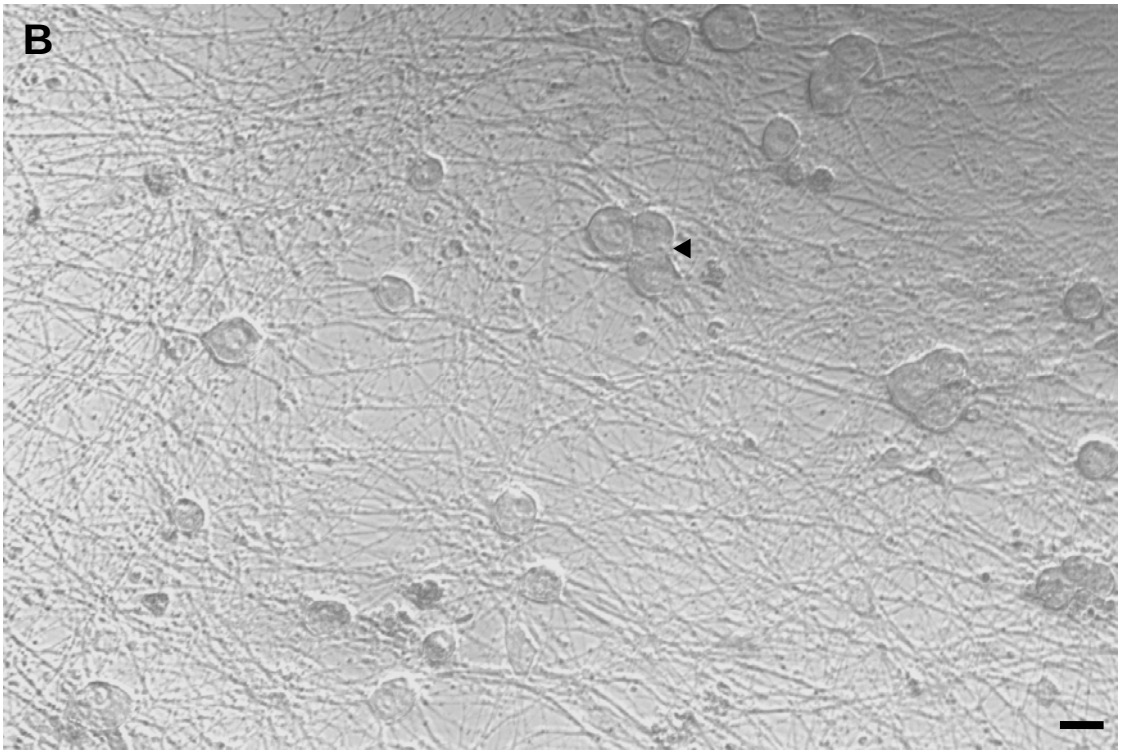
B

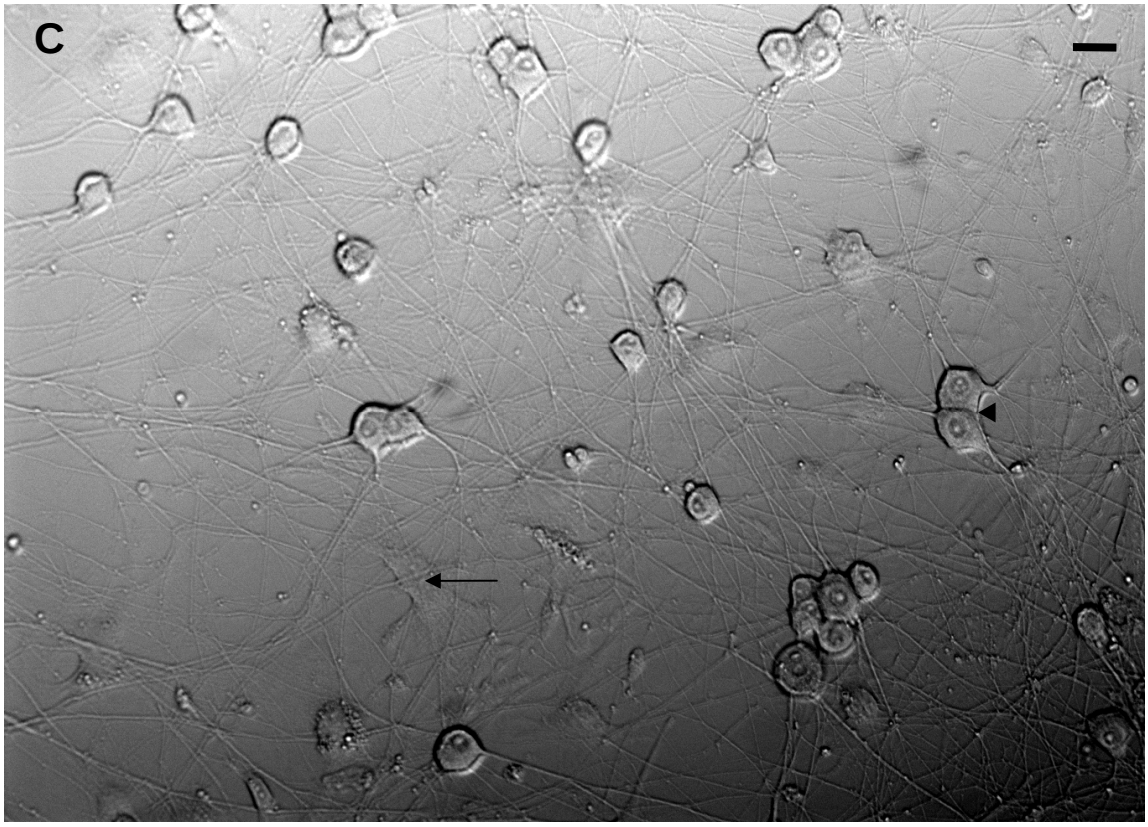

Fig. 3.1 Visualisation of the morphology of sensory neurons in cultured TGNs. *Cell cultures from (A) rat (P5) at 1DIV, (B) rat (P5) and (C) mouse (P5) at 7 DIV were viewed in an inverted Olympus IX71 microscope in phase contrast mode. Compared with 1 DIV, TGNs were enriched at 7DIV. Neuronal cells are indicated by arrow heads, A respresentive astrocyte is indicated by arrows, and a satellite cell is circled. Scale bar, 30 µm.*

3.2.2.2 Rat cultured TGNs display characteristics of sensory neurons: nociceptive markers and pain mediators

3.2.2.2.1 A large proportion of DAPI-stained cells are immuno-stained for NF-200 indicating enrichments for the neuron cells at DIV 5-7

NF-200 is a phosphorylated heavy chain of neurofilament, a major marker for neuronal cells. Neurofilament expression is developmentally regulated and all cells containing neuron-specific enolase epitopes also are labelled with NF200 (Trojanowski et al., 1986). A mAb against NF-200 stained both the cell soma and, strikingly, the processes of cultured TGNs (Fig. 3.2). After repetative treatment by Ara-C, there was only very limited contamination by non-neuronal cells, which cannot be totally removed by addition of anti-mototic regent because they proliferate slowly.

3.2.2.2.2 CGRP

The presence of a major pain-mediating peptide, CGRP, in most of the cells in TGN cultures was demonstrated by immuno-fluorescent microscopy and counter-staining with DAPI (Fig. 3.3). Striking punctate staining by a specific polyclonal antibody against CGRP was visualized on cell plasmalemma and along the fibres.

3.2.2.2.3 SP co-occurs with CGRP

Another pain peptide, SP, was found to co-occur with CGRP in cultured TGNs using a fluorescent inverted microscope (Fig. 3.4 A, B) and by confocal microscopy (Fig. 3.4 C, D, E). Both demonstrated predominant staining of the cell bodies with a mAb specific for SP and a polyclonal antibody against CGRP (as in Fig. 3.3) and less intense labelling of the extensive neurites. Confocal microscopy confirmed punctate staining for the two peptides throughout the cytoplasm and adjacent to the plasma membrane of the cell bodies and processes; the merged picture highlights the overlapping, but to some extent distinct, subcellular locations of CGRP and SP.

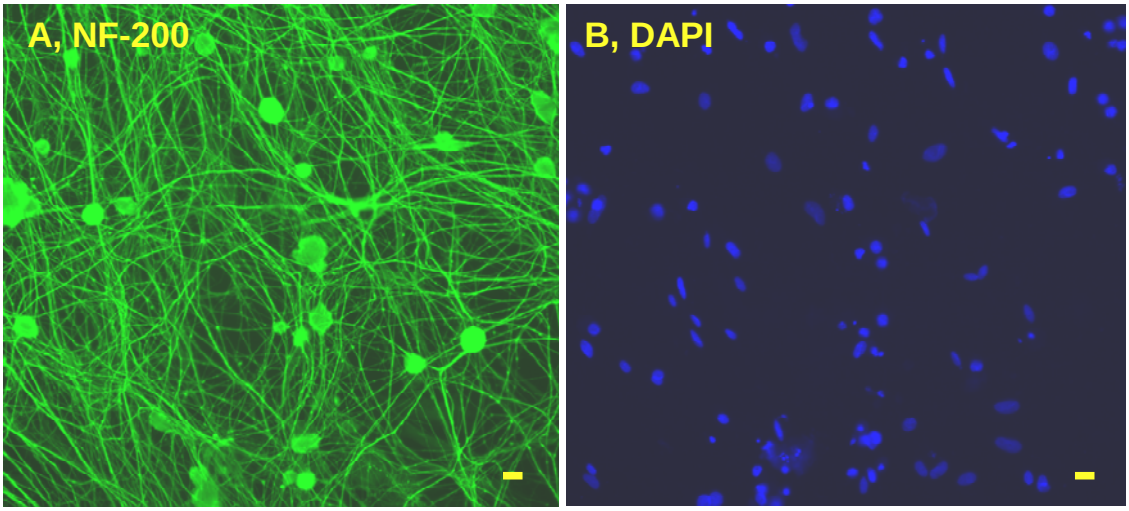

Fig. 3.2 Representative micrographs demonstrating that most of the cultured cells were NF-200 positive, indicative enrichment of neurons at 5 DIV. *Cells were grown on coverslips for 5 DIV, fixed and permeabilised prior to labelling overnight at 4 ºC with (A) mouse anti-NF-200 (1:500), followed by goat anti-mouse Alexa Fluor-488 (1:200) for 1 hour at room temperature. (B) Samples were counter-stained by DAPI before being mounted onto slides and viewed in an inverted microscope under fluorescent mode. Scale bar, 30 µm.*

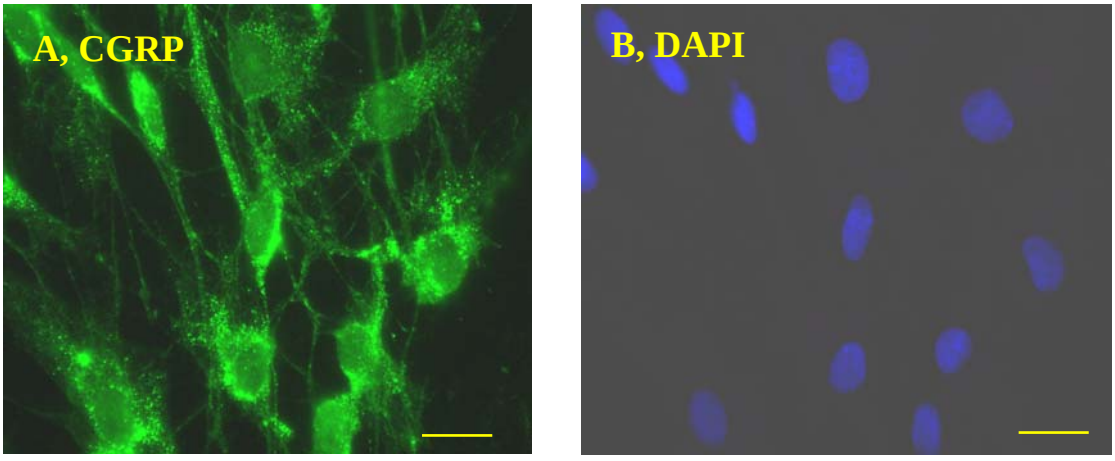

Fig. 3.3 Visualisation of CGRP immunoreactivity in cultured TGNs. *Rat TGNs grown on coverslips for 7 DIV were fixed, permeabilised and stained by rabbit anti-CGRP antibody (1:500) (A) , followed by fluorescently-labelled secondary goat anti-rabbit Alexa Fluor-448 (1:200); the specimens were counter-stained with DAPI (B) before samples were viewed in an inverted microscope in fluorescent mode. Scale bar, 20µm.*

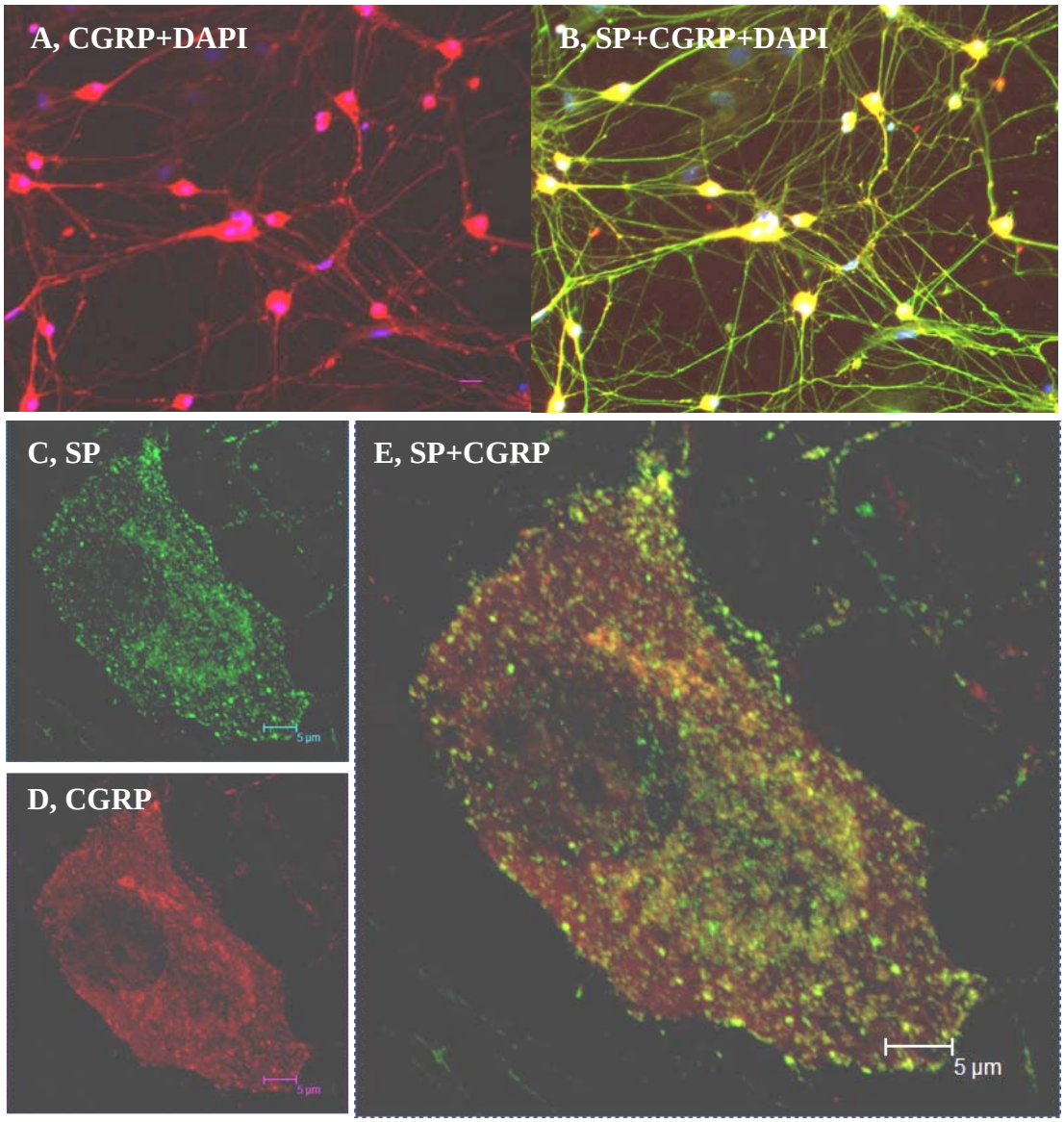

Fig. 3.4 Visualisation of CGRP and SP immunoreactivity in rat cultured TGNs. *CGRP and SP appeared to occur in the same neurons when visulaised under low-magnification microscopy (A, B) but confocal microscopy revealed some distinct distribution (C, D, E). Mouse mAb against SP (1:1000) (B, C, E) followed by goat anti-mouse Alexa Fluor-488 (1:200), and rabbit polyconal antibody against CGRP (1:200) (A, B, D, E) followed by goat anti-rabbit Alexa Fluor-546 (1:200), were applied. DAPI was used to counter-stain (A, B). Scale bars, 20µm (A, B) and 5µm (C-E).*

3.2.2.2.4 Vanilloid receptor type 1(VR1) - capsaicin receptor

The TGNs exihibited characteristics of differentiated pain sensory cells, as reflected by the staining patterns observed with antibodies to specific sensory markers. An antibody specific for VR1 — a vanilloid receptor type 1 which is responsive to capsaicin and occurs in peptidergic C fibres (Caterina et al., 1997) — labelled a majority of the rat neurons (Fig. 3.5). VR1 immunoreactivity resided predominantly on the cell bodies and to a much lesser extent on fibres.

3.2.2.2.5 VR1 and bradykinin receptor type 2 (BR2)

Another sensory marker, BR2 — a G protein-coupled receptor known to occur in nociceptive neurons (Steranka et al., 1988) — was detected in the VR1-positive cells, by labelling with a selective antibody (Fig. 3.6). Notably, the immunoreactivity appeared strongest in patches on the neurons (Fig. 3.6 B, C). Confocal microscopy clearly demonstrated BR2 protein located in a specific region (vascular-like distribution) and to a much lesser extent in the rest of cell membrane and cytoplasm (Fig. 3.6 E, G).

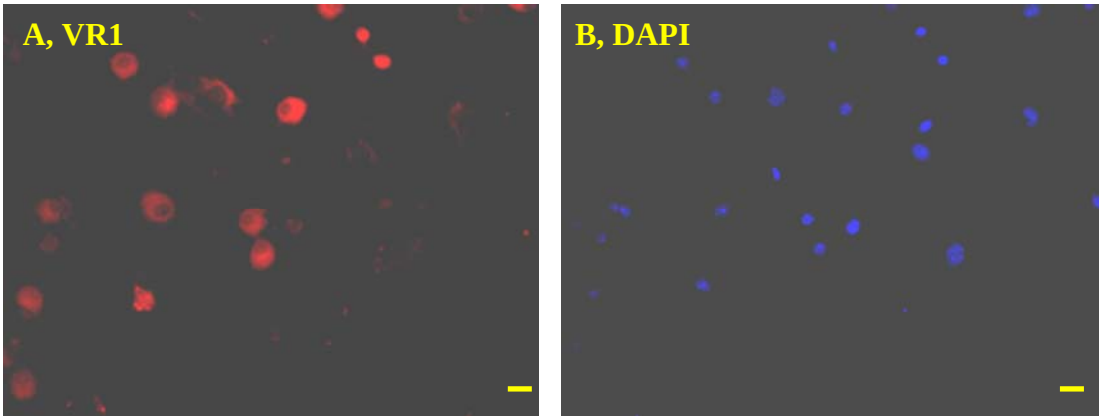

Fig 3.5 Visualisation of VR1 immunoreactivity in rat cultured TGNs. *TGNs grown on coverslips at 7 DIV were fixed, permeabilised and stained with rabbit anti-VR1 (1:1000) (A) followed by a fluorescently-labelled secondary goat anti-rabbit Alexa Fluor-546 (1:200); the specimens were counter-stained with DAPI (B) before viewing under low-magnification fluorescent microscopy. Scale bar, 30µm.*

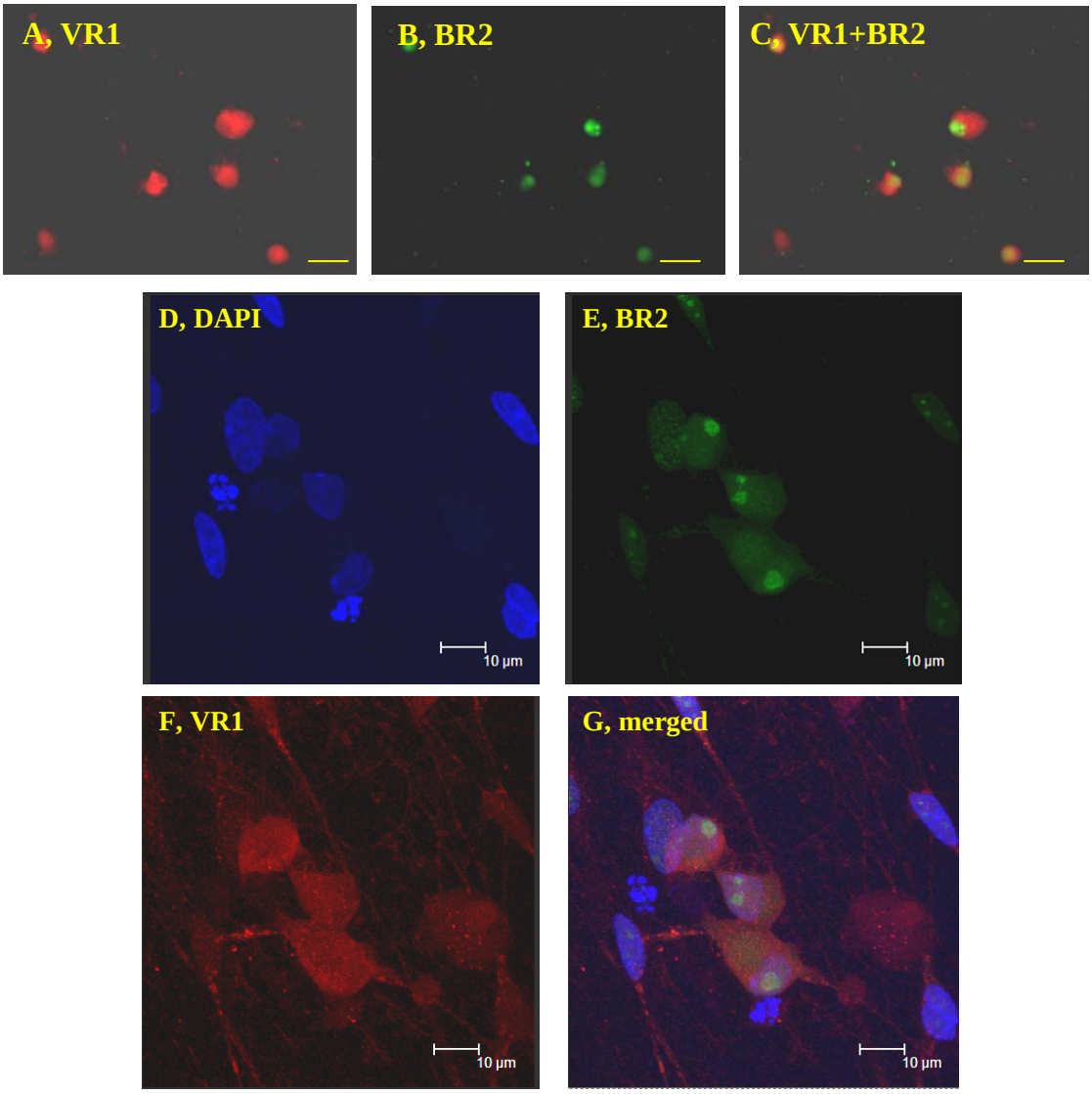

Fig. 3.6 BR2 expressed in many of VR1-positive neurons visualised by immunofluorescent microscopy. *Samples were viewed with an inverted microscope in fluorescent mode (A-C) or by confocal microscopy (D-G). Cells grown on coverslips at 7 DIV were fixed, permeabilised and stained with: rabbit anti-VR1 (1:1000) (A, C, F, G) followed by goat anti-rabbit Alexa Fluor-546 (1:200) or mAb against BR2 (1:500) (B, C, E, G) followed by goat anti-mouse Alexa Fluor-488 (1:200). The specimens were counter-stained with DAPI (D, G). Scale bars, 25µm (A-C) and 10µm (D-G).*

3.2.2.2.6 IB_4 binding and DAPI staining

Another nociceptive sensory neuron marker is revealed by a fluorescent conjugate of IB_4, an isolectin that binds to small nociceptive neurons in C fibres (Guo et al., 1999). It stained most of the cells counterstained by DAPI (Fig. 3.7); these are irregular in shape and vary in size. It has been suggested that IB_4-positive nociceptors mediate neuropathic pain, whereas IB_4-negative nociceptors mediate inflammatory pain. More evidence is needed to support this theory (Stucky et al., 2002).

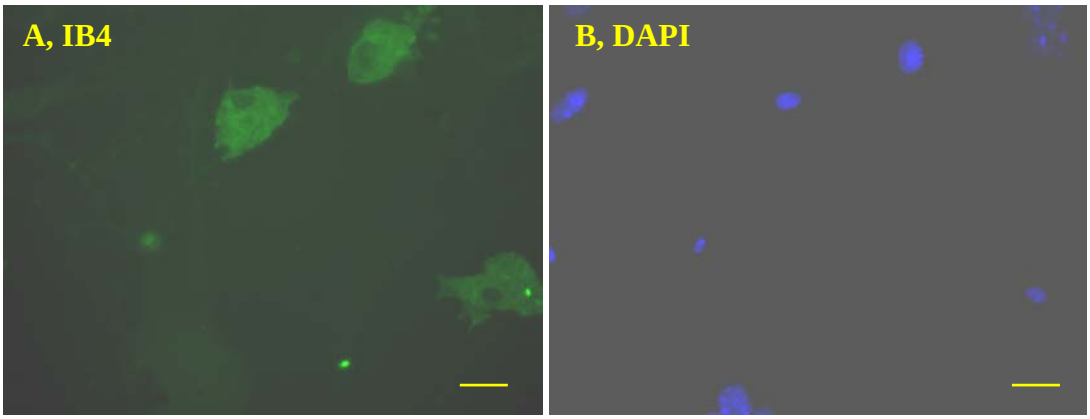

Fig 3.7 Fluorescence staining of IB_4 binding neurons. *Rat cultured TGNs at 7 DIV were fixed by 3.7% paraformadelhyde in CMF-PBS for 20 minutes at room temperature, followed by rinsing for 3 times with PBS. Staining was performed by 4 μg/ml FITC-IB_4 (A) in 0.1 M phosphate buffer (see Chapter 2), 0.1 mM $CaCl_2$, 0.1 mM $MgCl_2$, 0.1 mM $MnCl_2$ for 1 hour at room temperature. DAPI was applied for 5 minutes to counter-stain the samples (B). Specimens were viewed in an inverted microscope in fluorescent mode. Scale bar, 20μm.*

3.2.2.3 Sensory peptidergic TGNs contain all 3 SNAREs (SNAP-25, syntaxin, and Sbr) and synaptotagmin I/II which largely co-localise with CGRP

3.2.2.3.1 SNAP-25, SNAP-25 and CGRP, SNAP-25 and VR1

With regard to the molecular machinery underlying the regulated release of pain-peptides, it was important to identify the key isoforms of SNAREs and SNARE-related proteins present in sensory neurons, especially because of these being related to the sensitivity to BoNTs. Lower magnification micrographs showed that the majority of neurons were stained with a specific antibody against SNAP-25 (Fig. 3.8 A), a target substrate of BoNT/A and /E. SNAP-25 co-staining with CGRP could be visualised by confocal immuno-microscopy (Fig. 3.8 B). Labelling of SNAP-25 appeared on the membrane of cell bodies, axons (broad) and dendrites (fine); also, punctate staining was visible in the cytoplasm. Dual-labelling of VR1 and SNAP-25 indicated nearly all the VR1-positive cells express SNAP-25 (Fig. 3.8 C).

3.2.2.3.2 Syntaxin isoforms I, II, and III are expressed in TGNs

In rat synaptosomes, syntaxin I, II and III are known to be cleaved by BoNT/C1 (Schiavo et al., 1995). However, the presence of these proteins in nociceptive sensory neurons and their functions in pain-related peptides release are not clear. Herein, using immunofluorescence staining with isoform specific antibodies, it was demonstrated that these three isoforms are expressed in cultured TGNs.

3.2.2.3.2.1 Syntaxin I and CGRP

Labelling of the other t-SNARE, syntaxin I with a specific mAb gave a similar pattern of staining to that observed for SNAP-25. Lower magnification immunofluorescence micrographs demonstrated a majority of DAPI-stained cells expressing syntaxin I (Fig. 3.9 A). However, immunoreactivity towards syntaxin I seemed stronger in certain cells and lower in others. Confocal microscope (Fig. 3.9 B) demonstrated that labelling of syntaxin I definitely appeared on the cell membrane as well as processess; also, punctate staining was visualised in the cytoplasm near the nucleus. Clearly, CGRP occurs together with syntaxin I as revealed by dual-labelling (Fig. 3.9 B).

3.2.2.3.2.2 Co-staining of syntaxin II or III with NF-200

The presence of syntaxin II in cultured TGNs was confirmed by immuno-fluorescence microscopy, using a specific antibody against syntaxin II. Similar to syntaxin I, syntaxin II labelling appeared on the membrane of cell bodies, and to a much lesser extent on neurites, which were strongly labelled by NF-200 antibody (Fig. 3.10 A**)**. Syntaxin isoform III was also expressed in TGNs and showed similar distributions as isoform II (Fig. 3.10 B**).**

3.2.2.3.3 Sbr I and CGRP, Sbr II and CGRP

Both of the v-SNARE isoforms, Sbr I and II, which are the substrates of Sbr-cleaving toxins as listed in the Chapter 1, were visualised by low magnification microscope (Fig. 3.11 A), using antibodies selective for each. Focusing on the fine fibres at higher resolution revealed striking punctate labelling which co-localised well with CGRP (Fig. 3.11 A). Confocal microscopy also confirmed Sbr II staining was located predominantly in the cell body with 'vesicular-like' staining visible in the perinuclear area and to a lesser extent along the fibres. Additionally, the extensive network of neurites was clearly labelled (Fig. 3.11 B). Next, it was warranted to define which isoform could be involved in the release of transmitters.

3.2.2.3.4 Synaptotagmin I and CGRP

Finally, using confocal microscope to visualise the vesicle protein synaptotagmin I, a Ca^{2+} sensor whose N-terminal is exposed to the lumen of the synaptic vesicle, binds to SNAP-25 and also serves as a putative high-affinity protein acceptor for BoNT/B and /G. The micrographs showed a striking punctate pattern of staining for synaptotagmin I, both in the cell body and along all the fine processes (Fig. 3.12 A, C). Importantly, dual labelling with antibody reactive towards CGRP (Fig. 3.12 B, C) demonstrated that this protein and CGRP are strongly co-localized (Fig. 3.12 D). This indicates that this Ca^{2+} sensor might be involved in CGRP release.

In conclusion, CGRP occurs together with SNAP-25, syntaxin I, Sbr (I and II) and synaptotagmin I in the rat cultured TGNs. Although most of the cells became stained with all of these antibodies, some differences were apparent in the relative labelling intensity for CGRP and each of these proteins in individual neurons. The striking similarities apparent in the distribution patterns for Sbr I, synaptotagmin I and CGRP

are suggestive of functional implications (see later). These collective findings highlight that all 3 SNAREs and the putative Ca^{2+} sensor, synaptotagmin I, occur in CGRP-containing sensory neurons that, also, usually possess SP.

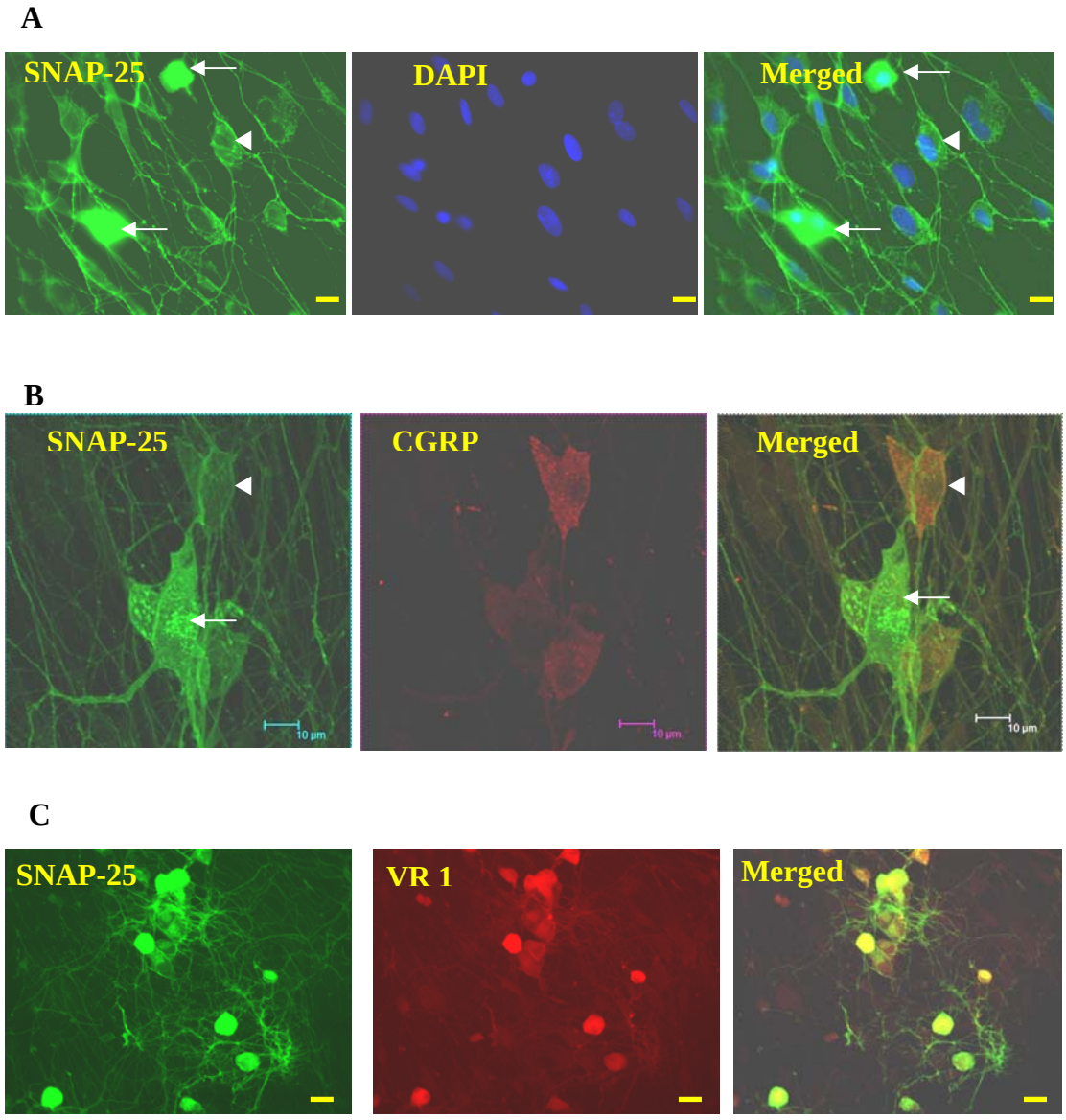

Fig. 3.8 Microscopic demonstration that SNAP-25 co-occurs with CGRP or VR1 in rat cultured TGNs*. Cells were grown on coverslips for 7 DIV, fixed and permeabilised prior to labelling with specific primary and secondary antibodies. (A) Mouse anti-SNAP-25 (1:500) and goat anti-mouse Alexa Fluor-488 (1:200) followed by counter-staining with DAPI; (B) mouse anti-SNAP-25 (1:500) (and goat anti-mouse Alexa Fluor-488 (1:200) and rabbit anti-CGRP (1:500) (and goat-anti rabbit Alexa Fluor-546 (1:200); (C) mouse anti-SNAP-25 (1:500) (and goat anti-mouse Alexa Fluor-488 (1:200)) and rabbit anti-VR1 (1:1000) (and goat-anti rabbit Alexa Fluor-546 (1:200). Normal (A, C) or confocal (B) fluorescent microscopes were taken. Merged images were shown at the right hand end of each panel. Notablly, immunoreactivity of SNAP-25 seemed higher in certain cells (arrows) and lower in others (arrow heads). Scale bars, 15µm (A, C) and 10µm (B).*

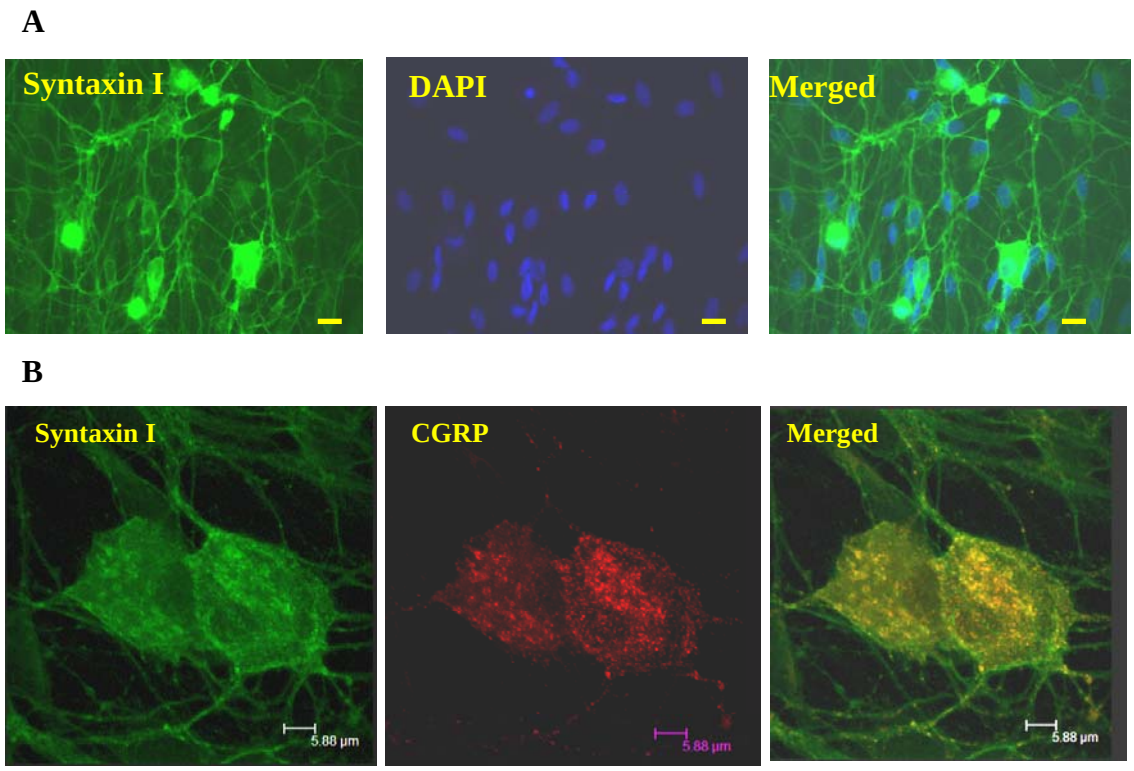

Fig. 3.9 Visualization of the presence of syntaxin I in rat TGNs together with CGRP. *Normal (A) or confocal immuno-fluorescence miscroscopy (B) were used to capture the images. Cells grown on coverslipes at 7 DIV were fixed, permeabilised and labelled with specific antibodies against (A) syntaxin I (1:500) followed by goat anti-mouse Alexa Fluor-488 (1:200) and counter-stained by DAPI, or (B) syntaxin I (1:500) (and goat anti-mouse Alexa Fluor-488 (1:200)) and CGRP (1:500) (and goat-anti rabbit Alexa Fluor-546 (1:200)). Scale bars, 15µm (A) and 5.88 µm (B).*

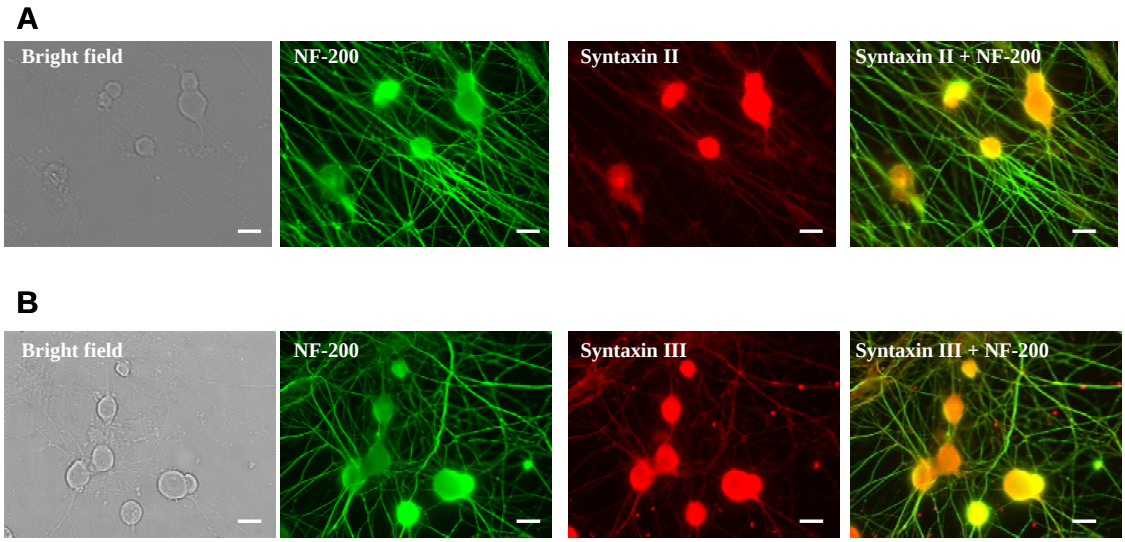

Fig. 3.10 Microscopic demonstration of the presence of syntaxin II and III in rat cultured TGNs. *The cells were grown on coverslips for 7 DIV, fixed and permeabalised prior to labelling with rabbit IgGs against (A) syntaxin II (1:1000) or (B) syntaxin III (1:1000) (and goat-anti rabbit Alexa Fluor-546 (1:200)) or mouse anti-NF-200 (1:200) (and goat anti-mouse Alex Fluor-488 (1:200)). Samples were viewed in an inverted microscope in phase contrast and fluorescent mode, as indicated in pictures. Syntaixn II and III labelling appeared predominantly on the neuron cell bodies and to a much lesser extent in processes. Scale bar, 20µm.*

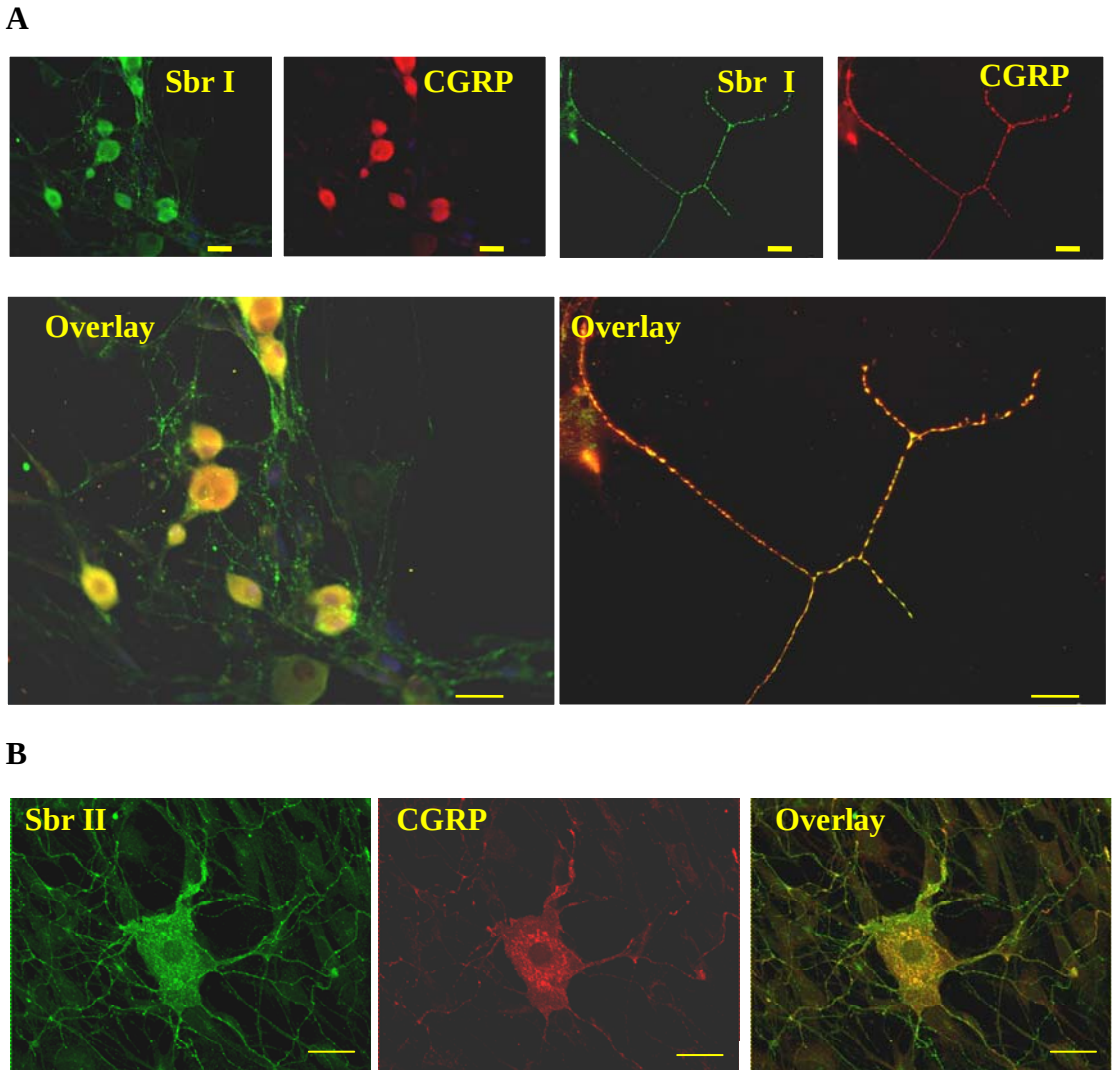

Fig. 3.11 Representative fluorescence micrographs showing the presence of Sbr I and II in CGRP-containing rat cultured TGNs. *Cells grown on coverslips for 7 DIV were fixed and permeabilised before staining with (A) rabbit anti-Sbr I (1:1000) (and donkey anti-rabbit IgG Cy2, 1:200), and mouse anti-CGRP (1:500) (and donkey anti-mouse IgG Cy3, 1:800) followed by counter-stained with DAPI or (B) rabbit anti-Sbr II (1:1000) and mouse anti-CGRP (1:500) followed by fluorescently-conjugated secondary antibodies, as used in (A). Specimens were viewed in a normal (A) or confocal miscroscopy (B). Scale bars, 20µm (A) or 30 µm (B).*

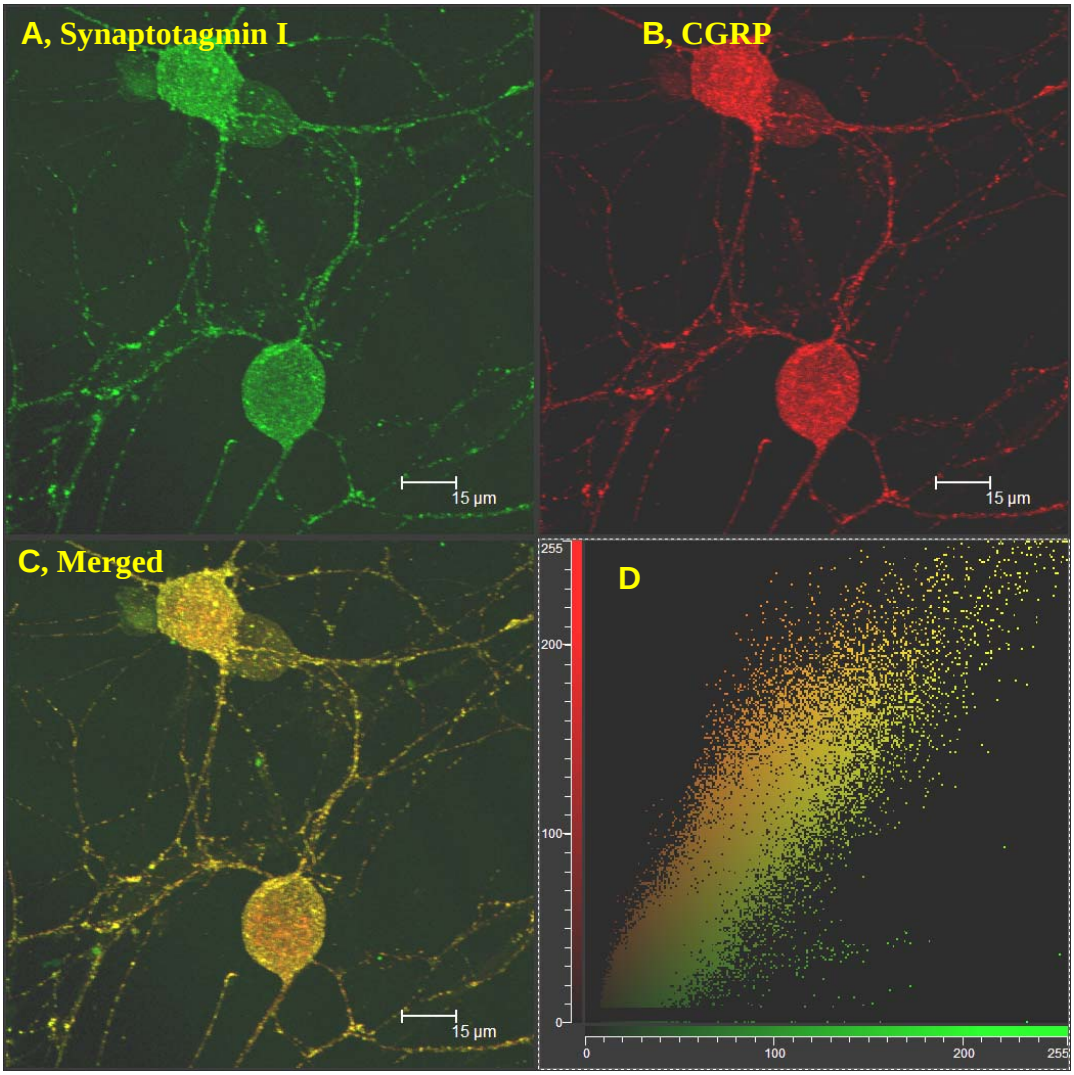

Fig. 3.12 Visualization of the punctate co-staining of synaptotagmin I and CGRP in rat cultured TGNs. *Cells grown on coverslips for 7 DIV were fixed and permeabilised before labelling with Mab against the lumenal domain of (A) synaptotagmin I (1:1000) followed by goat anti-mouse Alexa Fluor-488 (1:200), or (B) rabbit antibody against CGRP (1:500) followed by goat anti-rabbit Alexa Fluor-546 (1:200). (C) Merged picture showing overlapped signals. (D) The axes represent density of each fluorescent signal and the analysis graph shows the extent of co-localization of two fluorescence signals. Scale bar, 15µm.*

3.2.3 Evoked-release of neurotransmitters from rat cultured TGNs

3.2.3.1 K^+ depolarisation-, capsaicin- or bradykinin-elicited release of CGRP and SP from cultured TGNs are Ca^{2+}-dependent and show different levels

After culturing TGNs for 7 days, the amounts of CGRP released under basal and stimulated conditions were quantified by EIA. The optimal stimulation time was 30 minutes (Fig. 3.13 A). A minimal quantity of 'resting' release occurred in 3.5 mM K^+/2.5 mM Ca^{2+} compared to the amounts evoked by elevated [K^+], 60 mM K^+ giving an optimal ~ 14-fold increase over the basal level (Fig. 3.13 B). Nearly all of this increment could be prevented by removal of Ca^{2+} from the external medium (Fig 3.13 B), demonstrating a Ca^{2+}-dependency. Likewise, K^+ depolarisation-evoked SP release is also Ca^{2+}-dependent but the extent of this increment (2.5-fold over basal) was much lower than that for CGRP (Fig. 3.13 C). Consistent with TGNs containing the VR1 protein (demonstrated earlier), capsaicin-triggered CGRP release was Ca^{2+}-dependent; 1 μM gave a maximum of 3.3-times increment over basal (Fig. 3.14 A). Consistent with the occurrence of BR2 protein in the TGNs described earlier, bradykinin stimulated CGRP release is also Ca^{2+}-dependent (Fig. 3.14 B). A maximum increment of 3.9-times over basal was achieved with 0.1 μM bradykinin. Collectively, the stimulation of Ca^{2+}-dependent CGRP release from TGNs by K^+, capsaicin and bradykinin accords with their efficacies in elevating the efflux of peptidergic transmitters in brain, as measured in perfusates (Gazerani et al., 2006).

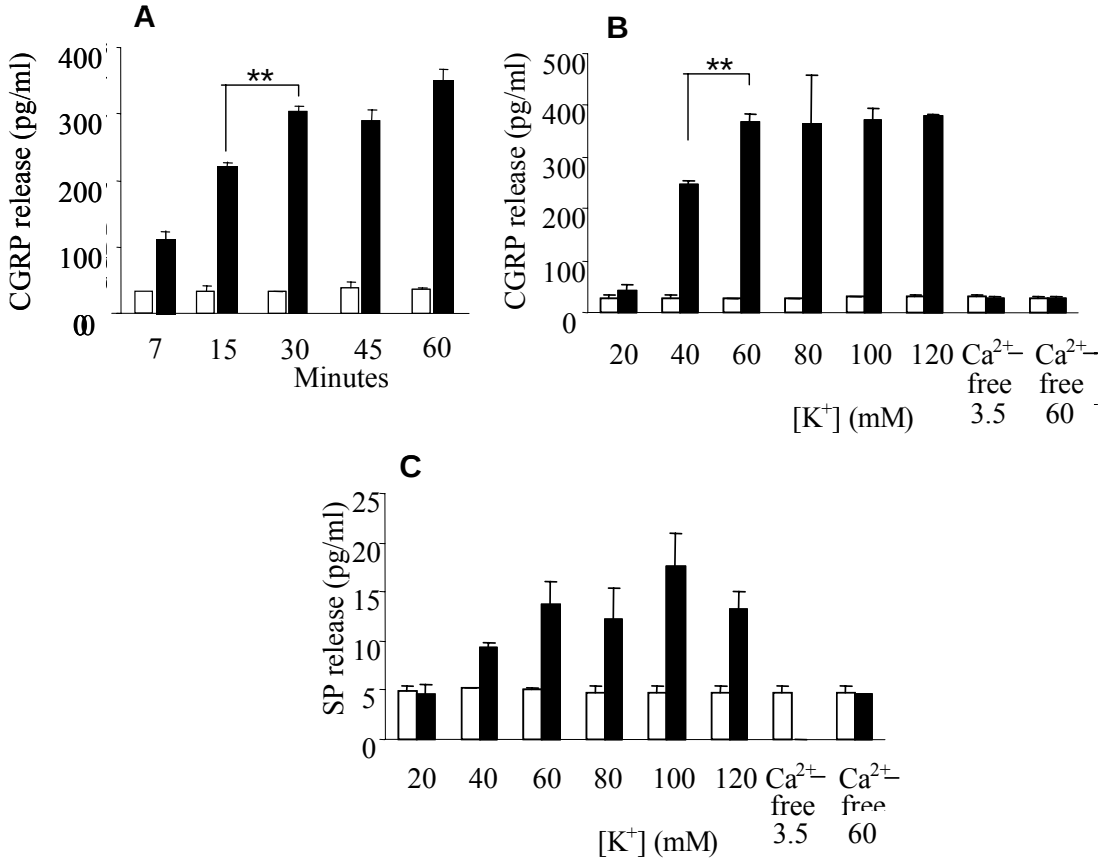

Fig. 3.13 CGRP and SP release evoked by K^+ from TGNs are K^+-concentration and Ca^{2+}-dependent: 30 minutes proved optimal. *After 7 DIV, rat cultured TGNs were incubated in BR-HBS at 37 °C with varying times for basal release (hollow bars) followed by incubation in BR-HBS in the presence of 60 mM of K^+, for the same period as for basal, to stimulate CGRP release. Buffer bathing the cells were carefully removed and quantity of released CGRP was measured by EIA; 30 minutes incubation time proved to be optimal (A). In order to optimize the concentration of K^+ used for stimulation of CGRP (B) or SP release (C), basal release over 30 minutes was measured in BR-HBS (hollow bars), then supplemented with various concentrations of K^+ (isotonically-balanced Na^+ concentration) for the same period as for stimulated release (filled bars). Release stimulated by 60 mM [K^+] represented 30% (CGRP) or 8% (SP) of the total content in cells. Ca^{2+}-independent release was determined using Ca^{2+}-free BR-HBS containing 2 mM EGTA. Data plotted are means ± S.D.; n = 4; student's unpaired t-test: **, $p<0.01$.*

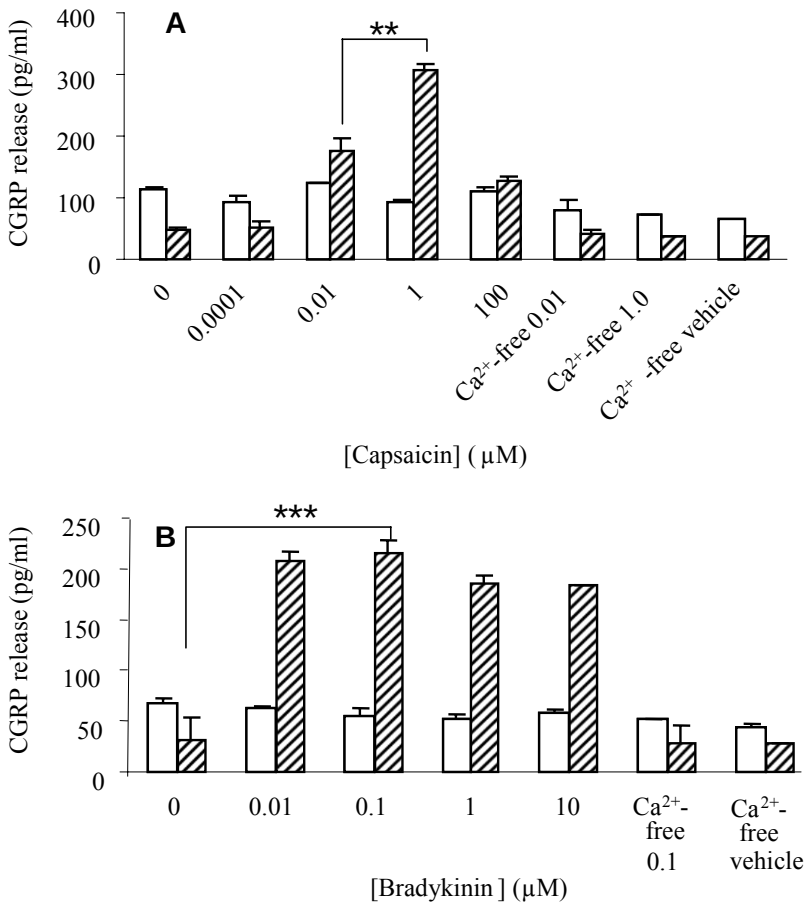

Fig 3.14 CGRP release evoked by capsaicin or bradykinin from TGNs is concentration and Ca^{2+}-dependent. *After 7 DIV, the rat cultured TGNs were incubated in BR-HBS with the addition of vehicle (see Chapter 2) for measurement of basal release (hollow bars), and then incubated in BR-HBS in the presence of varying concentrations of capsaicin (A) or bradykinin (B) for the determination of stimulated release (hatched bars). 1 μM capsaicin- or 0.01 or 0.1 μM bradykinin- stimulated release represents 20 or 15% of the total content, respectively. Likewise, Ca^{2+}-independent release was determined in Ca^{2+}-free BR-HBS containing 2 mM EGTA. Values are the means ± S.D.; n = 4; student's unpaired t-test: **, p<0.01; ***, p<0.001.*

3.2.3.2 Crudely fractionated SP- and CGRP-containing LDCVs showed similar sedimentation velocity and contain SNAREs plus associated proteins

TGs were dissected from ~35 P3-5 neonatal rats and homogenized (see Chapter 2); Microsomes were collected by ultracentrifugation and lysed in resuspension buffer. Vesicles were seperated by continuous sucrose gradient centrifugation according to their density (see Chapter 2). Fractions (600 µl) were collected from the bottom to top of the centrifuge tube using a peristaltic pump. Amounts of SP and CGRP in each fraction were quantified by EIA assay. The neuropeptides-enriched fractions are those with high ratio of peptides concentration relative to total protein concentrations (Fig. 3.15 B). Theortically, SCSVs should be collected in later fractions than LDCVs because they have slower sedimentation. Fractions from no. 5-13 seemed to be enriched in SP (Fig. 3.15 A). The occurrence of both CGRP and SP in fractions 7-10 suggests that at least some of the vesicles containing peptides have similar sedimentation behaviour; possibly, to some extent, both peptides reside in the same vesicles (Fig. 3.15 A, B). Notably, fractionated CGRP level was lower than that of SP; whereas in culture, CGRP was released at higher level than SP (Fig. 3.13). This finding is consistent with that NGF supplementation in culture upregulates CGRP expression (Price et al., 2005). Neurotansmitters in SCSVs fractions could not be detected because of lower content (see Section 3.2.3.3).

The presence of SNAREs and synaptophysin were detected in the collected fractions by SDS-PAGE and Western blotting, using specific antibodies. Note that the Sbr III antibody used was also able to detect isoforms I and II but signals were weaker. It is deduced that synaptophysin, syntaxin I, SNAP-25 and three isoforms of Sbr are all present in the LDCVs fractions (Fig. 3.15 C).

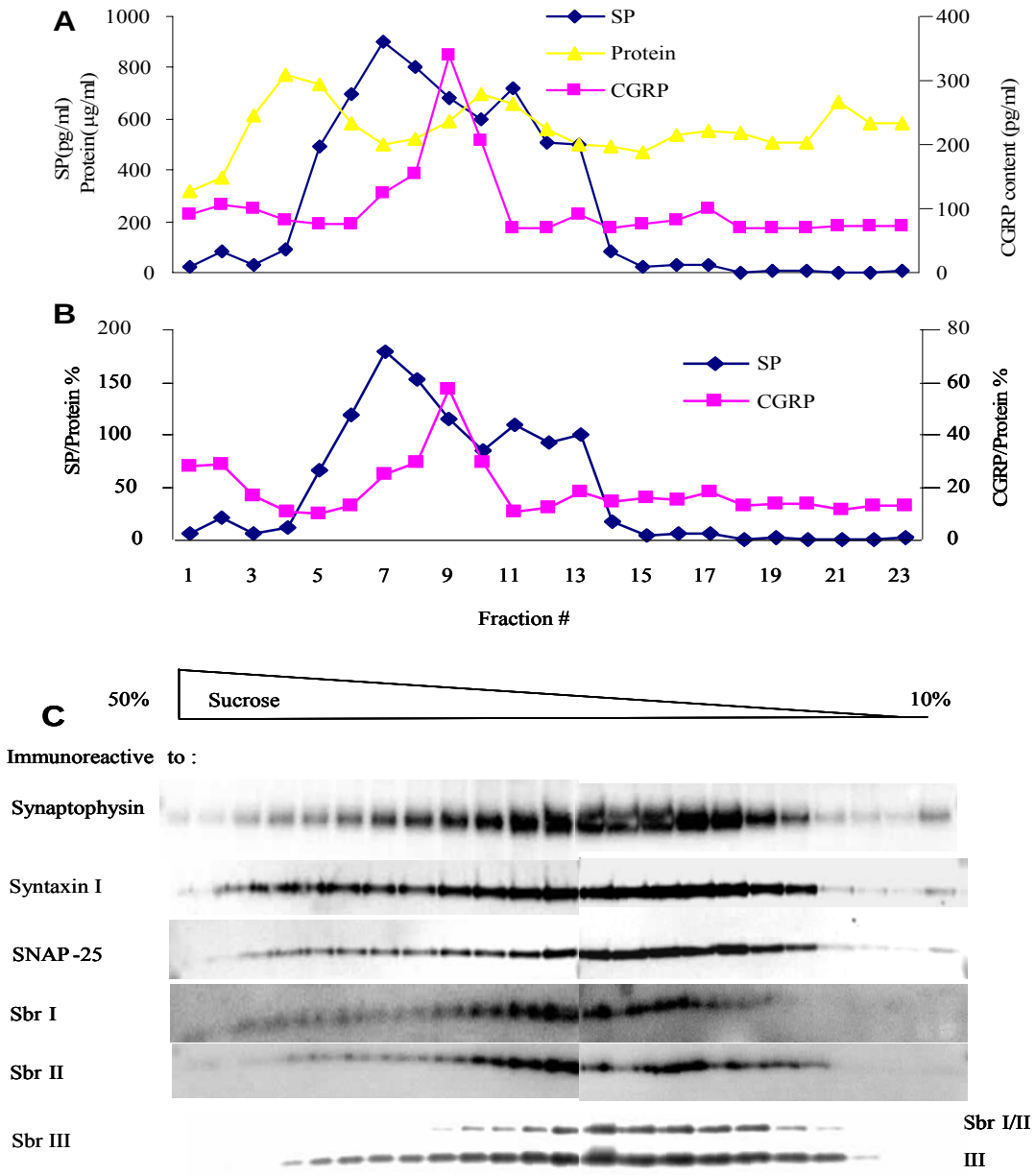

Fig. 3.15 Crude separation of CGRP- and SP-containng LDCVs by sucrose gradient sedimentation. *Microsomes prepared from TGs were lysed in resuspension buffer and layered on a 10-50% continuous sucrose gradient for centrifugation (detailed in Chapter 2). Fractions were collected and analysed for CGRP (pink) and SP (blue) by EIA as shown in (A); the protein concentration of each collected fraction was measured by BCA kit (A, yellow), and ratios % of neuropeptide content relative to protein concentration (pg/µg) was calculated and plotted in (B). Presence of SNAP-25, syntaxin I, Sbr (I, II and III) and synaptophysin in fractions were confirmed by immunoblot analysis in (C) using specific antibodies against synaptophysin, syntaxin I, SNAP-25, Sbr I, II except for a pan antibody used for Sbr III which recogises all three isoforms but with different affinities.*

3.2.3.3 Release of other transmitters from TGNs

Attempts were made to measure additional LDCV-contained transmitters such as NPY, VIP and serotonin by EIA, but their levels of stimulated release from rat cultured TGNs were under the detection limit. Table 3.1 shows the total cellular content of these neurotransmitters in 10^6 cells/well (plating number). It proved difficult to detect stimulated release of classic transmitters (such as glutamate, aspartate, GABA and glycine) from SCSVs by a radioisotopic method, using the same stimulation protocol as for CGRP exocytosis. In conclusion, CGRP and SP are the main transmitters released from cultured TGNs.

Table 3.1 NPY, VIP and serotonin are present at low levels in rat cultured TGNs

Neurotransmitters	**Total content (pg) / 10^6 cells***
NPY	~5
VIP	~20
Serotonin	~10

** ~10^6cells/well of dissociated TGNs were cultured for 7 DIV, solubilised in 2 M acetic acid/ 0.1% TFA followed by freeze/thaw thrice and high speed-vaccum drying. Cell pellets were dissolved in EIA buffer and contents of NPY, VIP and serotonin were measured using EIA (see Chapter 2).*

3.3 Discussion

Deciphering the molecular details of transmitter release from sensory neurons has been neglected, despite its great importance in understanding the propagation of painful stimuli. Also, there is an urgent need for drugs with capabilities to control chronic pain, in a variety of clinical conditions (e.g. migraine, low back pain, tension headache) where existing drugs are not effective in all patients. Lack of progress with investigations is in part due to difficulties in obtaining adequate quantities of pain-propagating cells for biochemical work. This problem was overcome herein by using cultured TGNs which were chosen because they comprise a major pain-relay centre, and their release of CGRP and SP is elevated in migraine (Durham and Russo, 1999; Liu et al., 2003). The model was validated by showing that TGNs maintained in culture retain the morphological and histochemical properties reported for sensory neurons *in situ* (Baccaglini and Hogan, 1983; Guo et al., 1999; Price et al., 2005), as well as an

ability to release peptidergic transmitters in a Ca^{2+}-dependent manner in response to different stimuli. However, the proportion of neurons in the cultures staining positive for VR1 and CGRP is higher than those observed in sections of TG (Durham and Cady, 2004; Price et al., 2005); such a difference has been attributed to their upregulation by NGF added to the culture medium (Durham and Cady, 2004). In fact, this can be viewed as making the TGN model more similar to the situation in migraine in which there is also an increase in the level of NGF (Durham and Cady, 2004). Such elevation is known to be involved in the development of nociceptive sensitization in a number of pathological states; NGF raises the sensitivity of sensory neurons to capsaicin and enhances its stimulation of CGRP release from TGNs *in vitro* (Price et al., 2005). Likewise, NGF raises the response to bradykinin of capsaicin-sensitive small neurons cultured from rat dorsal root ganglia (Kasai et al., 1998). Virtually all of the neurons identified by fluorescence microscopy to contain CGRP also possessed SP. The higher resolution offered by confocal microscopy revealed that the intracellular distribution of both peptidergic transmitters overlapped but were distinct in some respects. For example, an area resembling the endoplasmic reticulum/ Golgi network showed dual staining; on the other hand, SP occurred along the plasmalemma whereas CGRP seemed to have a more diffuse but 'vesicle-like' distribution. The latter indicates that these two peptides do not reside in the same vesicles at least to some extent, in accordance with the report that CGRP occurs only in LDCVs whilst SP can also exist in smaller vesicles from spinal cord sensory neurons (De Biasi and Rustioni, 1988; O'Connor and van der Kooy, 1988). Sucrose gradient centrifugation further suggested CGRP and SP had a similar sedimentation pattern but with some dissimilarity indicating not all of them reside in the same vesicles.

A prime objective of our investigation was to find agents capable of blocking the evoked release of CGRP because of its pivotal role as a pain mediator. This required firstly establishing the complement of SNAREs in these sensory neurons, and then identifying which isoforms are involved in their release from LDCVs, compared to those known to mediate exocytosis from SCSVs.

For the first time, all 3 SNAREs and synaptotagmin I were visualised in the sensory neurons by confocal microscopy. Each displayed some characteristic distribution features. For example, syntaxin I staining gave a 'cloud-like' appearance throughout the soma together with more defined labelling in the bigger neurites; syntaxin II, III also gave a similar pattern in neuronal cell bodies and comparably weaker signals in

neurites, as revealed by conventional fluorescent microscopy. SNAP-25 showed a similar pattern but with intracellular punctate staining and definite labelling of the membrane of the cell bodies and major processes. Finally, similar pictures were obtained for the vesicular proteins, Sbr II and synaptotagmin I, which included intense and fairly uniform staining of the cell bodies as well as punctate deposition of stain on even the smallest neurites. Isoform I of Sbr was visualized predominantly on the cell bodies together with a distinctive punctate pattern of staining on the fine neurites. Most importantly, conventional microscopy demonstrated co-occurrence of each of the exocytotic proteins with CGRP, and images with high resolution revealed some similarities and differences in their subcellular locations. Puncate staining of Sbr I co-localised with CGRP on the fine fibres; in the case of Sbr II and synaptotagmin I, there is a striking degree of co-localisation whereas the granular band of CGRP staining of Sbr isoform II differs from the more widespread distribution of synaptotagmin I in the cytoplasm and on the plasmalemma. Notably, there is a differential intensity of the relative staining for SNAP-25 and CGRP in adjacent neurons. In summary, these sensory neurons possess several components of the exocytotic machinery though the requirement for each, or a particular isoform, had to be established by other means.

A large increment of Ca^{2+}-dependent CGRP release could be evoked by all three stimuli tested, with a rank order of K^{+}> capsaicin > bradykinin; the respective values represents 30, 20, and 15 % of the total content. These figures suggest that some stimulants can only trigger the release of a limited pool of transmitter, in keeping with different signalling pathways being involved. In this regard, it is notable that the quantities of CGRP release elicited by capsaicin or bradykinin relative to that for K^{+} depolarisation approximate to the respective proportions of the cultured cells shown to contain VR1 and BR2, which overlapped as assessed by immunofluorescence staining. SP release was also detected from rat cultured TGNs but at a lower level.

Clearly, sensory peptidergic neurons cultured from rat TGs contain the exocytotic machinery and release CGRP in response to depolarization or pain stimuli. However, involvement of SNARE proteins, and particular isoforms, in Ca^{+}-regulated CGRP release needs to be established by using BoNTs, which are known to cleave distinct SNARE substrates and inhibit transmitters release in a number of neuron types. *In vitro,* cultured TGNs with their highly desirable properties used in combination with

recombinant BoNT make it feasible to examine the basic mechanisms of pain transmission.

4.0 CGRP exocytosis from sensory neurons is SNARE-dependent and unique in requiring Sbr I: inhibition by BoNTs reflects their anti-nociceptive potential

4.1 Overview

Although BoNTs have proved instrumental in demonstrating that all three SNAREs are essential for Ca^{2+}-regulated exocytosis in a number of neuron types, this remains to be established for cultured TGNs. As stimulation of neurotransmitter release by K^+, capsaicin and bradykinin relies on somewhat different signalling mechanisms and in the two latter cases, occur in sub-populations possessing VR1 or BR2, determining their susceptibilities to BoNT serotypes is a prerequisite for the attractive prospect of engineering a variant that could be targeted and, thus, preferentially inhibit CGRP secretion in certain varieties of sensory neurons.

4.2 Results

4.2.1 Truncation of SNAP-25 by BoNT/A gives distinct inhibition of CGRP release evoked by 3 stimuli

TGNs were incubated overnight at 37°C with BoNT/A and Ca^{2+}-dependent CGRP secretion was measured in response to different stimuli, before the same cells were solubilised and subjected to SDS-PAGE and Western blotting of the SNAREs. SNAP-25 was detected with an antibody exhibiting equal reactivity with both the intact and the toxin-truncated SNARE (Fig. 4.1 A). Increasing BoNT/A concentrations cleaved SNAP-25 as reflected by appearance of a faster-migrating product, giving an EC_{50} = 0.3 nM derived from densitometric scanning of 5 replicate gels (Fig. 4.1 B). Only trace amounts of the BoNT/A-resistant homologue, SNAP-23, could be visualised (Fig. 4.1 C). K^+-evoked CGRP release was inhibited by BoNT/A with a concentration dependence identical to that for SNAP-25 cleavage (Fig. 4.1 B). By contrast, it proved less potent in blocking exocytosis elicited by bradykinin (Fig. 4.1 B). The CGRP release elicited by 1μM capsaicin was least susceptible to BoNT/A, with only ~ 15% reduction seen even at 100 nM toxin (Fig. 4.1 B); this minimal sensitivity is not attributable to lack of the receptors on these particular neurons because synaptic vesicle protein 2A, B and C were detected in VR1-positive cells (Fig. 4.1 D; see Discussion). Morever, K^+-evoked SP release, assayed in an aliquot of the sample used for measuring CGRP release, was also blocked by BoNT/A (Fig. 4.1 B inset). Such disparate BoNT/A susceptibilities of neuro-exocytosis triggered by various stimuli differ from the rank order observed for type D (see later).

Fig. 4.1. BoNT/A cleaves SNAP-25 and differentially inhibits Ca^{2+}-dependent CGRP release evoked from rat TGNs by three stimuli: the toxin's acceptors occur on VR1-positive cells. *TGNs were exposed to BoNT/A, release of CGRP over 30 minutes assayed; then the cells were solubilized in LDS-sample buffer and equal volumes subjected to SDS-PAGE and Western blotting, using an antibody that recognises intact and truncated SNAP-25. The proportion of substrate remaining was calculated relative to an internal syntaxin control, using digital images of the gels. (A) Immunoblot showing the cleavage by the neurotoxin of SNAP-25 but not syntaxin I. (B). Dose response curvse for BoNT/A-induced blockade of CGRP release evoked by 60 mM K^+ (■) which correlates with the % of SNAP-25 remaining (▼). Lesser extents of inhibition by BoNT/A were observed for release evoked by 0.1 μM bradykinin (▲) and, especially, 1 μM capsaicin (●). Data plotted are means ± s.e.m.; n = 5. Inset shows inhibition of 60 mM K^+-evoked SP release by 0.1 nM BoNT/A (data plotted are means ± s.e.m.; n = 3). Note, there was no detectable SP release evoked by 60 mM K^+ after treatment with 1 nM. (C) A Western blot of TGNs visualised with antibodies specific for syntaxin I or SNAP-23 (*). (D) Representative micrographs demonstrating VR1 and SV2A, B and C in rat TGNs. Fluorescent images were obtained after labelling the cells with antibodies raised in guinea pig specific for VR 1 (1:1000) and in rabbit for SV2A or SV2B (1:1000) or in goat for SV2C (1:100). The controls were treated similarly except in the absence of primary antibodies but incubated with fluorescently-labelled secondary IgGs against rabbit (goat anti-rabbit Alexa Fluor-546, 1:200) and guinea pig (goat anti-guinea pig Alexa Fluor-488, 1:200) (1) or goat (donkey anti-goat Cy3, 1:800) and guinea pig (donkey anti-guinea pig Cy2, 1:200) (2). Scale bars are 20 μm. It is noteworthy that all the SV2 isoforms are present in VR1-positive neurons.*

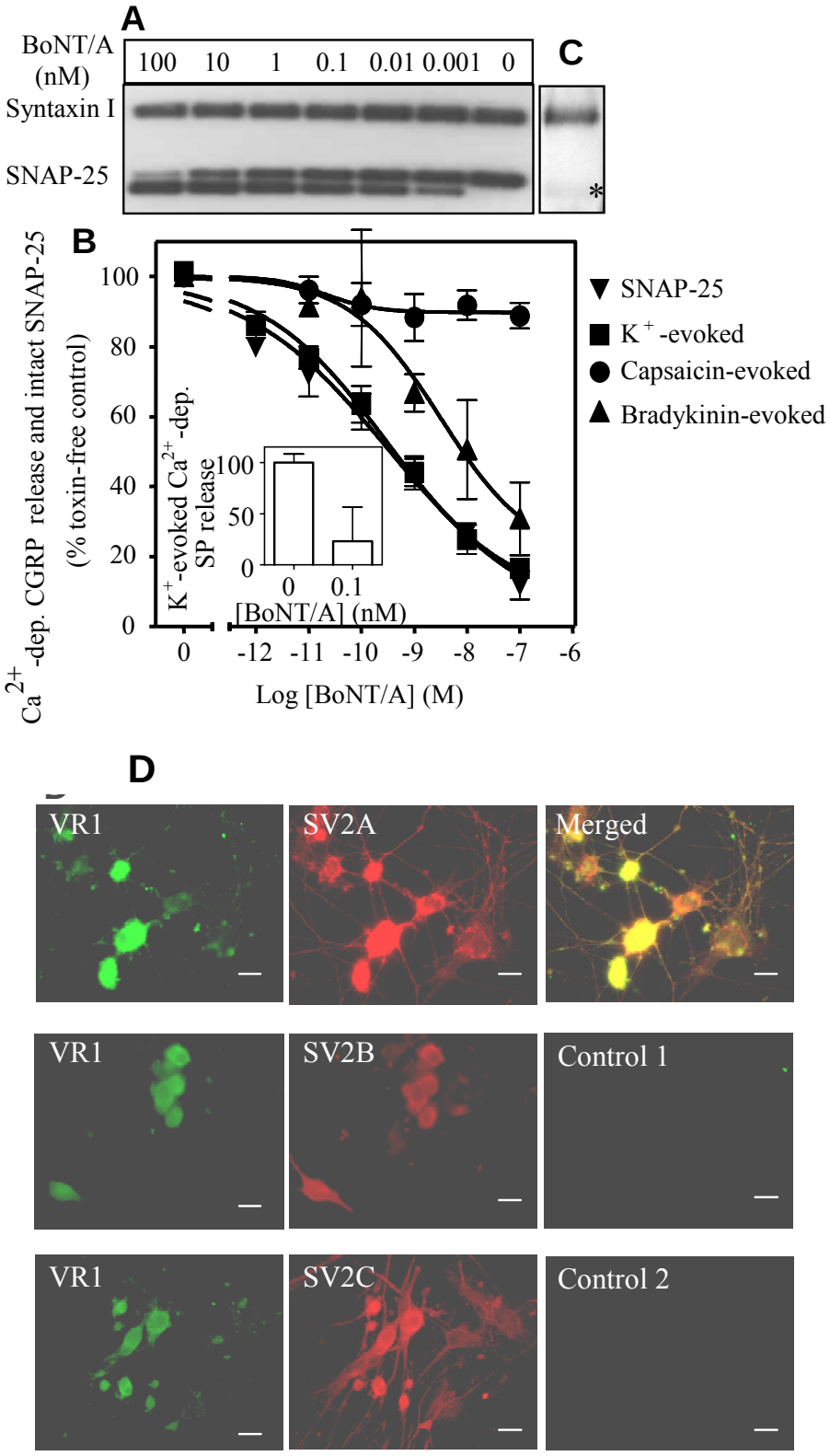
A
BoNT/A (nM)
100 10 1 0.1 0.01 0.001 0
Syntaxin I
SNAP-25
C
*
B
Ca2+-dep. CGRP release and intact SNAP-25 (% toxin-free control)
100
80
60
40
20
0
0 -12 -11 -10 -9 -8 -7 -6
Log [BoNT/A] (M)
K+-evoked Ca2+-dep. SP release
100
50
0
0 0.1
[BoNT/A] (nM)
SNAP-25
K+-evoked
Capsaicin-evoked
Bradykinin-evoked
D
VR1
SV2A
Merged
VR1
SV2B
Control 1
VR1
SV2C
Control 2

4.2.2 Limited cleavage of syntaxin I and SNAP-25 by BoNT/C1 partially blocks exocytosis induced by all the stimuli

Incubation of TGNs with BoNT/C1 (under the conditions outlined above for BoNT/A) resulted in partial cleavage of syntaxins IA and/or IB as indicated by the decreased intensities on the Western blots, stained with a monoclonal antibody reactive with both isoforms of intact syntaxin I which were not resolved (Fig. 4.2 A). Moreover, the toxin also truncated SNAP-25 (Fig. 4.2 A); the dose-response curves, derived from analysis of several blots, are similar for the toxin's partial cleavage of both substrates (Fig. 4.2 B). BoNT/C1 caused a minimal reduction in CGRP exocytosis and with little discrimination between the stimuli used (Fig. 4.2 C). Syntaxin II, III and IV (not shown) were also detected in TGNs by Western blotting but only isoforms II and III are BoNT/C1 sensitive (Schiavo et al., 1995); the limited cleavage was accentuated by the toxin's limited uptake, as reflected in the partial inhibition of CGRP release (Fig. 4.2). Although the function of these syntaxin isoforms in CGRP exocytosis is not clear, the presence of SNARE complexes containing either isoform II or III with SNAP-25, Sbr I or II were demonstrated by co-immunoprecipitation of detergent soluabilized lysate of rat TGNs (Fig. 4.3). Sbr isoforms could be detected after their release from the complexes by boiling; SNAP-25 signal was stronger than that for non-boiled samples. The simplest interpretations of these results are that the native BoNT/C1 has low potentcy or this toxin only enters a fraction of the responsive neurons or all the cells with poor efficiency; the contribution of its cleavage of syntaxin I to CGRP inhibition could not be determined because SNAP-25 also gets truncated.

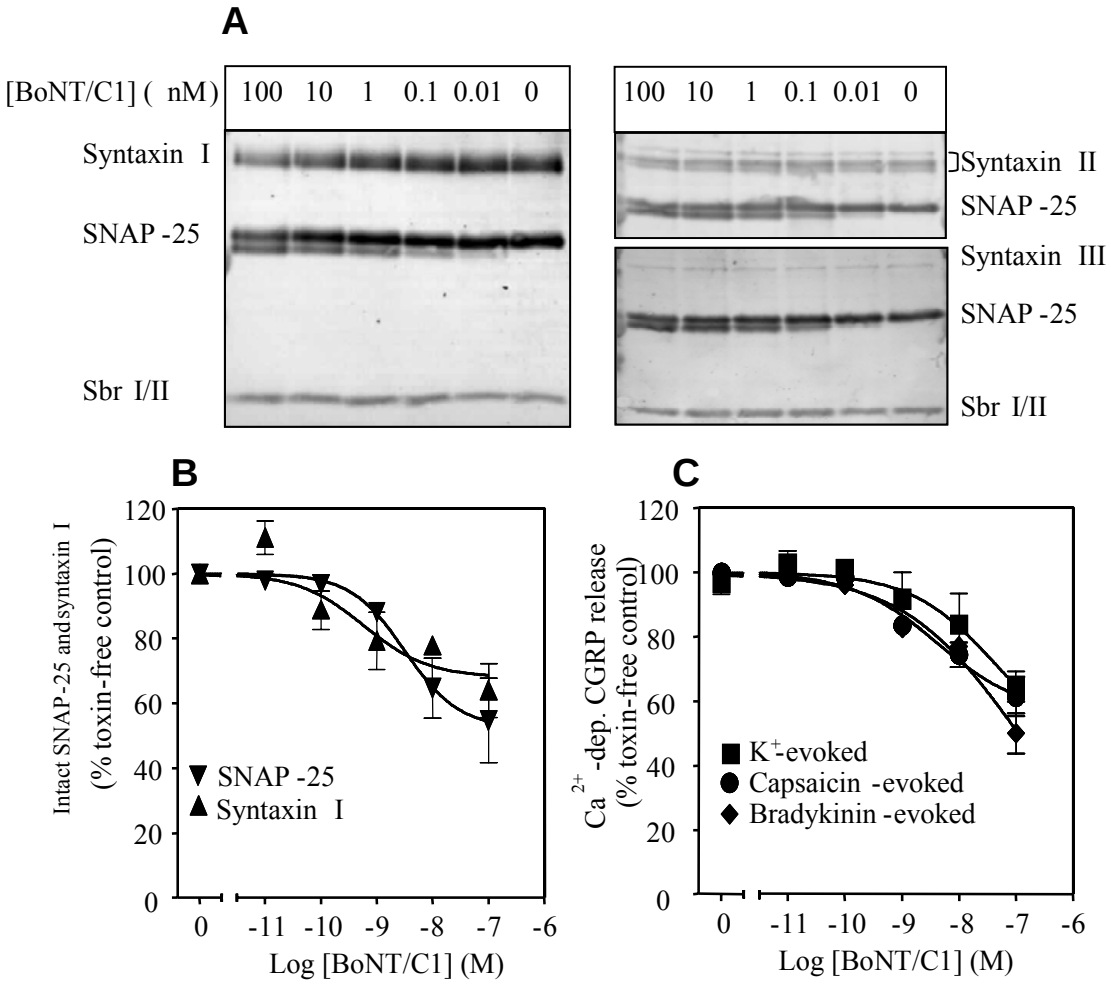

Fig 4.2 BoNT/C1 incompletely cleaves SNAP-25 and syntaxin I, and partially inhibits Ca^{2+}-dependent CGRP release evoked by three stimuli. *TGNs at 7 DIV were treated with BoNT/C1, release of CGRP was assayed and Western blotting performed. Results were calculated as described in Fig. 4.1 A, B but relative to the Sbr I/II control. (A) Partial cleavage of SNAP-25 by BoNT/C1 shown with the IgG used in Fig. 4.1, and decrease in syntaxin I revealed with an antibody only reactive with this intact SNARE. Syntaxin II, and especially III, proved difficult to quantify and, thus, cleavage by toxin was not detectable. (B) Dose response curves for BoNT/C1-induced cleavage of SNAP-25 (▼) and syntaxin I (▲). (C) Inhibition by toxin of CGRP release evoked by 60 mM K^+ (■), 0.1 μM bradykinin (◆) or 1 μM capsaicin (●). Data plotted are means ± s.e.m.; $n \geq 3$.*

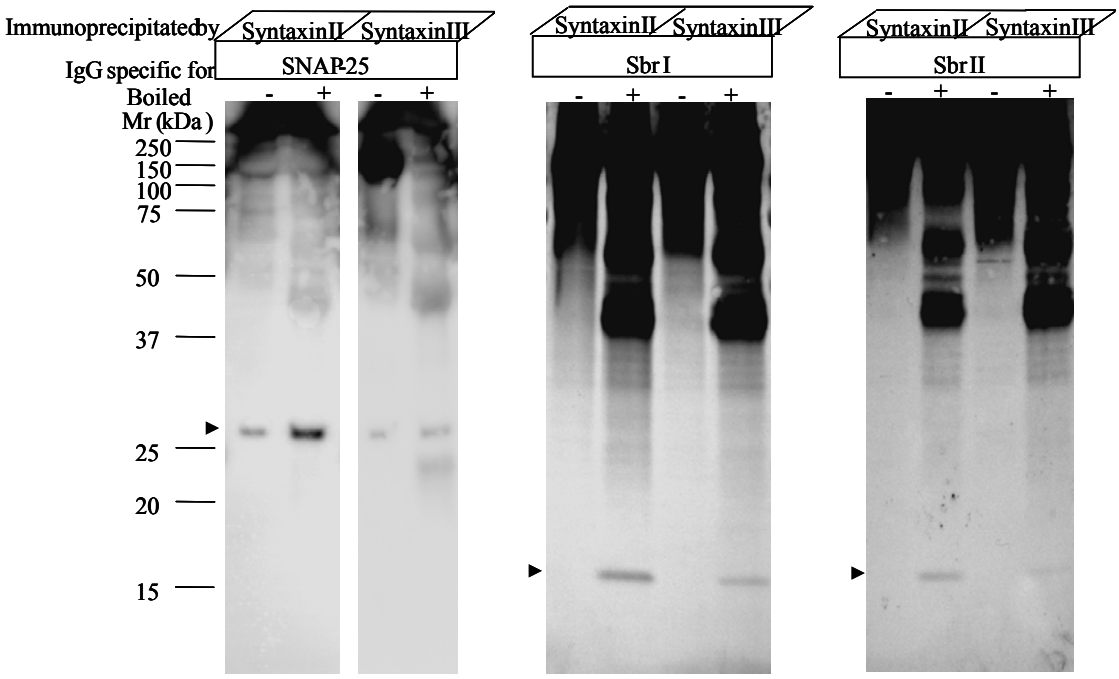

Fig. 4.3 Syntaxin II and III complexes with SNAP-25, Sbr I or II in TGNs. *The pelleted cells were extracted in 1 ml of buffer containing 1% (v/v) triton X-100 (see Chapter 2) for 1 hour at 4°C, followed by a centrifugation. The supernatant was incubated at 4°C overnight with anti-syntaxin II or III IgG (as used in Fig. 4.2) coupled to protein A-agarose. After sedimentation and extensive washing with the extraction buffer, the beads were suspended in 2xLDS sample buffer for SDS-PAGE (± boiling for 10 minutes) under non-reducing conditions, followed by Western blotting using antibodies specific for each SNARE. Note, excessive staining of the rabbit IgG overlapped with the SNARE complexes on the top halves of gels; however, multiple bands were shown in boiled samples in contrast to the one major broad band before boiling, indicating the the complex was dissociated; free Sbr isoforms were only detected in the boiled samples. Free SNARE proteins are indicated by arrow heads.*

4.2.3 BoNT/D cleaves all Sbr isoforms and inhibits CGRP release: the importance of Sbr I is unveiled by BoNT/B-induced blockade of exocytosis from mouse but not rat TGNs even though they possess its acceptor

TGNs were treated with BoNT/D as above, before visualising Sbr isoforms on Western blots with specific antibodies. Increasing concentrations of BoNT/D gave a progressive reduction in the staining for Sbr II or Sbr I and Sbr III bands (Fig. 4.4 A), indicative of their cleavage. When Sbr II or Sbr I were individually labelled with isoform-specific antibodies, and the averaged intensities of each band normalised to an internal control (SNAP-25), the resultant plots (Fig. 4.4 B) demonstrated that BoNT/D cleaves Sbr I somewhat more effectively than Sbr II (EC_{50} = 3.6 and 14.6 nM, respectively). Such treatment of the cells with BoNT/D blocked K^+- and capsaicin-evoked CGRP release (Fig. 4.4 B, C); the dose-dependence for K^+-evoked CGRP release is very close to that for Sbr I cleavage. Likewise, CGRP exocytosis elicited by bradykinin was reduced by the toxin but with a lower potency (Fig. 4.4 C). This differential inhibition of evoked release may relate to distinct BoNT/D susceptibilities of sensory neuron populations that respond to capsaicin or bradykinin. Basal efflux was also decreased (Fig. 4.4 C inset), as found with this toxin in other neurons (Hua et al., 1998). Notably, BoNT/D also blocked K^+-evoked SP release from rat cultured TGNs (Fig. 4.4 B inset).

In order to exclude that BoNT/D-induced diminution of CGRP exocytosis is due to death of TGNs, a short time course study was performed. Rat cultured TGNs were incubated with or without 10 nM BoNT/D or /B for 24 hours. Toxins were washed away, and cells were tested immediately or fresh medium was replaced and cells were maintained for the time indicated. There was no observable difference in the levels of SNAP-25 and syntaxin I in control cells and these were not reduced by day 6, indicating no toxin-induced cell death (Fig. 4.5). K^+-evoked CGRP release was inhibited by BoNT/D at day 1, 3, and 6, but there was no drop in the total cellular content of CGRP over time (the increase in CGRP total content in BoNT/D treated cells may be caused by the accumulation of CGRP intracellularly due to the blockade of release), confirming BoNT/D-induced CGRP inhibition is directly caused by proteolysis of Sbr isoforms. In contrast, BoNT/B failed to give any inhibition even though it decreased the total immuno-signals for Sbr I and Sbr II.

It was necessary to ascertain if cleavage of one or more isoforms of Sbr is required for the blockade of exocytosis. Involvement of Sbr II was addressed using BoNT/B (Fig. 4.6 A) because it does not cleave Sbr I in rat (Schiavo et al., 1992). Incubation of the

TGNs with BoNT/B decreased the intensity of Sbr II and III bands (Sbr I remained unchanged consistent with it being resistant) that were detected with the broad specificity HV-62 antibody (Fig. 4.6 A). Notably, the mAb specific for Sbr II showed a more complete cleavage of this isoform compared with HV-62 because the latter would have labelled the persisting BoNT/B–resistant Sbr I (Fig. 4.6 A). Despite this extensive cleavage of Sbr II and III, BoNT/B failed to inhibit K^+-evoked CGRP release (Fig. 4.6 B). Likewise, K^+-evoked SP release from rat cultured TGNs was not affected by BoNT/B treatment (Data not shown). The possibility of BoNT/B-resistant release occurring from a sub-population of neurons that are unable to bind and internalize this toxin seems unlikely because of the complete cleavage of Sbr II observed (unless they lack Sbr II). Moreover – synaptotagmin I and II – the toxin's acceptor, were detected in all TGNs containing CGRP (Fig. 4.6 E). Thus, the lack of blockade of CGRP release by BoNT/B raised the question whether the insensitive Sbr isoform I is involved; this idea was reinforced by the co-occurrence of Sbr I and CGRP on the cell bodies and, particularly, their striking punctate location on the neurites (Fig. 3.11 A). As murine Sbr I is susceptible to BoNT/B, experiments were repeated with TGNs prepared from P5 mice; the resultant cultured cells displayed similar morphology and purity (Fig 3.1 B). Importantly, type B toxin caused a pronounced inhibition of K^+-elicited CGRP release from the mouse TGNs (Fig. 4.6 D) similar to seen with BoNT/D although higher doses were required (Fig. 4.6 D inset); moreover, capsaicin-evoked CGRP release was inhibited. Accordingly, BoNT/B cleaved Sbr I in mouse TGNs as revealed by the concentration-dependent reduction in labelling with an antibody exclusively reactive with this isoform (Fig. 4.6 C, D). Therefore, it is reasonable to deduce that CGRP release from LDCVs can utilise Sbr I.

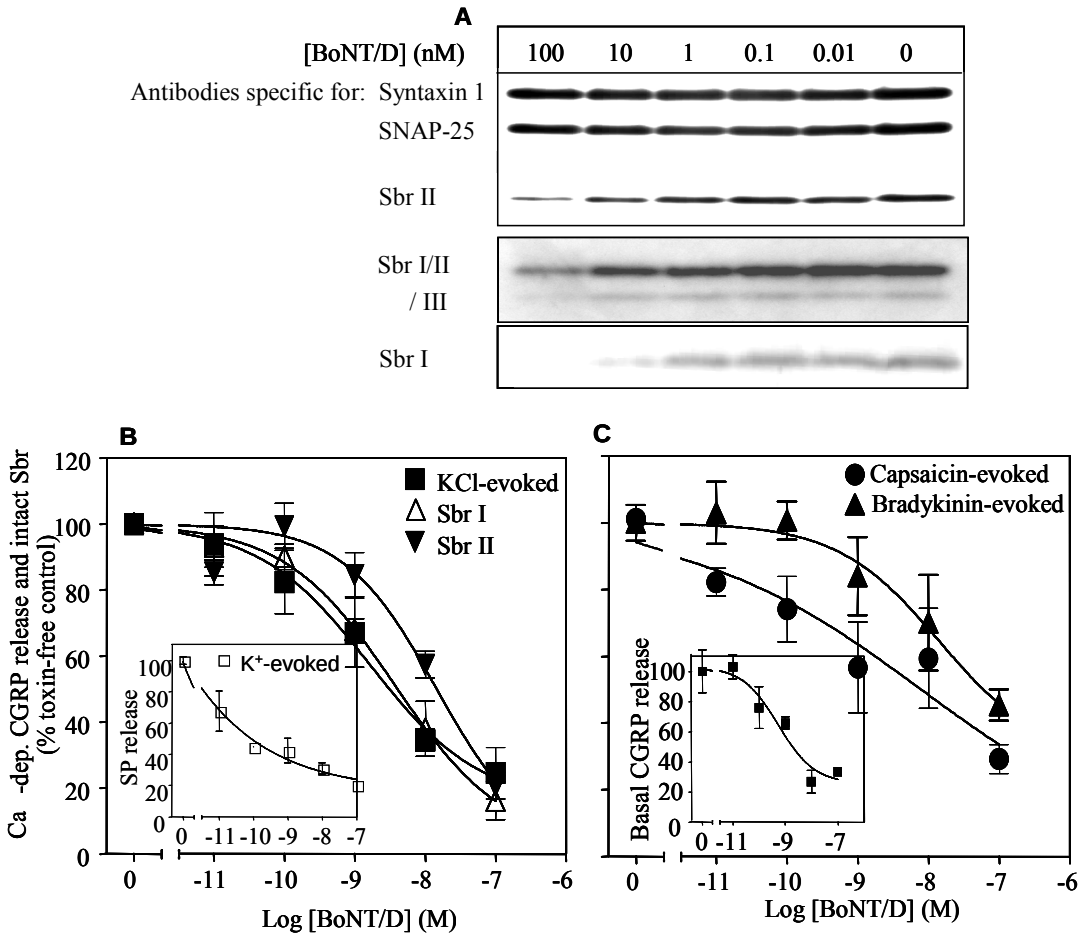

Fig. 4.4 BoNT/D blocks evoked Ca^{2+}-dependent CGRP release and cleaves 3 Sbr isoforms. *The amounts of Ca^{2+}-dependent basal and evoked release of CGRP for each stimulus were measured in cells treated with BoNT/D as in Fig. 4.1 (A). Three Sbr isoforms were detected using antibodies against Sbr I, or Sbr II, or Sbr I, II and III together (HV-62); isoform I and II co-migrate. (B) Dose response curves for the remaining intact Sbr II (▼) and Sbr I (Δ), and for inhibition of release evoked by 60 mM K^+ (■). Inset shows dose-dependent inhibition of K^+-evoked SP release by BoNT/D (□); (C) Dose response curves for inhibition of release evoked by 1 μM capsaicin (●) or 0.1 μM bradykinin (▲). Inset shows the reduction of basal release by BoNT/D (■). The values plotted are means ± s.e.m.; n = 8 except inset in B; n = 2 performed in duplicates.*

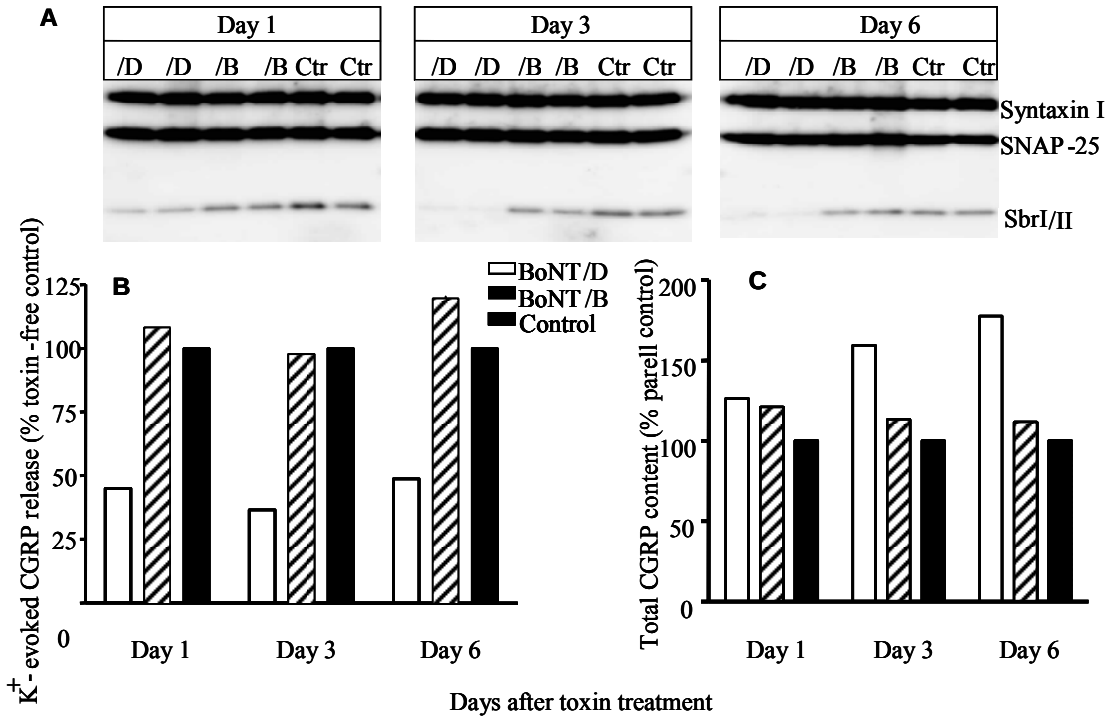

Fig. 4.5 The time course of BoNT/D-induced inhibition of K^+-evoked Ca^{2+}-dependent CGRP release implicates cleavage of its substrates rather than cell death. *Rat cultured TGNs at 7 DIV were incubated in culture medium with 10 nM BoNT/D or /B for 24 hours. After removal of toxins by washing, the neurons were tested immediately (day 1) or the medium was replaced. Cells at day 3 and 6 were analyzed as described in Fig. 4.1. Released and cellular CGRP contents were assayed by EIA. (A) Sbr isoforms I and II were detected using HV-62 antibody (I and II co-migrated). BoNT/D cleaved both isoforms at all time points, whereas, BoNT/B only cleaved Sbr II (cf Fig. 4.6); the latter caused lesser reduction in total signal for isoforms I and II. (B) BoNT/D blocked K^+-evoked CGRP release, whereas, BoNT/B proved ineffective (cf. Fig. 4.6). (C) Intracellular CGRP content relative to that of equivalent toxin-free control (filled bars) remained unchanged after expose to BoNT/B (hatched bars) but was increased by BoNT/D (open bars). Data plotted are average from n = 2 performed in duplicates.*

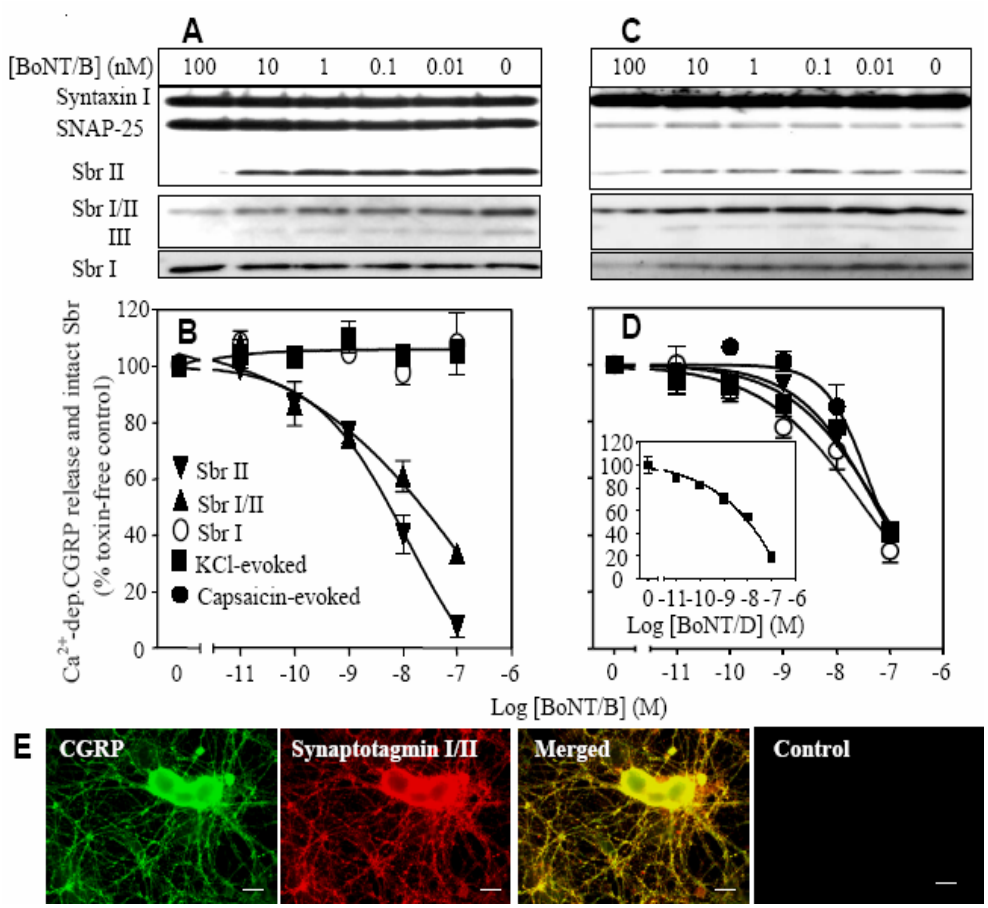

Fig. 4.6 BoNT/B proteolyses Sbr II and III in rat TGNs but does not reduce K^+-evoked CGRP release despite the presence of its receptor: in mouse TGNs, Sbr I is also cleaved and exocytosis blocked. *TGNs were cultured from rat (A, B, E) and mouse (C, D) for 7 DIV before exposure to BoNT/B; EIA of released CGRP and Western blotting were carried out as described in Fig. 4.1. Results presented are means ± s.e.m.; n = 8. (A, C) Immuno-blots showing the disappearance of 2 Sbr isoforms for rat (Sbr II and III) and 3 for mouse (Sbr I, II and III) relative to the internal standard (SNAP-25) that remained unchanged. (B, D) Dose response curves for inhibition of CGRP release evoked by 60 mM K^+ (■), capsaicin (●) and remaining Sbr II (▼), Sbr I and II (▲), and Sbr I (○). Inset illustrates the inhibition by BoNT/D of K^+-evoked CGRP release from mouse TGNs, for comparison. (E) Representative fluorescent micrographs showing that the putative protein receptors of BoNT/B, synaptotagmin I and II, are present in CGRP positive neurons. Specimens were stained using rabbit anti-CGRP (1:500) (and donkey anti-rabbit IgG Cy2, 1:200) and goat anti-synaptotagmin I/II (1:100) (and donkey anti-goat IgG Cy3, 1:800). The control was treated in the absence of primary antibodies but incubated with secondary fluorescently-labelled IgGs against goat and rabbit. Scale bars are 20 μm.*

4.2.4 Pre-incubation of rat cultured TGNs with BoNT/D but not BoNT/B inhibits BoNT/A binding/uptake

Previous studies reported that incubation with BoNT/A in K^+ depolarization buffer results in increased cleavage of SNAP-25 by /A in various cultured neuronal cells because this toxin's acceptor, SV2 isoforms, are located on secretory vesicles and the luminal domains for BoNT/A binding are only exposed to the extracellular domain during exocytosis (Dong et al., 2006), indicating BoNT/A uptake occurs in an activity-dependent manner. Consistent with this, K^+ depolarization significantly increased uptake of BoNT/A into TGNs (Fig. 4.7 A). Because BoNT/D cleaved all three Sbr isoforms and inhibited CGRP exocytosis in rat cultured TGNs, the toxin might be expected to inhibit BoNT/A uptake; on the other hand, BoNT/B was unable to cleave rat Sbr I and failed to inhibit CGRP exocytosis from LDCVs and should, thus, allow BoNT/A binding to the luminal domain of SV2 proteins during exocytosis. Therefore, it was important to determine whether cleavage by BoNT/B of Sbr II and Sbr III, the SNARE which normally mediate classical transmitters release, will inhibit BoNT/A internalization. To address this question, rat cultured TGNs were pre-treated with 50 nM BoNT/B or /D for 24 hours to allow cleavage of their substrates. After removal of the toxins by washing, the neurons were exposed to 50 nM BoNT/A in depolarization buffer for 5 mins. Unbound toxin was removed by washing with pre-warmed culture medium , and the cells were maintained in culture medium for 24 hours to allow internalized BoNT/A to cleave SNAP-25. The extent of BoNT/A binding/uptake was reflected by the observed cleavage of SNAP-25. Immunoblots demonstrated that both BoNT/B and BoNT/D cleaved Sbr II to similar extent (Fig. 4.7 B, C); however, pre-treatment of BoNT/B only slightly reduced BoNT/A binding to rat TGNs because 60% of SNAP-25 became cleaved which is very similar to that for treatment with BoNT/A only. In constrast, pre-treatment with BoNT/D significantly inhibited BoNT/A uptake, as reflected by only ~15% SNAP-25 cleavage (Fig. 4.7 C). Negligible inhibition of BoNT/A binding by BoNT/B might implicate there are very small amounts of SCSVs in rat cultured TGNs or Sbr I is also presents in SCSVs and mediates SCSVs recycling. It can be deduced that binding of BoNT/A to the luminal domain of SV2 proteins must be significantly reduced due to the impaired exocytosis induced by /D; BoNT/A uptake remained almost unaltered after /B treatment because the latter failed to prevent vesicle recycling even though it cleaved Sbr II and Sbr III (Fig. 4.6). Our results suggest that Sbr II or III are somewhat redundant in CGRP release from rat TGNs.

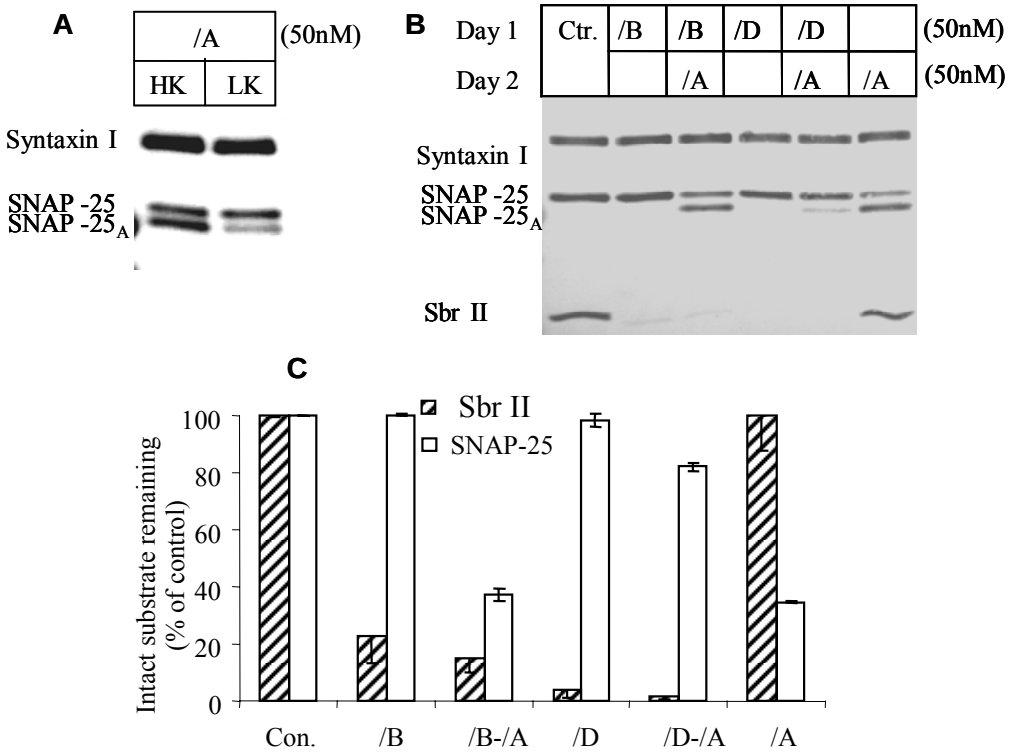

Fig. 4.7 SNAP-25 cleavage by BoNT/A upon depolarization of rat cultured TGNs was significantly reduced by pre-treatment with BoNT/D but not /B. *Rat cultured TGNs at 7 DIV were pretreated with 50 nM BoNT/B or /D for 24 hours. The washed cells were then exposed to 50 nM BoNT/A for 5 minutes in 60 mM K^+ depolarization buffer. After removal of unbound toxin by pre-warmed culture medium, the latter was replaced and cells were further incubated for 24 hours at 37°C to allow internalized BoNT/A to cleave SNAP-25. Cells were then solubilized in 2xLDS sample buffer and subject to SDS-PAGE and Western blotting. The proportion of remaining substrate was calculated relative to an internal uncleaved syntaxin I control. (A) SNAP-25 cleavage were demonstrated from samples that treated by BoNT/A for 5 minutes in K^+ depolarization buffer (HK) or basal buffer (LK) followed by 24 hours of incubation in toxin-free medium; (B) Representative immunoblot showing the similar extent of cleavage of Sbr II by BoNT/B and /D; SNAP-25 cleavage by BoNT/A after pre-treatment with BoNT/B is only slightly less than that for BoNT/A alone, whereas pre-exposure to BoNT/D significantly reduced SNAP-25 cleavage by BoNT/A. (C) Percentage of intact SNAP-25 (open bar) or Sbr II (filled bar) remaining, calculated relative to parallel toxin-free control after scanning of 3 blots from 3 independent experiments.*

4.2.5 Novel BoNT chimeras AB and BA generated with ability to block pain-peptide release reaffirm the involvement of Sbr I in CGRP exocytosis

4.2.5.1 Designs of BoNT chimeras AB (LC-H_N/A-H_C/B) and BA (LC-H_N/B-H_C/A)

To further confirm that the lack of inhibition by BoNT/B of CGRP release in rat is not due to its failure to bind TGNs but because of its inability to cleave Sbr I, I designed two novel chimeras AB and BA. Chimera AB comprises the LC-H_N domains from BoNT/A (LC-H_N/A) fused to the binding domain of BoNT/B (H_C/B) to ascertain whether a /B-receptor exsists on rat TGNs by determining of SNAP-25 cleavage could be detected by its delivered /A protease activity. Likewise, the LC-H_N domains from BoNT/B were fused to H_C/A to address if Sbr I cleavage occurred when the protease of /B was delivered via the known /A-acceptor. A schematic of the toxin's design strategy is shown in Fig. 4.8.

4.2.5.2 Generation of chimera AB and BA

Construction, expression and purification of chimera AB and BA were performed by Dr Wang J (our unpublished data). Briefly, chimera AB and BA were expressed in *E. coli* BL21 (DE3) and purified as SC polypeptides that upon SDS-PAGE migrated as Mr~150 k bands, in either the absence or presence of the reducing agent DTT (Fig. 4.9 A). Controlled nicking of chimera AB with Trypzean gave near-complete conversion of the SC to disulphide-linked DC, as demonstrated by the appearance of HC and LC upon SDS-PAGE in the prescence of DTT; continued migration at ~150 k (Fig. 4.9 A) in the absence of DTT indicates that the inter-chain disulphide was formed in virtually all of the DC. Likewise, chimera BA was also successfully converted from SC to DC form by incubation with thrombin (Fig. 4.9 B). Western blotting with antibodies against LCA, BoNT/A or BoNT/B demonstrated the expected domains from each parental toxin were incorported into chimera AB and BA.

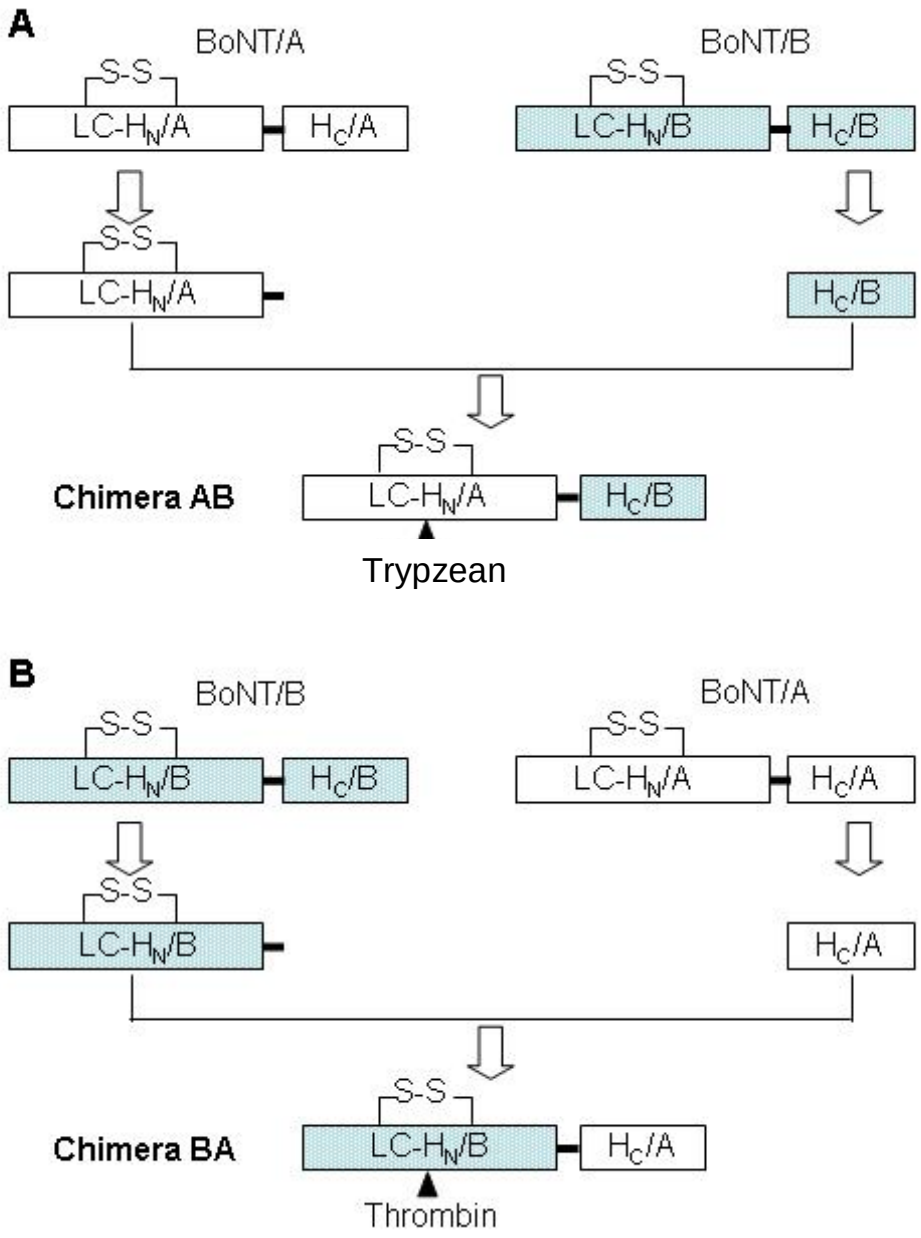

Fig. 4.8 Design strategy for chimera AB and BA. *(A) Chimera AB SC gene comprises LC and H_N gene fragments from BoNT/A fused to binding domain from BoNT/B. Likewise, LC-H_N/B was fused to HC/A to generate chimera BA transgene (B). The nicking sites are indicated with (▲).*

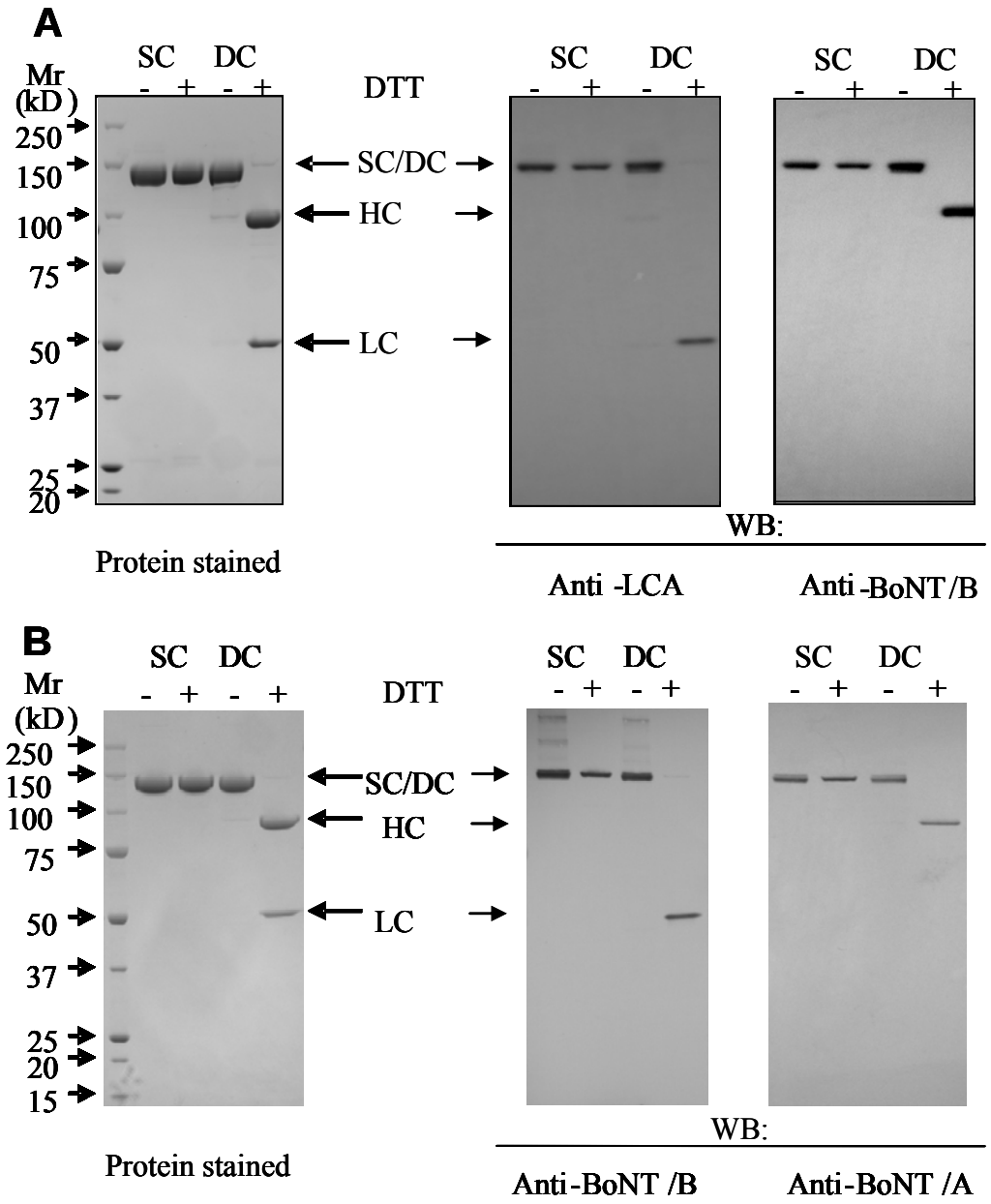

Fig. 4.9 Expressed chimera AB and BA toxins. *The purified chimera AB (A) and BA (B) SCs which were subsequently converted to DC forms by controlled nicking (see Chapter 2; the gels were provideded by Dr Wang J) before SDS-PAGE in the absence or presence of DTT (as indicated), followed by Coomassie protein staining or Western blotting (WB) with the antibodies specified.*

4.2.5.3 Chimera AB and BoNT/A equi-potently cleaved SNAP-25 whereas BA cleaved Sbr II to a similar extent as BoNT/B in cultured CGNs: chimeras exhibit protease activity of their parents

CGNs are a useful model of central nerves for evaluating potency of BoNT due to their ease of preparation, with large yield and high sensitivity to the toxins. Cultured CGNs at 7 DIV were incubated with chimeric toxins AB and BA, as well as their parental toxins BoNT/A and /B for 24 hours (Fig. 4.10). Dose response curves for SNAP-25 cleavage by BoNT/A and chimera AB overlapped, indicating both toxins have similar potency (Fig. 4.10 A). Moreover, Sbr II cleavage by chimera BA is similar to that by native BoNT/B (Fig. 4.10 B). Thus, changing the binding domains does not affect their potency for SNARE cleavage in rat cultured CGNs.

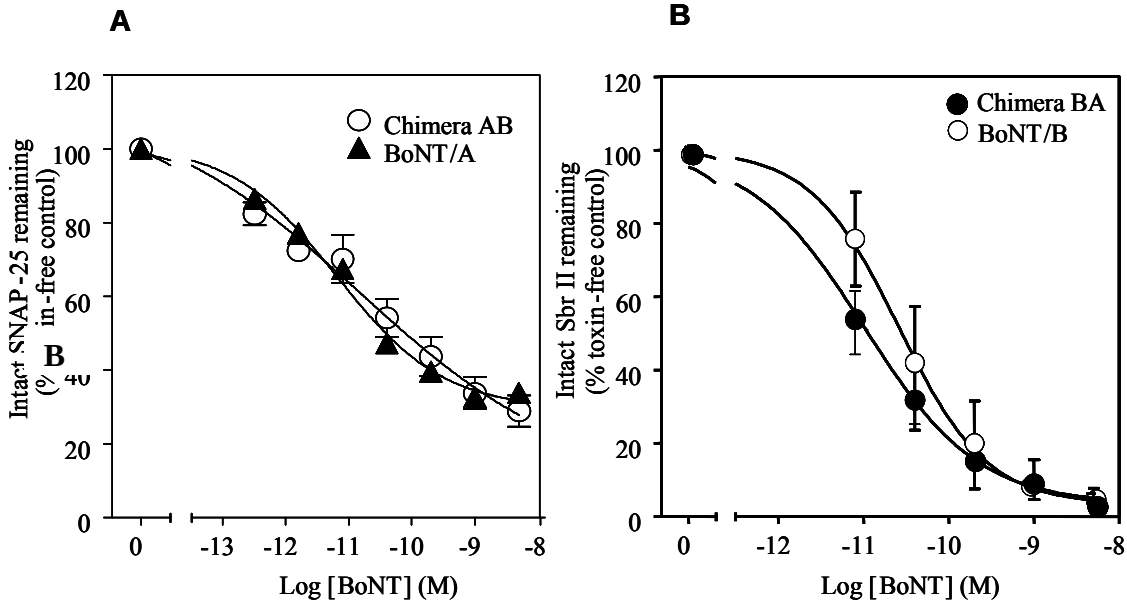

Fig. 4.10 The potencies in cultured CGNs of chimera AB and BA in cleaving their respective substrates are similar to that of their parental toxins containing the same protease. *CGNs at 7 DIV were incubated with toxins for 24 hours in culture medium with the specified concentrations. After removal of toxins by washing, cells were then solubilized in 200 µl 2xLDS-sample buffer and equal volume of protein subjected to SDS-PAGE and Western blotting. The proportion of remaining substrate was calculated relative to an internal un-cleaved syntaxin control. (A, B) Dose response curves for remaining intact SNAP-25 (A) or Sbr II (B) after treatment with BoNT/A (▲), chimera AB (○), BoNT/B (○) or chimera BA (●). Data plotted are means ± s.e.m.; n=3.*

4.2.5.4 Inhibition of CGRP release by chimera AB demonstrated the presence of acceptors for BoNT/B in rat cultured TGNs: lack of inhibition of CGRP exocytosis by chimera BA accords with BoNT/B-resistant Sbr being required

Rat cultured TGNs were incubated with chimera AB, BA, BoNT/A or BoNT/B in culture medium for 24 hours at 37°C and K^+-evoked Ca^{2+}-dependent. CGRP release was measured, before the same cells were subjected to SDS-PAGE and Western blotting. Chimera AB gave dose-dependent cleavage of SNAP-25 and inhibition of K^+-evoked CGRP release (Fig. 4.11 A, B). Notablly, 100 nM of chimera AB gave the same inhibition of CGRP release as BoNT/A (Fig. 4.11 B). Due to chimera AB having the binding domain from BoNT/B, it seemed rat TGNs contains a functional BoNT/B receptor which led to intracellular delivery of the /A protease giving the cleavage of SNAP-25 (Fig. 4.11 A). In contrast, 100 nM chimera BA nearly cleaved all of Sbr II whereas Sbr I is resistant (Fig. 4.11 C); however, chimera BA did not inhibit K^+-evoked CGRP release from rat TGNs just like BoNT/B (Fig. 4.11 D). This further demonstrated the inability of BoNT/B to inhibit CGRP release is not due to BoNT/B being unable to enter the cells becase chimera BA also failed to give any inhibtion even though it was targeted to BoNT/A-susceptible neurons. Clearly, lack of inhibition of CGRP release is due to a lack of cleavage of rat Sbr I by type B toxins (chimera BA and BoNT/B).

4.2.5.5 Chimera AB- and BA-induced inhibition of CGRP exocytosis from mouse TGNs correlates with the cleavage of their respective substrates: SNAP-25 and Sbr I

Mouse cultured TGNs at 7 DIV were incubated overnight at 37°C with various concentrations of chimera AB and BA and Ca^{2+}-dependent CGRP release was measured. K^+-evoked CGRP release was inhibited by chimera AB with a concentration dependence identical to that for SNAP-25 cleavage. In comparison with its parental toxin BoNT/B, inhibition by chimera AB is much more effective even though they share same binding domain (Fig. 4.12 A, B; cf. Fig. 4.6). Increasing concentration of chimera BA gave a progressive cleavage of Sbr I (Fig. 4.12 C, D), as revealed by Western blotting with isoform-specific antibodies. The dose-response curves derived from analysis of several blots demonstrated that chimera BA dose-dependently cleaved Sbr I and induced inhibition of K^+-evoked CGRP release (Fig. 4.12 C, D).

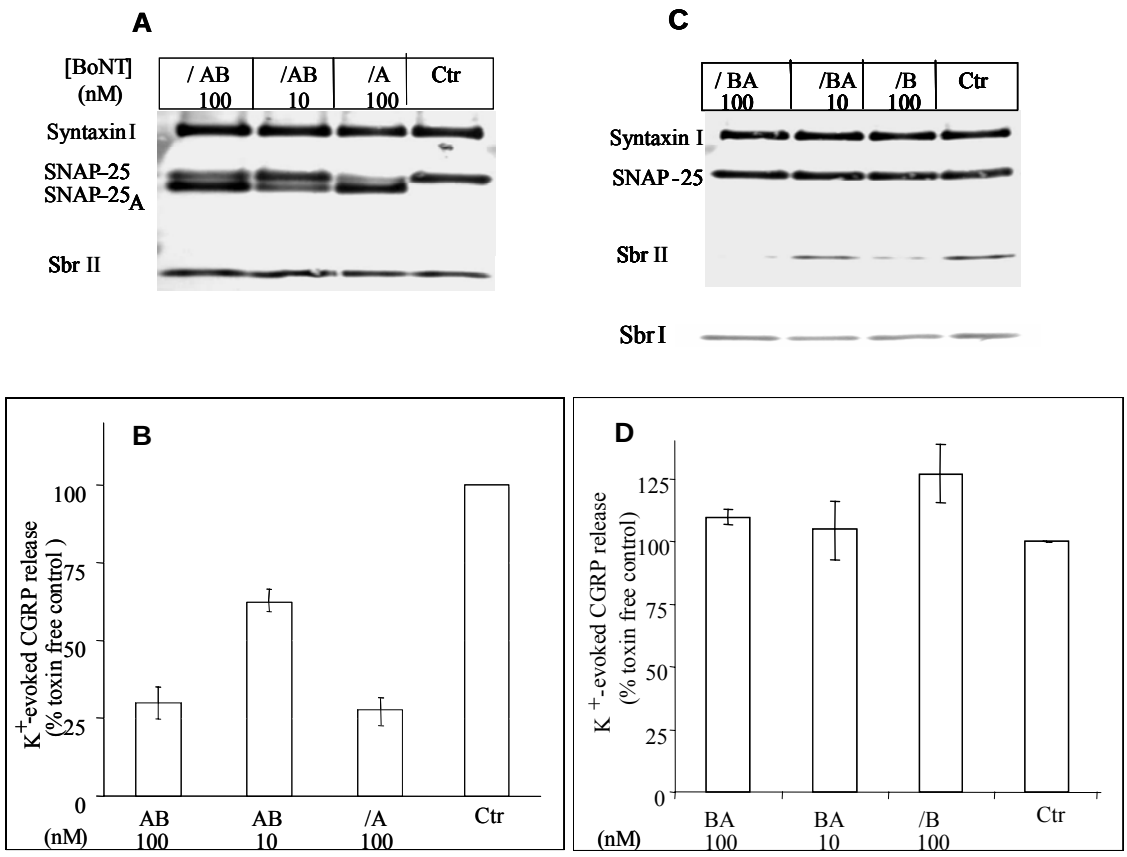

Fig. 4.11 Chimera AB cleaves SNAP-25 and inhibits K^+-evoked CGRP release from rat TGNs to a similar extent as BoNT/A; in contrast, BA gives no inhibition, just like BoNT/B, though both cleave Sbr II. *Rat cultured TGNs at 7 DIV were exposed to chimera AB or BoNT/A (A, B), or chimera BA or BoNT/B (C, D) at 37°C for 24 hours. CGRP release was assayed and the cells were solubilised in 2xLDS sample buffer for SDS-PAGE and Western blotting. Immunoblots illustrate the cleavage of SNAP-25 (A) or Sbr II (C) by the toxins treatment and the effects on (B, D) K^+-evoked CGRP release. Data plotted are means±s.e.m.; n=3.*

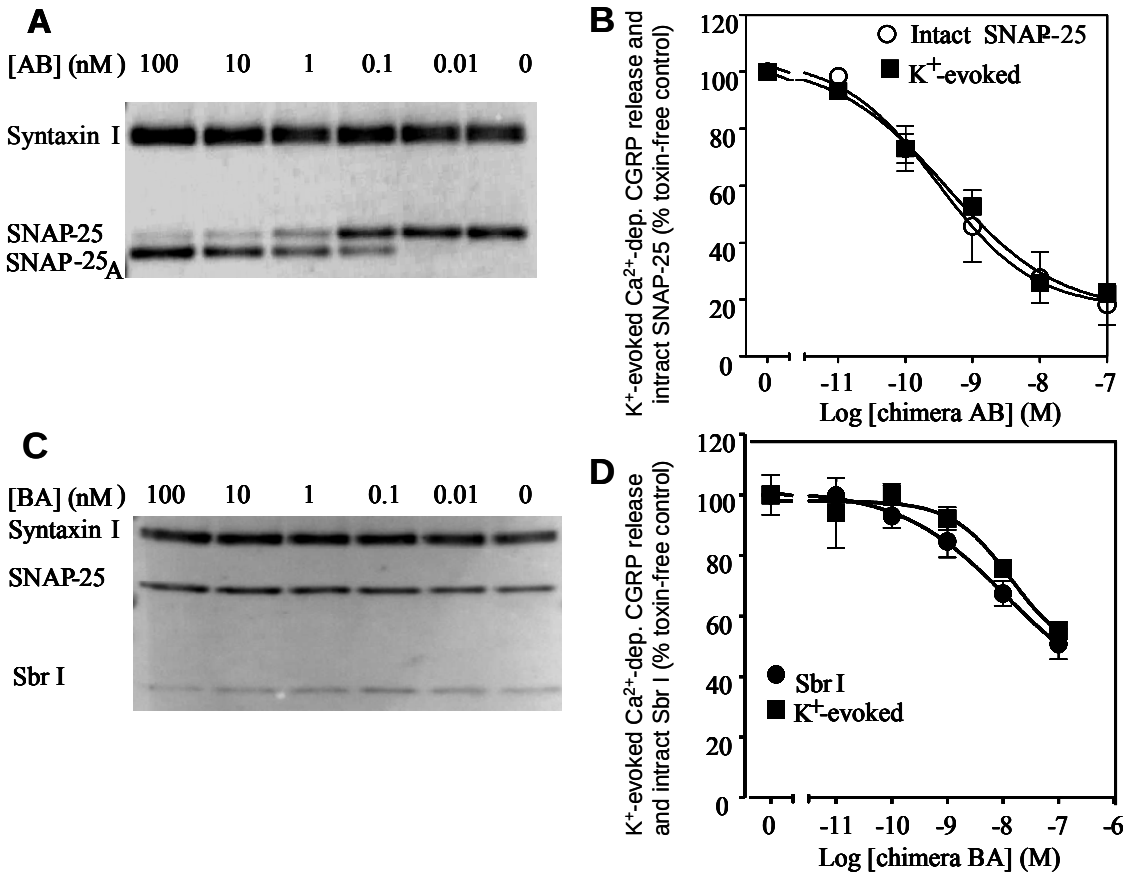

Fig. 4.12 Chimera AB potently cleaves SNAP-25 and inhibits K^+-evoked CGRP release from mouse cultured TGNs whereas BA incompletely cleaves Sbr I and partially blocks CGRP release. *Mouse cultured TGNs at 7 DIV were exposed to various concentrations of chimera AB or BA at 37 ° C in culture medium for 24 hours. K^+-evoked CGRP release was assayed, Western blotting performed and results calculated (see Fig. 4.1). (A, C) Immunoblots illustrate the cleavage of SNAP-25 by chimera AB, or Sbr I by chimera BA. (B, D) Dose response curves for chimera AB- or BA-induced inhibition of K^+-evoked CGRP release (■) correlate with remaining intact (B) SNAP-25 (○), or (D) Sbr I (●), respectively. Data plotted are means±s.e.m.; n=3.*

4.2.6 CGRP–containing vesicles possess Sbr I and II: each can form a separate SNARE complex

4.2.6.1 Immuno-isolation of CGRP containing vesicles

BoNT/B- or chimera BA-induced cleavage of Sbr II (and III) in rat TGNs failed to reduce K^+-evoked CGRP exocytosis, whereas the additional cleavage of Sbr I in the mouse neurons resulted in blockade. This indicates that isoform I can mediate exocytosis from these peptidergic LDCVs. Evidence to support this hypothesis was obtained by precipitating vesicles including CGRP- containing LDCVs from a TGN lysate with IgG that is known to be exclusively reactive with Sbr I (Fig. 4.4 A). The resultant vesicles were found to be enriched in CGRP (Fig. 4.13 A) relative to the level observed in the control (prepared with non-immune IgG beads). Moreover, analysis of these isolated vesicles by SDS-PAGE and Western blotting revealed the expected presence of Sbr I which was absent from the control (Fig. 4.13 B). Notably, the immuno-isolated vesicles also contained isoform II (Fig. 4.13 B). Clearly, Sbr II co-exists with isoform I on CGRP-containing vesicles because both were found in the immuno-isolates irrespective of whether IgGs specific for Sbr II (Fig. 4.13) or I were used. This is in agreement with our eailer findings that Sbr I and II are present in the fractionated SP- or CGRP- containing vesicles (cf. Fig. 3.15).

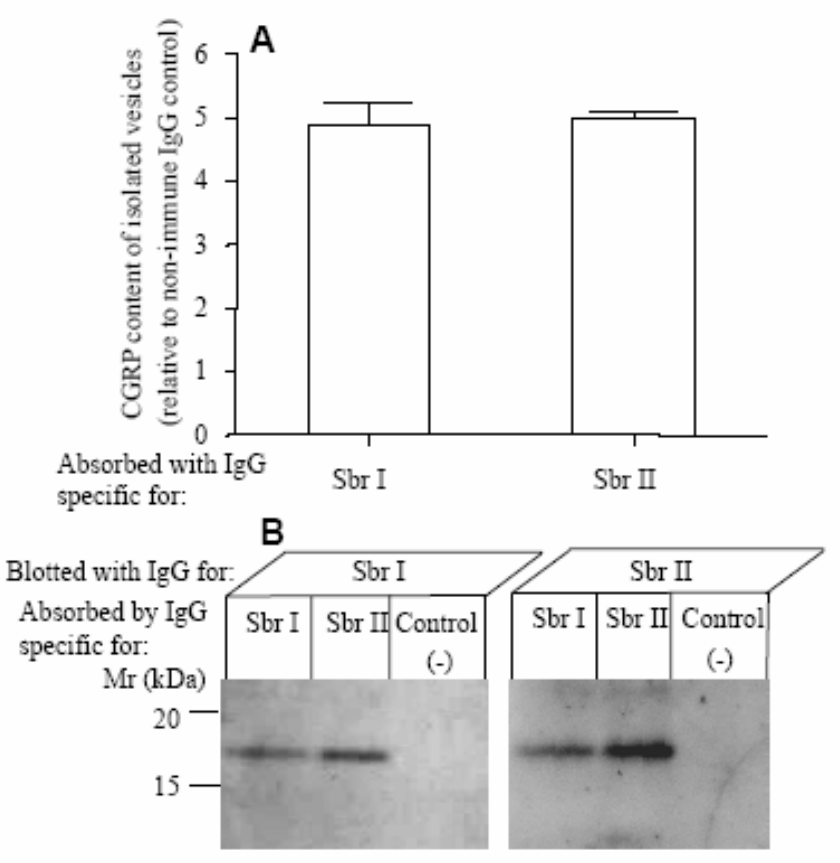

Fig. 4.13 Immuno-absorption of vesicles from TGNs by antibodies against Sbr I and II. *Equal amounts of the total membrane fraction from lysed TGNs were incubated overnight at 4℃ with protein A-agarose coupled to IgGs specific for Sbr I or II, or rabbit non-immune IgG (control). After extensive washing, equivalent aliquots of the beads were sedimented and pellets dissolved in LDS sample buffer for SDS-PAGE and Western blotting, as in Fig. 4.3. Alternatively, 2M acetic acid with 0.1% TFA was added to replicate samples for CGRP determination. (A) CGRP contents (± s.e.m.) measured in two separate preparations show the large enrichment in vesicles obtained using beads containing Sbr I or Sbr II relative to the control. (B) Western blots of the two vesicle preparations and the control, using antibodies specific for Sbr I or II.*

4.2.6.2 Immuno-precipitation of SNARE complexes

The functionality of Sbr I in these vesicles was confirmed by its demonstrated presence in characteristic SDS-resistant SNARE complexes separated from an extract of TGNs, in non-denaturing detergent with IgG specific for Sbr I, coupled to protein A beads. The sedimented proteins were solubilized in LDS sample buffer, subjected to SDS-PAGE and Western blotting. One aliquot of each sample was boiled before the analysis. A sensitive protein reagent (Sypro-ruby) stained a major broad band of complexes (Mr>100 k) before boiling. Boiling reduced the amount of apparent intact complexes and resulted in additional lower molecular weight bands (Fig. 4.14 A). Immunblots of the samples before boiling, with antibodies specific for SNAP-25 or syntaxin I, visualised a broad band corresponding to the main SNARE complexes (Mr > 100 k); much lower levels of these free constituents were present (Fig. 4.14 B). Boiling raised the proportions of dissociated SNAP-25 and syntaxin I whilst decreasing the relative amounts of the complex, although substantial protein remained (Fig. 4.14 B). As expected, some free Sbr I was found in the unheated sample but its level increased after boiling (Fig. 4.14 B); this accords with the corresponding decreased intensity of the major immuno-reactive protein complexes (Mr > 100 k) upon boiling (cf. Fig. 4.14 A). Notably, Sbr II could not be detected in the non-boiled or boiled samples (Fig. 4.14 B). In conclusion, the collective evidence presented here suggests, for the first time, that Sbr I can mediate regulated CGRP exocytosis from TGNs.

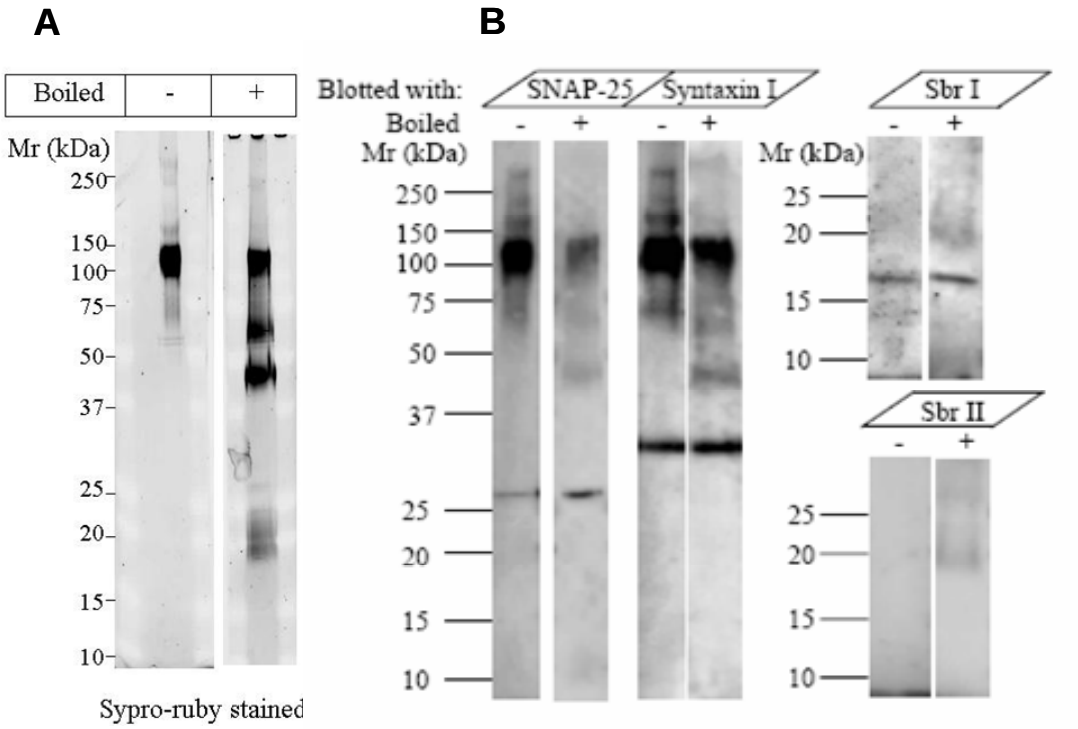

Fig. 4.14 Sbr I complexes with SNAP-25 and syntaxin I in TGNs. *The pelleted cells were extracted in 1 ml of buffer containing 1% (v/v) Triton X-100 (see Chapter 2) for 1 hour at 4°C, followed by centrifugation. The supernatant was incubated at 4°C overnight with anti-Sbr I IgG coupled to protein A-agarose. After sedimentation and extensive washing with the extraction buffer, beads were suspended in LDS sample buffer for SDS-PAGE (with and without boiling for 10 minutes) under non-reducing conditions, followed by Sypro-ruby staining (A) or Western blotting using antibodies specific for each SNARE (B). Only the lower halves of the gels blotted for Sbr I or II are shown because of excessive staining of the rabbit IgG that overlapped the SNARE complex. Note that boiling raised the proportion of dissociated SNAP-25, syntaxin I and Sbr I; this corresponds to the decrease in the complex.*

4.2.7 Sbr I requirement in CGRP release also applies to other types of sensory neurons, such as DRGs

Various BoNTs are known to be effective in cleaving their substrates and inhibiting SP release from cultured rat embryonic DRGs (Welch et al., 2000), whereas BoNT/B did not give significant inhibition though it cleaved its substrate Sbr II.

Considering the dramatic co-localization of CGRP and SP in sensory neurons and reported co-release of both peptides from LDCVs [our results described earlier and (Skofitsch and Jacobowitz, 1985)], it was necessary to establish whether the CGRP released from DRGs is also mediated by Sbr I.

4.2.7.1 Phase contrast microscopy of DRGs showing their similar morphology to TGNs

DRG neurons were successfully maintained in culture using the methods described (Chapter 2). Similar to cultured TGNs, 24 hours after plating cells start to develop neurites, and after 7 days in medium supplemented with Ara-C and NGF DRG neuronal cells became enriched and formed an extensive neurite network (Fig. 4.15).

4.2.7.2 BoNT/B inhibited K^+-evoked CGRP exocytosis from mouse but not rat cultured DRG neurons whereas BoNT/D blocked release from both implicating Sbr I in CGRP release

K^+-evoked CGRP release was monitored from rat cultured DRG neurons at 7DIV, and its release was found to be significantly inhibited by 100 nM BoNT/D but not by /B (Fig. 4.16 A); in constrast, both of these toxins could inhibit CGRP release from mouse DRG neurons (Fig. 4.16 B). This is consistent with what we found in TGNs, which indicated that Sbr I may be essential for other CGRP releasing sensory neurons.

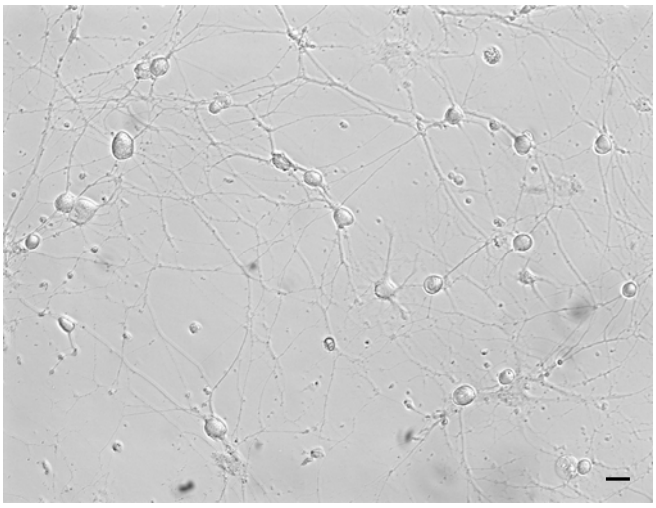

Fig. 4.15 Representative phase contrast micrograph of rat cultured DRGs at 7 DIV. *Rat DRGs were dissected from P5 rats, dissociated and cultured following the procedures as described in Chapter 2. Image was taken at 7 DIV with an inverted microscopy in phase contrast mode. At 7 DIV neurites were well developed and neuronal cells enriched. Scale bar = 20µm.*

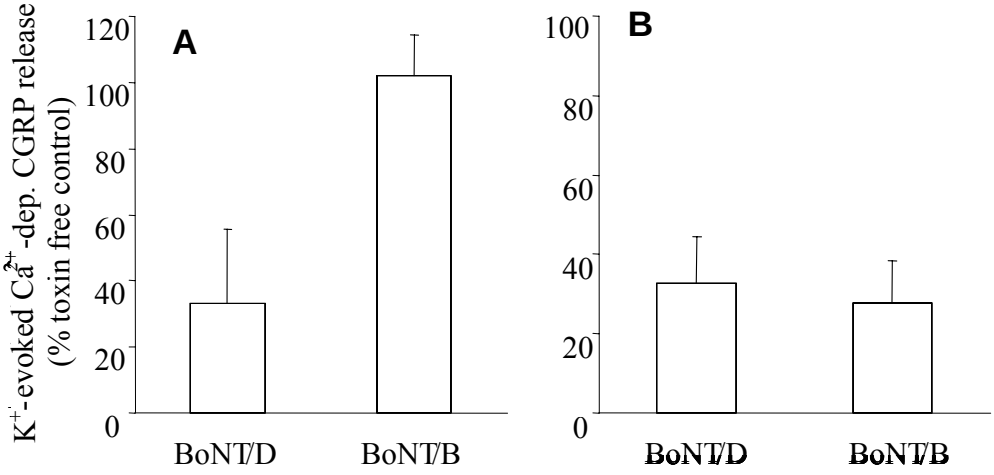

Fig. 4.16 BoNT/D but not /B inhibited K^+-evoked CGRP release from rat cultured DRG cells, whereas both blocked release from mouse DRG neurons. *DRGs were dissected from P5 Wistar rats (A) and TO mice (B), dissociated and cultured (described in Matherials and Methods). DRG neurons at 7 DIV were exposed to 100 nM BoNT/D or /B in culture medium for 24 hours at 37°C; 60mM K^+-evoked Ca^{2+}-dependent CGRP release was assayed using EIA. Results are means ± s.e.m.; n = 3.*

4.2.8 Knock down of Sbr I gene expression by shRNA resulted in a substantial reduction of CGRP exocytosis directly pinpointing Sbr I as being required

ShRNA is a short sequence of RNA which makes a tight hairpin turn and can be used for stable and long-term gene silencing. Sbr I shRNA lentiviral transduction particles supplied by Sigma contains 5 clones for knock down of mouse Sbr I gene expression. Each clone targets a specific sequence, as indicated in Fig. 4.17A.

Mouse cultured TGNs at 7 DIV were infected with individual clones of Sbr I shRNA lentiviral particles for 8 days before basal and K^+-evoked CGRP release were monitored (see Chapter 2). After release, cells were then solubilised in LDS-sample buffer and subject to SDS-PAGE and Western blotting. Sbr I and Sbr II were visualized using isoform-specific antibodies. Other SNARE proteins, SNAP-25 and syntaxin I were also detected using their specific antibodies. All 5 individual clones knocked down expression of Sbr I as shown in Fig. 4.18 A. In contrast, Sbr II and internal control proteins (syntaxin I, SNAP-25) remained unaltered (Fig. 4.18 A). Knock down of expression of Sbr I did not significantly affect basal release (data not shown) but caused nearly 45% reduction of CGRP release evoked by 60 mM [K^+] from mouse TGNs (Fig. 4.18 B), which directly pinpoint a pivotal role of Sbr I in mediating exocytosis of this transmitter. The same procedures were performed in rat TGNs though all these 5 clones of shRNA were originally designed for knock-down of mouse Sbr I gene. According to gene sequence alignment, clone #2 perfectly matches the rat gene sequence and clone #4 has only 1 nucleotide mismatch (Fig. 4.17 B). Subsequently, both of them significantly reduced rat Sbr I expression (Fig. 4.18 C); the control proteins, SNAP-25, syntaxin I and Sbr II remained unchanged. For the reduced expression level of Sbr I, K^+-evoked Ca^{2+}-dependent CGRP release was decreased ~55% by clone #2 (Fig. 4.18 D).

From Western blotting, Sbr I protein was hardly detected from shRNA lentiviral particles infected cells. However, immunocytochemical staining using the same antibodies against Sbr I with different dilution indicated there was residual Sbr I after shRNA treatment (Fig. 4.19). Mouse cultured TGNs grown on coverslips were treated with clone #3, followed by fixation, permeabilisation and staining with antibodies specific for Sbr I or II. Notably, Sbr I signal is significantly reduced on the neurites and cell bodies relative to the untreated samples; in contrast, Sbr II signal remained same as control. Such differences were more apparent in the merged images (Fig. 4.19).

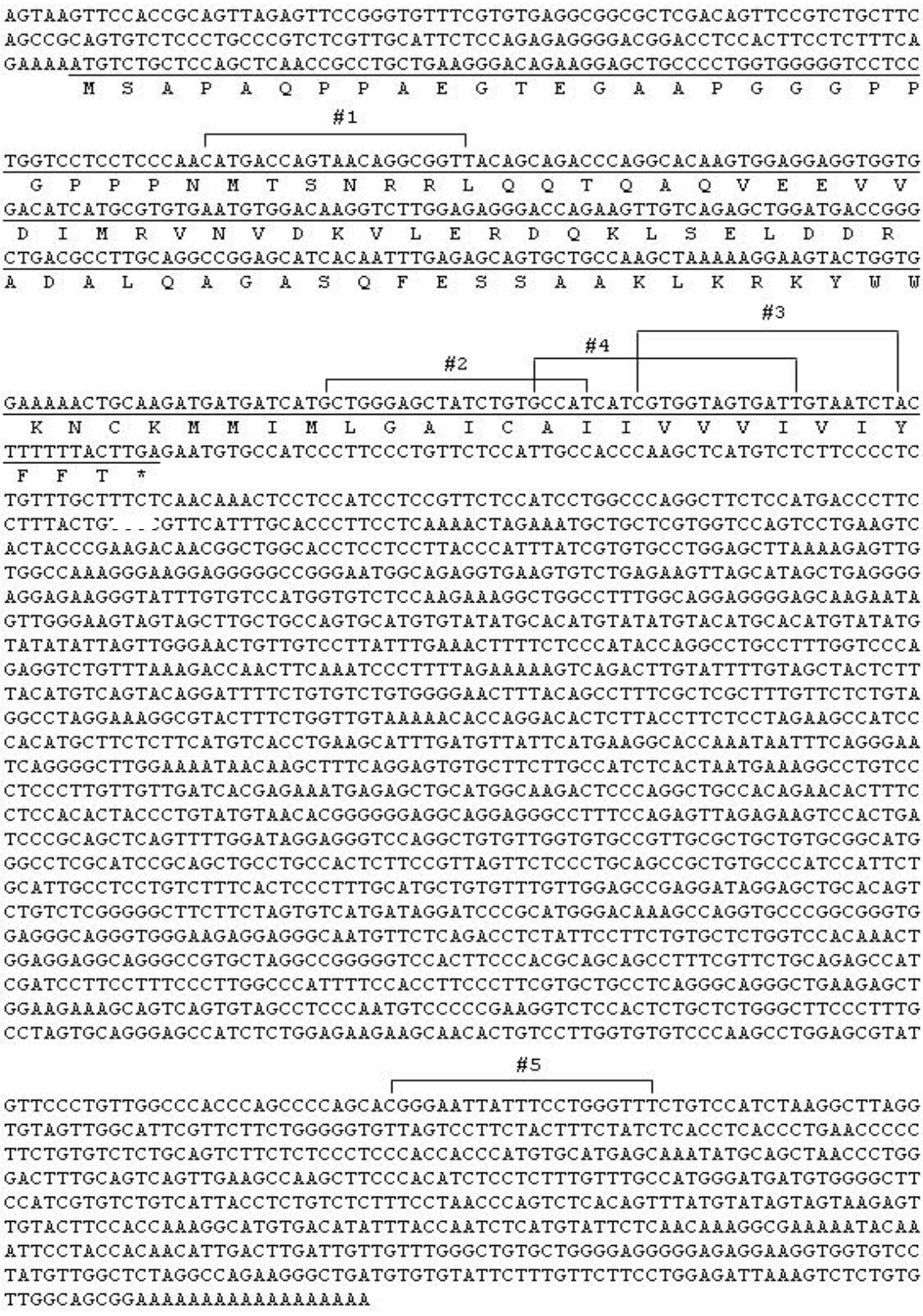

Fig. 4.17A. Mouse Sbr I cDNA sequence (GenBank accession No. NM_009496). *5 shRNA targeting regions are indicated***.**

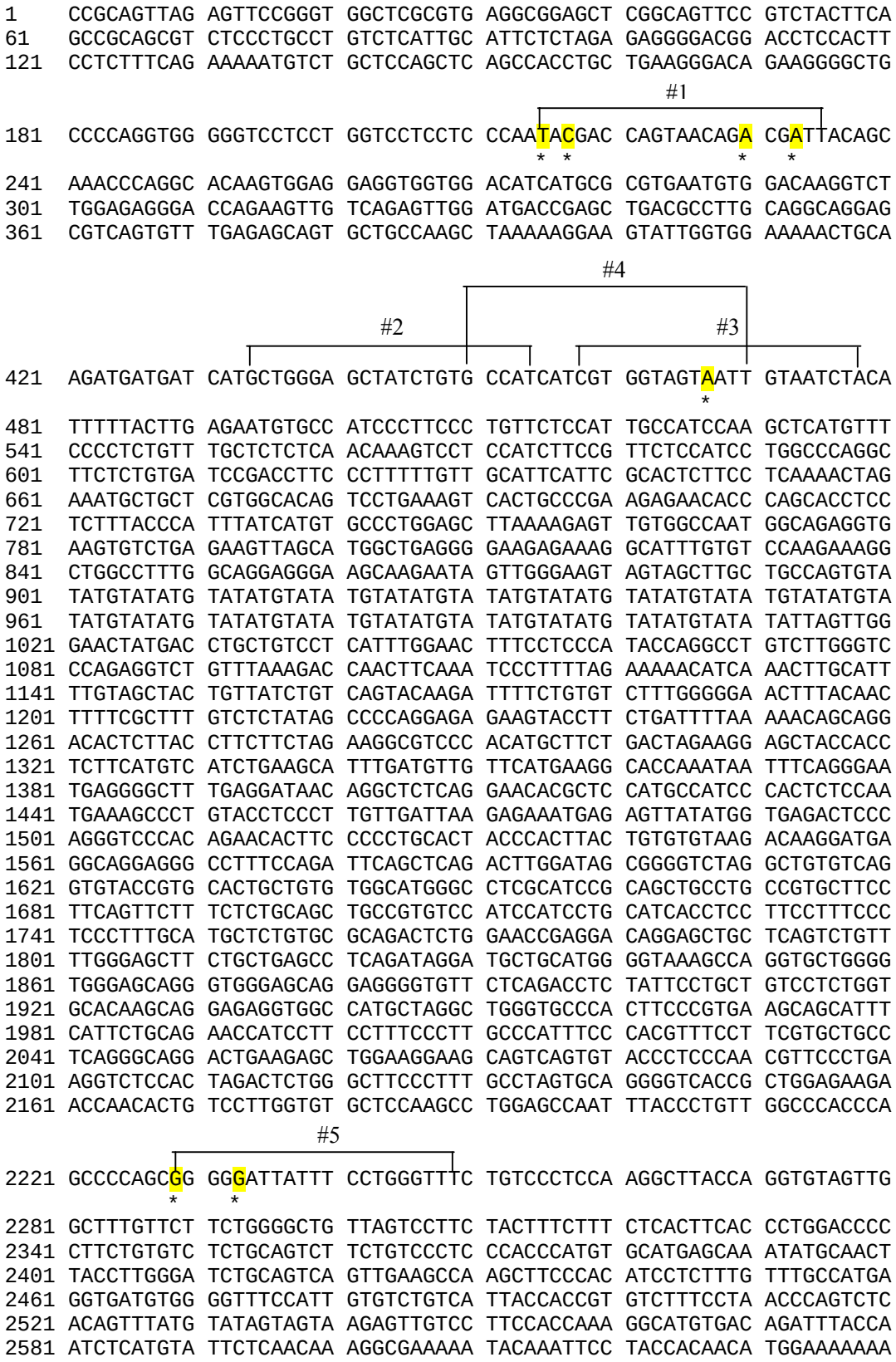


```
1    CCGCAGTTAG AGTTCCGGGT GGCTCGCGTG AGGCGGAGCT CGGCAGTTCC GTCTACTTCA
61   GCCGCAGCGT CTCCCTGCCT GTCTCATTGC ATTCTCTAGA GAGGGGACGG ACCTCCACTT
121  CCTCTTTCAG AAAAATGTCT GCTCCAGCTC AGCCACCTGC TGAAGGGACA GAAGGGGCTG

181  CCCCAGGTGG GGGTCCTCCT GGTCCTCCTC CCAATACGAC CAGTAACAGA CGATTACAGC
                                      * *             *   *

241  AAACCCAGGC ACAAGTGGAG GAGGTGGTGG ACATCATGCG CGTGAATGTG GACAAGGTCT
301  TGGAGAGGGA CCAGAAGTTG TCAGAGTTGG ATGACCGAGC TGACGCCTTG CAGGCAGGAG
361  CGTCAGTGTT TGAGAGCAGT GCTGCCAAGC TAAAAAGGAA GTATTGGTGG AAAAACTGCA

421  AGATGATGAT CATGCTGGGA GCTATCTGTG CCATCATCGT GGTAGTAATT GTAATCTACA
                                            *

481  TTTTTACTTG AGAATGTGCC ATCCCTTCCC TGTTCTCCAT TGCCATCCAA GCTCATGTTT
541  CCCCTCTGTT TGCTCTCTCA ACAAAGTCCT CCATCTTCCG TTCTCCATCC TGGCCCAGGC
601  TTCTCTGTGA TCCGACCTTC CCTTTTTGTT GCATTCATTC GCACTCTTCC TCAAAACTAG
661  AAATGCTGCT CGTGGCACAG TCCTGAAAGT CACTGCCCGA AGAGAACACC CAGCACCTCC
721  TCTTTACCCA TTTATCATGT GCCCTGGAGC TTAAAAGAGT TGTGGCCAAT GGCAGAGGTG
781  AAGTGTCTGA GAAGTTAGCA TGGCTGAGGG GAAGAGAAAG GCATTTGTGT CCAAGAAAGG
841  CTGGCCTTTG GCAGGAGGGA AGCAAGAATA GTTGGGAAGT AGTAGCTTGC TGCCAGTGTA
901  TATGTATATG TATATGTATA TGTATATGTA TATGTATATG TATATGTATA TGTATATGTA
961  TATGTATATG TATATGTATA TGTATATGTA TATGTATATG TATATGTATA TATTAGTTGG
1021 GAACTATGAC CTGCTGTCCT CATTTGGAAC TTTCCTCCCA TACCAGGCCT GTCTTGGGTC
1081 CCAGAGGTCT GTTTAAAGAC CAACTTCAAA TCCCTTTTAG AAAAACATCA AACTTGCATT
1141 TTGTAGCTAC TGTTATCTGT CAGTACAAGA TTTTCTGTGT CTTTGGGGGA ACTTTACAAC
1201 TTTTCGCTTT GTCTCTATAG CCCCAGGAGA GAAGTACCTT CTGATTTTAA AAACAGCAGG
1261 ACACTCTTAC CTTCTTCTAG AAGGCGTCCC ACATGCTTCT GACTAGAAGG AGCTACCACC
1321 TCTTCATGTC ATCTGAAGCA TTTGATGTTG TTCATGAAGG CACCAAATAA TTTCAGGGAA
1381 TGAGGGGCTT TGAGGATAAC AGGCTCTCAG GAACACGCTC CATGCCATCC CACTCTCCAA
1441 TGAAAGCCCT GTACCTCCCT TGTTGATTAA GAGAAATGAG AGTTATATGG TGAGACTCCC
1501 AGGGTCCCAC AGAACACTTC CCCCTGCACT ACCCACTTAC TGTGTGTAAG ACAAGGATGA
1561 GGCAGGAGGG CCTTTCCAGA TTCAGCTCAG ACTTGGATAG CGGGGTCTAG GCTGTGTCAG
1621 GTGTACCGTG CACTGCTGTG TGGCATGGGC CTCGCATCCG CAGCTGCCTG CCGTGCTTCC
1681 TTCAGTTCTT TCTCTGCAGC TGCCGTGTCC ATCCATCCTG CATCACCTCC TTCCTTTCCC
1741 TCCCTTTGCA TGCTCTGTGC GCAGACTCTG GAACCGAGGA CAGGAGCTGC TCAGTCTGTT
1801 TTGGGAGCTT CTGCTGAGCC TCAGATAGGA TGCTGCATGG GGTAAAGCCA GGTGCTGGGG
1861 TGGGAGCAGG GTGGGAGCAG GAGGGGTGTT CTCAGACCTC TATTCCTGCT GTCCTCTGGT
1921 GCACAAGCAG GAGAGGTGGC CATGCTAGGC TGGGTGCCCA CTTCCCGTGA AGCAGCATTT
1981 CATTCTGCAG AACCATCCTT CCTTTCCCTT GCCCATTTCC CACGTTTCCT TCGTGCTGCC
2041 TCAGGGCAGG ACTGAAGAGC TGGAAGGAAG CAGTCAGTGT ACCCTCCCAA CGTTCCCTGA
2101 AGGTCTCCAC TAGACTCTGG GCTTCCCTTT GCCTAGTGCA GGGGTCACCG CTGGAGAAGA
2161 ACCAACACTG TCCTTGGTGT GCTCCAAGCC TGGAGCCAAT TTACCCTGTT GGCCCACCCA

2221 GCCCCAGCGG GGGATTATTT CCTGGGTTTC TGTCCCTCCA AGGCTTACCA GGTGTAGTTG
               *   *

2281 GCTTTGTTCT TCTGGGGCTG TTAGTCCTTC TACTTTCTTT CTCACTTCAC CCTGGACCCC
2341 CTTCTGTGTC TCTGCAGTCT TCTGTCCCTC CCACCCATGT GCATGAGCAA ATATGCAACT
2401 TACCTTGGGA TCTGCAGTCA GTTGAAGCCA AGCTTCCCAC ATCCTCTTTG TTTGCCATGA
2461 GGTGATGTGG GGTTTCCATT GTGTCTGTCA TTACCACCGT GTCTTTCCTA ACCCAGTCTC
2521 ACAGTTTATG TATAGTAGTA AGAGTTGTCC TTCCACCAAA GGCATGTGAC AGATTTACCA
2581 ATCTCATGTA TTCTCAACAA AGGCGAAAAA TACAAATTCC TACCACAACA TGGAAAAAAA
```

Fig. 4.17B. Rat Sbr I cDNA sequence (GenBank accession No. NM_013090). *5 shRNA targeting regions are indicated and the nucleotides differing from mouse gene are pointed by * and highlighted in yellow.*

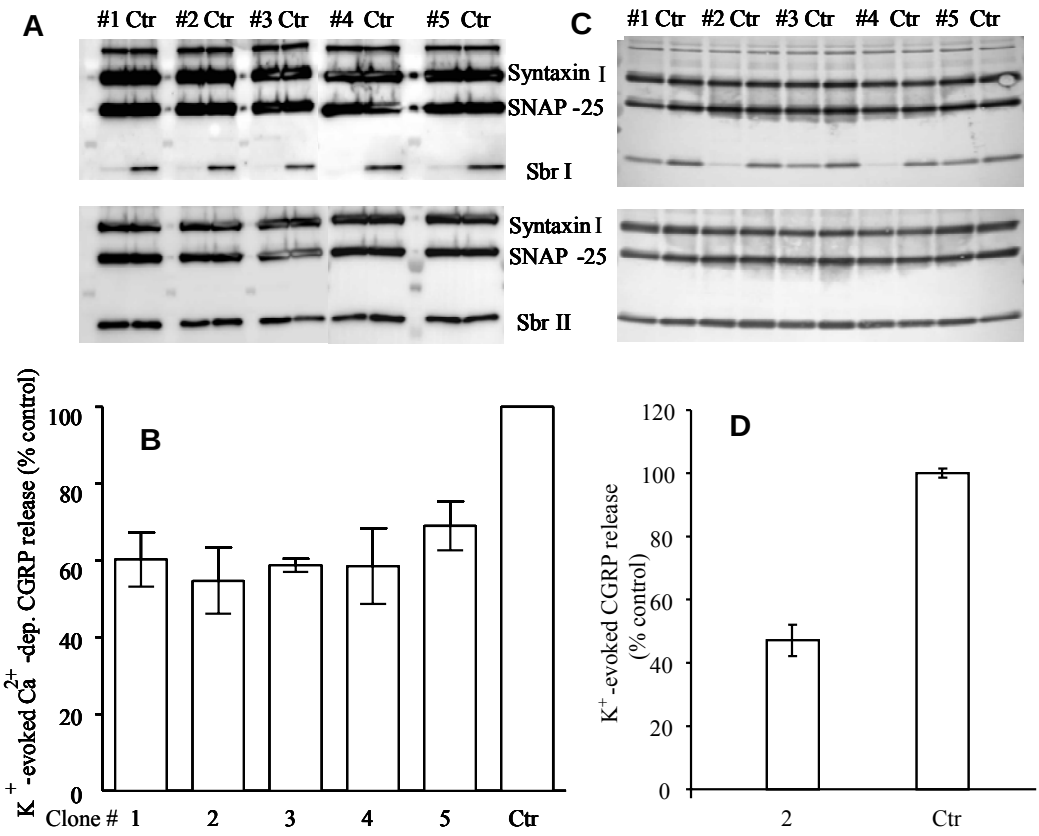

Fig. 4.18 Knock down of Sbr I by shRNA caused significant reduction of K^+-evoked CGRP release. *TGNs at 7 DIV were separately infected by 5 different Sbr I shRNA lentiviral particles (3x 10^5 each). At 8-10 days post-infection, release of CGRP from infected- and non-infected control cells under basal and 60 mM [K^+] stimulation conditions were assayed. Released cells were then solubilised in 2xLDS sample buffer and equal volumes (1/10) of samples were subjected to SDS-PAGE and Western blotting. The same samples were loaded onto two different gels seperately blotted with antibodies against SNAP-25, syntaxin I and Sbr I or Sbr II. Representative immunoblots showing Sbr I protein level in all 5 clones infected mouse TGNs (A) or clone #2- and #4-infected rat TGNs (C) was significantly decreased compared to non-infected control cells, whereas shRNA did not affect Sbr II expression. Other SNARE proteins, SNAP-25 and syntaxin I also maintained unchanged in treated cells and non-treated cells. The antibodies used for Sbr I and II are isoform-specific with no cross-reactivity with each other. Knock down of Sbr I expression caused substantial reduction of K^+-evoked CGRP release in mouse (B) and in rat (D) compared to non-infected control. Data plotted are means ± s.e.m.; n = 4 (mouse) or 2 (rat).*

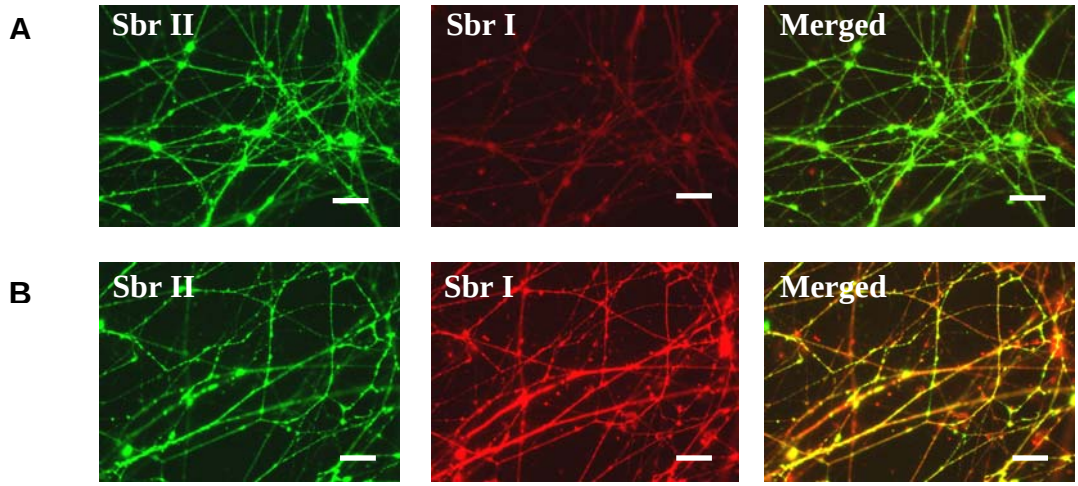

Fig. 4.19 Immuno-fluorescence staining demonstrated reduction of Sbr I expression in the shRNA-treated samples compared to control cells. *Mouse TGNs grown on coverslips at 7 DIV were infected by clone #3 shRNA lentiviral particles. At 8 days post infection, cells were fixed, permeabilised and stained with rabbit anti-Sbr I (1:1000) followed by donkey anti-rabbit Alexa Fluor 546 (1:200) or mouse anti-Sbr II (1:1000) followed by donkey anti-mouse Alexa Fluor 488 (1:200). Representative micrographs show the reduced Sbr I expression and unchanged Sbr II level in the (A) shRNA treated relative to the (B) un-treated control specimens, by indirect immuno-cytochemistry staining. ShRNA clone #3 treated cells were chosen as a representative example. Scale bar=20μm.*

4.3 Discussion

The evidence obtained for SNAP-25 being essential for K^+-evoked CGRP release is clear-cut because BoNT/A caused near-complete inhibition (~ 90%) and an equivalent extent of cleavage. This accords with its putative acceptor ─ synaptic vesicle protein 2A, B and C (Dong et al., 2006; Mahrhold et al., 2006) ─ being found in the TGNs. In contrast, capsaicin-elicited exocytosis of CGRP from TGNs proved largely non-susceptible to BoNT/A; this corresponds to the a minimal inhibition of SP release by this toxin from rat dorsal root ganglionic neurons (Purkiss et al., 2000). As VR1-positive TGNs express SV2, BoNT/A should be able to enter the capsaicin-responsive neurons. Although SNAP-23 is non-susceptible to BoNT/A, only a low level was detected in TGNs; therefore, this seems inadequate to explain the lack of inhibition of CGRP exocytosis from capsaicin-sensitive neurons. Thus, the observed lower efficiency of BoNT/A in blocking capsaicin–evoked release of CGRP may be due to the known ability of elevated intra-neuronal Ca^{2+} concentration to partially reverse BoNT/A-induced inhibition [(Sakaba et al., 2005; Verderio et al., 2004), see Chapter 5]; this could result from a large, capsaicin-triggered Ca^{2+} influx through the non-selective cation channel of the VR1 receptor (Caterina et al., 2000) and, also, causes Ca^{2+}-induced Ca^{2+} release form the internal Ca^{2+} store (Karai et al., 2004). Contrary to the consistent outcome of this study and that of (Purkiss et al., 2000), there is a single report that a haemagglutinin–toxin complex of type A blocks capsaicin-evoked CGRP release from TGNs (Durham and Cady, 2004); however, the latter result could not be reproduced and a more indepth mechanism study was conducted to investigate the inability of BoNT/A inhibitions CGRP release elicited by capsaicin (see Chapter 5). Unlike SNAP-25, determination of the contribution of syntaxin I to exocytosis from TGNs was not possible because a near-equal cleavage of syntaxin I and SNAP-25 by BoNT/C1 precluded assessment of their individual contributions to its partial inhibition of CGRP release.

Evidence for Sbr being essential for CGRP release evoked by K^+, capsaicin or bradykinin was provided by the inhibition of each with BoNT/D associated with cleavage of Sbr I, II and III; moreover, basal efflux seemed to be reduced which accords with its ability to reduce spontaneous release at crayfish motor synapses (Hua et al., 1998). As this neurotoxin cleaved all 3 isoforms of Sbr, assessment of their relative contributions to exocytosis necessitated carrying out additional experiments with type B which is unable to cleave Sbr I in rat (Fig. 4.6 A). Despite near-complete

cleavage of Sbr II (and III) by 100 nM BoNT/B, its observed inability to cause any detectable inhibition of K^+-evoked CGRP release indicated that these two isoforms are not essential as their roles can be taken by Sbr I. The possibility of BoNT/B-resistant CGRP release occurring from a sub-population of neurons unable to internalize this toxin was excluded by the complete cleavage of Sbr II and, especially, the demonstrated presence of synaptotagmin I/II in all of the CGRP-positive neurons because these proteins act as acceptors for the /B toxin (Chai et al., 2006; Dong et al., 2003; Jin et al., 2006). Participation of Sbr I in CGRP exocytosis is an interesting and novel feature of TGNs, also seen with K^+-evoked Ca^{2+}-dependent release of SP from rat TGNs which proved non-susceptible to BoNT/B but was inhibited by serotypes /D or /A. Importantly, BoNT/B did cleave Sbr I and blocked exocytosis of CGRP from mouse TGNs. Use of newly-generated chimera AB and BA have shed significant light on the functionality of Sbr I. Chimera AB with its H_C/B domain was found to enter rat TGNs, cleave SNAP-25 and cause inhibition of CGRP release to the same extent as BoNT/A. This demonstrated the presence of functional receptors for BoNT/B on all rat TGNs, consistent with immuno-fluorescence staining results showing synaptotagmin I/II present on CGRP positive rat TGNs. Chimera BA, harnessing the H_C/A domain was found to readily enter TGNs (rat and mouse) cleaving almost all Sbr II at a concentration of 100 nM; this blocked CGRP release from mouse but not rat, further confirming Sbr I involvement in CGRP release from TGNs. Knock down of Sbr I gene by shRNA resulted in a substantial reduction in CGRP release. Thus, it is reasonable to conclude that isoform I can mediate CGRP release from LDCVs, at least in sensory neurons. This is supported by co-immunoprecipitation experiments on TGNs showing that Sbr I occurs in SNARE complexes that contain SNAP-25 and syntaxin I. A large proportion of these complexes proved resistant to SDS-denaturation and showed Mr > 100 k on SDS-PAGE unless the samples were boiled, in which case the signals for the individual SNARE components were increased due to complex disassembly. These features are characteristic of neuronal SNARE complexes (Hayashi et al., 1994; Otto et al., 1997). Moreover, CGRP-containing vesicles immuno-isolated by Sbr I-specific IgGs possessed Sbr I and II; accordingly, LDCVs isolated by density gradient centrifugation were shown to contain CGRP as well as the SNAREs (Sbr I, II and III together with SNAP-25 and syntaxin I). In rat where Sbr I is non-susceptible to BoNT/B, this toxin can nevertheless block exocytosis from central neurons of several transmitters (e.g. glutamate, γ-amino-butyrate) (Foran et al., 2003; Schoch et al., 2001;

Verderio et al., 2004). These published data indicate that the majority of Ca^{2+}-dependent exocytosis from SCSVs in these neurons (at least 80% of glutamate release from rat cerebellar neurons) requires Sbr II and/or III; thus, it seems Sbr I is not essential for the latter. Likewise, a major role for Sbr II in exocytosis from SCSVs (Takamori et al., 2006) accords with its predominance therein and correlates with a 100-fold reduction in Ca^{2+}-triggered fast transmitter release in knock-out mice lacking this isoform (Schoch et al., 2001). Hence, the ability of Sbr I to support exocytosis in TGNs is not replicated in all neuron types, possibly due to the reported differential expression of Sbr I and II (Aguado et al., 1999; Trimble et al., 1990). Unfortunately, the release of detectable levels of classical SCSV transmitters could not be elicited from the TGNs with the stimulation methods used for CGRP and, thus, it was not possible to investigate the responsible Sbr isoform. Utilisation of Sbr I may be a characteristic of sensory neurons because studies on rat derived preparations, in which this isoform is BoNT/B-resistant, have shown that cleavage of Sbr II/III blocks exocytosis of noradrenaline release from 'large dense-core like' vesicles in cerebrocortical synaptosomes and PC-12 cells (Ashton and Dolly, 1997; Lomneth et al., 1991). Although this is the first demonstration that Sbr I can mediate regulated exocytosis in TGNs, it is noteworthy that dopamine release from LDCVs in rat brain nerve terminals can be reduced by BoNT/B but not its somato-dendritic release (Bergquist et al., 2002). Therefore, considering this together with our direct evidence leads to the deduction that Sbr I participates in toxin B-resistant release from rat TGNs at sites remote from the active zones in the presynaptic membrane where CGRP exocytosis has been shown to occur (Bernardini et al., 2004). Indeed, as BoNT/B was completely ineffective in reducing CGRP release (despite cleaving all the Sbr II and III in rat TGNs), it must largely arise from vesicles that contain Sbr I. Based on all these consistent findings, it is apparent that Sbr I can underlie this special type of exocytosis which would allow the released CGRP to activate its receptor on blood vessels in the vicinity (Edvinsson, 2004). This also seems to apply to other sensory neurons because K^{+}-evoked CGRP release from DRG neurons from mouse, but not rat, is blocked by BoNT/B. Furthermore, our proposal is supported by the lack of statistically significant inhibition of SP release by BoNT/B (unlike other serotypes) in cultured neurons from embryonic rat DRGs (Welch et al., 2000). In fact, the demonstrated involvement of Sbr I in peptide exocytosis from LDCVs in sensory neurons may contribute to the neurological defects found in mice with a Sbr I null mutation that die soon after birth

(Nystuen et al., 2007). Undoubtedly, identifying SNARE isoforms used preferentially in exocytosis from different vesicle types in other varieties of secretory cells, and pinpointing the inherent functional advantages, should shed light on subtle dissimilarities likely to exist in the exocytotic processes and/or their fine control in eukaryotic cells.

Colletively, BoNTs and the newly developed chimeric toxins proved instrumental in dissecting the exocytosis pathway, providing evidence for the functionality of the SNAREs and, in one case, pinpointing Sbr I involvment in the pain-peptides release from sensory neurons. Also, the chimeric toxins may have distinctive pharmacological potential. Although BoNT/D served as a universal blocker of the release from sensory neurons, human neuromuscular junction has been demonstrated to be insensitive to BoNT/D due to lack of its receptor (Coffield et al., 1997), which excludes it as a therapeutic for humans. Another toxin, BoNT/A blocked K^+- and bradykinin- evoked release, but hardly affected capsaicin-elicited release; the latter is a specific stimulant for C-fibres, indicating the requirement for an alternative (see Chapter 5), or a variant toxin. The information gained from this chapter provides new insights for designing novel recombinant chimeric BoNTs with improved anti-nociceptive function over natural BoNTs that should be effective on human sensory neurons (see Chapter 5).

5.0 Capsaicin-evoked CGRP release from nociceptive neurons is resistant to BoNT/A due to sustained increased $[Ca^{2+}]_i$ but can be inhibited by a re-targeted E/A chimera

5.1 Overview

Initial reports on the clinical applications of BoTOX for alleviating the symptoms of migraine indicated beneficial outcomes in just a certain group of sufferers (Mauskop, 2002; Silberstein et al., 2000). However, the impressive improvement in these responders, whose symptoms had proved resistant to other therapeutic regimes, highlights the importance of in-depth neurochemical examination of the inhibitory action of BoNT variants on the release of pain mediators from sensory neurons. Further justification is provided by the likelihood that an effective BoNT-based therapy will emerge for tension headache and other forms of chronic pain (Foran et al., 2003; Gupta, 2005) because of the occurrence in various neuron types of the toxin's target, SNAP-25. Such an important prospect is heightened by the remarkable success of BoTOX in treating numerous conditions arising from hyper-activity of nerves innervating muscles (Dolly, 2005) or secretory glands (Kim et al., 2006), due to cleavage of SNAP-25 by its LC protease (Dolly and Lawrence, 2007). Already, it is becoming apparent that the anti-nociceptive effects of BoTOX arise from peripheral inhibition of the release of transmitters/pain mediators (e.g. CGRP, SP and glutamate) which, in turn, minimise sensitisation of pain relay systems in the brain (Aoki, 2005). Nevertheless, though attenuation of nociception by this toxin has been demonstrated in animal pain models (Bach-Rojecky et al., 2005; Cui et al., 2004), other studies have found it to be ineffective (Schulte-Mattler and Martinez-Castrillo, 2006; Voller et al., 2003).

TGNs, maintained in culture, provide a suitable model (Durham and Cady, 2004) for biochemical investigation of the inhibition by BoNTs of Ca^{2+}-dependent CGRP exocytosis, a process known to involve SNAP-25, Sbr I and, probably, syntaxin I (Chapter 4). CGRP release can be triggered from TGNs by K^{+}-depolarisation, bradykinin or capsaicin; bradykinin acts on its type 2 receptor and causes acute sensation of pain whereas capsaicin activates C-fibres by binding to VR1, opening its non-selective cation channel and, thereby, inducing pain (Caterina et al., 2000). Type A BoNT was found to inhibit CGRP exocytosis induced by elevated $[K^{+}]$ or bradykinin but to exert minimal effect on that evoked by capsaicin despite TGNs containing the toxin's acceptor and target (Chapter 4). To gain insights into this enigma, BoNT/E was investigated because it shares the same intracellular SNARE target as /A but cleaves 26 rather than 9 residues off the C-terminus of SNAP-25 (Binz et al., 1994). Furthermore, it could offer additional features attractive for future therapeutic purposes, namely, faster neuro-paralysis than /A (Lawrence et al., 2007; Simpson, 1980; Simpson and

DasGupta, 1983) indicating a more rapid translocation into neurons (Keller et al., 2004). Surprisingly, the present study found BoNT/E to be virtually ineffective in cleaving SNAP-25 and blocking CGRP release from TGNs. As this raised the suspicion of these lacking a high-affinity acceptor for /E (its identity remains unknown), the H_C binding moiety of BoNT/E was replaced by its counterpart from /A (Wang et al., 2008). By availing of the toxin's independent domains (Stevens et al., 1991), this EA chimera exploits the most active moieties of the two serotypes. It was shown that EA entered cultured rat CGNs faster than BoNT/A and potently cleaved SNAP-25 in TGNs, blocked the transfer of synaptic vesicle proteins to the cell surface and inhibited CGRP release elicited by all stimuli, including capsaicin.

5.2 Results

5.2.1 Capsaicin-evoked CGRP release from TGNs is only partially inhibited by BoNT/A and virtually resistant to /E

Although BoNT/A entered TGNs and displayed a dose-dependent cleavage of SNAP-25 (up to ~ 85% with 1 μM; Fig. 5.1 A) that correlates with its inhibition of K^+-evoked CGRP release (cf. Fig. 4.1), secretion elicited by bradykinin was blocked to a slightly lesser extent and the exocytotic response to capsaicin was only reduced by <20% even at 1 μM toxin (Fig. 5.1 B). As this suggests that the 9 residues removed from the C-terminus of SNAP-25 by BoNT/A are not essential for inhibiting capsaicin-triggered CGRP release, the effects of deleting a total of 26 amino acids with type E were examined because it potently blocks exocytosis from central and peripheral neurons (Foran et al., 2003; Lawrence et al., 2007). Surprisingly, TGNs proved virtually insensitive to BoNT/E, as reflected by the absence of SNAP-25 cleavage except for a trace at high concentations (Fig. 5.1 C) and the observation that neither K^+- nor capsaicin-triggered CGRP release were reduced by more than 15% (Fig. 5.1 D). These findings suggest that TGNs lack a high-affinity acceptor for BoNT/E, unlike motor nerve terminals and cultures of other neuron types which internalise it more rapidly than /A (Keller et al., 2004; Wang et al., 2008). Alternatively, it is possible that capsaicin could stimulate release via a mechanism utilising an /E-insensitive homologue. Clearly, an alternative strategy was required to examine the role of SNAP-25 in CGRP release elicited by capsaicin from these sensory neurons. Hence, a chimera

consisting of the acceptor-binding domain (H_C) of /A together with SNAP-25 cleaving LC of /E and H_N/E was utilised.

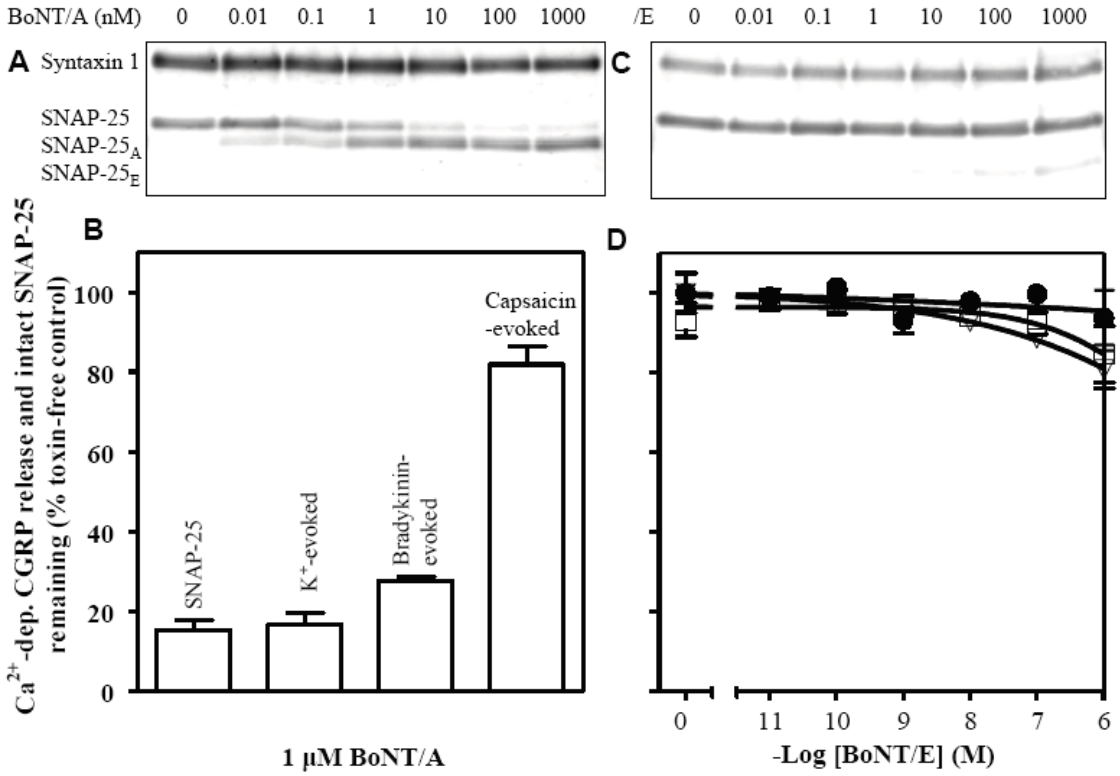

Fig. 5.1 BoNT/A cleaves SNAP-25 in TGNs and inhibits CGRP release evoked by K^+ >bradykinin>>capsaicin whereas BoNT/E is ineffective. *Rat cultured TGNs at 7 DIV were exposed to BoNT/A (A, B) or /E (C, D) at 37°C in culture medium for 24 hours. Evoked release of CGRP (B, D) over 30 minutes at 37°C was measured by EIA (see Chapter 2). Cells were then solubilised in LDS-sample buffer and equal volumes subjected to SDS-PAGE and Western blotting (A, C), using an antibody that recognises intact and truncated SNAP-25. The proportions of intact substrate remaining (B, D) were calculated relative to the internal control, uncleaved syntaxin, by visualisation with its specific antibody and analysis of digital images of the gels. SNAP-25 was extensively cleaved by BoNT/A (A, B) but not /E (C, D, ▽). BoNT/A inhibited CGRP exocytosis (B) triggered by K^+ or bradykinin but gave a minimal reduction in that evoked by capsaicin; there was negligible inhibition by /E (D) of the release evoked by 60 mM K^+ (□) or 1 µM capsaicin (●). Data plotted are means ± S.E.M.; n ≥ 3.*

5.2.2 Generation of chimera EA toxin: its design, production and characterisation

As BoNT/A binds to cell surface acceptors via the C-terminal moiety of its HC, H_C, delivery of the BoNT/E protease activity (i.e. its LC) into TGNs was attempted by swapping its H_C domain with the corresponding region of /A. For this purpose, a synthetic DNA fragment encoding the LC and H_N portions of BoNT/E had been ligated to that encoding BoNT/A H_C, expressed as a single-chain (SC) in *E. coli,* purified and converted to the activated disulphide-linked dichain (DC) form (Wang et al., 2008).The schematic construction map is described in Fig. 5.2.

5.2.3 Chimera EA toxin displays the desired properties

EA was expressed and purified as a SC polypeptide whose major protein band migrated as Mr~145 k band upon SDS-PAGE in either the absence or presence of DTT; a minor amount of larger, aggregated material (that disappeared upon reduction) was detected by Coomassie staining and Western blotting (Fig. 5.3). Western blotting demonstrated the presence of BoNT/E LC and epitopes from BoNT/A (Fig. 5.3 B, C) in the SC and confirmed the absence of truncated forms. Controlled proteolytic nicking converted the SC to a disulphide-linked DC which, as expected, showed different behaviour in SDS-PAGE in either the absence or presence of DTT (Fig. 5.3 A). Incubation with Trypzean achieved complete nicking of the chimera, as demonstrated by the appearance of Mr~97 k HC and Mr~47 k LC upon SDS-PAGE of the DC in the presence of DTT, whereas it appeared as a Mr~145 k band in the absence of reducing agent indicating that the inter-chain disulphide bond had been formed in the vast majority of the toxin (Fig. 5.3 A). The presence of the requisite moieties (LC/E and H_C/A) in EA DC and the successful removal of the His_6 tag were confirmed by Western blotting (Fig. 5.3). Therefore, the expected domains from each parental toxin were demonstrated to be incorporated into chimera EA (Fig. 5.3).

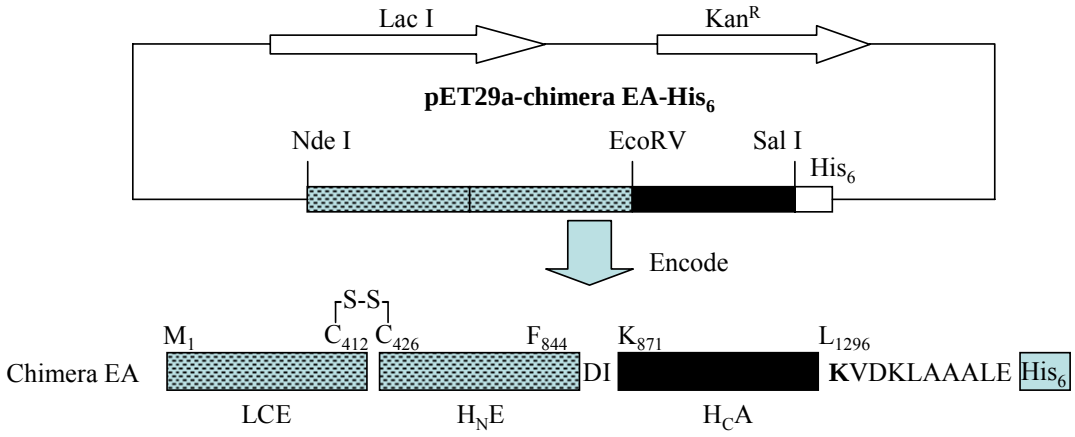

Fig. 5.2 Schematic representation of the novel EA chimeric construct generated. *Chimera EA gene consists of synthetic LC-H_NE (hatched box) and H_CA (black box) gene fragments which were cloned into pET29a vector followed by C-ter His_6 sequence (Wang et al., 2008). Numbers refer to residue positions in the amino acid sequences (GenBank^{TM} accession numbers AF488749 and X62683) of corresponding parental BoNTs. S-S denotes the interchain disulphide bridge formed between LC and HC. Letters between bars specify amino acids in the single letter code that were chosen as linkers between domains.*

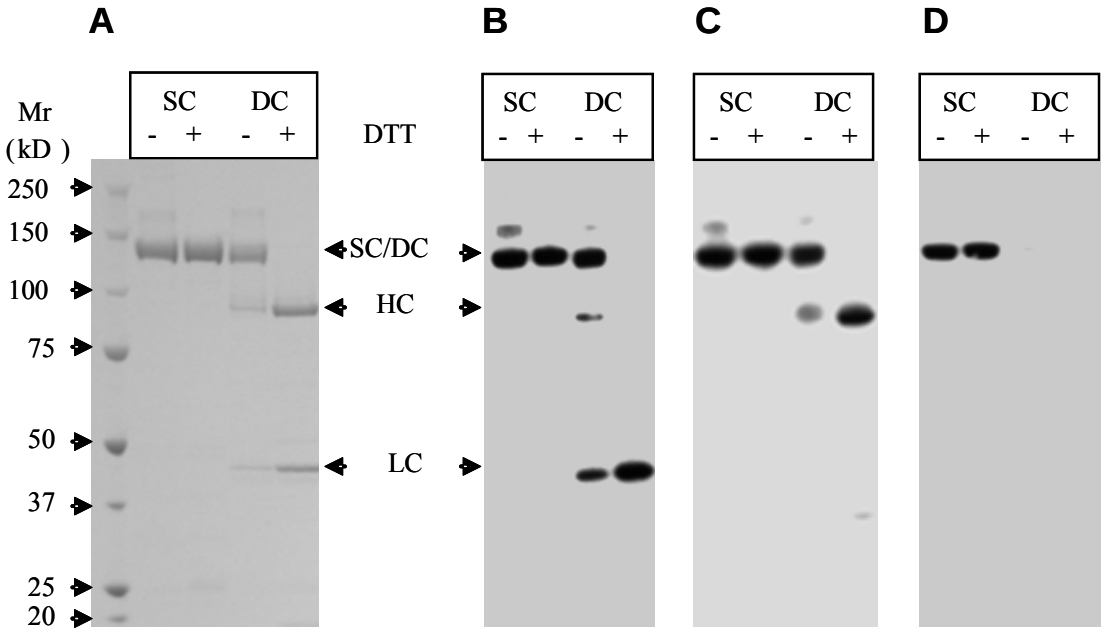

Fig. 5.3 Properities of chimera EA: a highly purified and completely nicked recombinant protein. *EA toxin was expressed in E.coli, purified by immobilized metal affinity and cation exchange chromatography (Wang et al., 2008); the resultant SC toxin was converted to the DC form using trypzean (8 μg/mg BoNT incubated at room temperature for 1 hour). Aliquots were subjected to SDS-PAGE on 4-12% Bis-Tris gels in the absence or presence of 25 mM DTT (as indicated), followed by either Coomassie staining (A) or Western blotting (B-D) with antibodies against LC/E (B), BoNT/A (C) and His_6(D). Arrows indicate the positions of SC/DC, HC and LC.*

5.2.4 EA binds to the SV2C acceptor for /A and cleaves SNAP-25 like /E

To examine if EA had acquired the binding selectivity of BoNT/A, its interaction with the fourth intra-lumenal loop of SV2C (SV2C-L4) (Fig. 5.4 A) was examined because this together with gangliosides act as acceptors for H_C/A (Dong et al., 2006; Mahrhold et al., 2006). A SV2C fragment fused to GST (GST-SV2C-L4) and immobilised on glutathione-Sepharose was incubated with BoNT/A, /E or EA plus gangliosides before assessing toxin binding by Western blotting (see Chapter 2). As expected, BoNT/A was recovered with the glutathione-Sepharose when GST-SV2C-L4 was present (Fig. 5.4 B); on omitting the fusion protein from control incubations no association with glutathione-Sepharose could be detected (data not shown). In contrast, BoNT/E failed to bind the fusion protein-beads, confirming that BoNT/A but not /E binds to SV2C (Mahrhold et al., 2006). Importantly, the DC form of EA was recovered with the affinity resin containing SV2C-L4, demonstrating that substitution of the H_C of BoNT/E with the corresponding domain of /A conferred the acceptor specificity of the latter onto the chimera. As SC EA also bound the SV2C fusion protein (Fig. 5.4 B), nicking is not essential for interaction with the acceptor. EA also proved enzymically active towards a model substrate GFP-SNAP-25(134-206)-His_6 (Wang et al., 2008) yielding a truncated fragment that co-migrated on SDS-PAGE with the product of BoNT/E but not /A (Fig. 5.4 C). This established the presence of /E-like protease activity in EA.

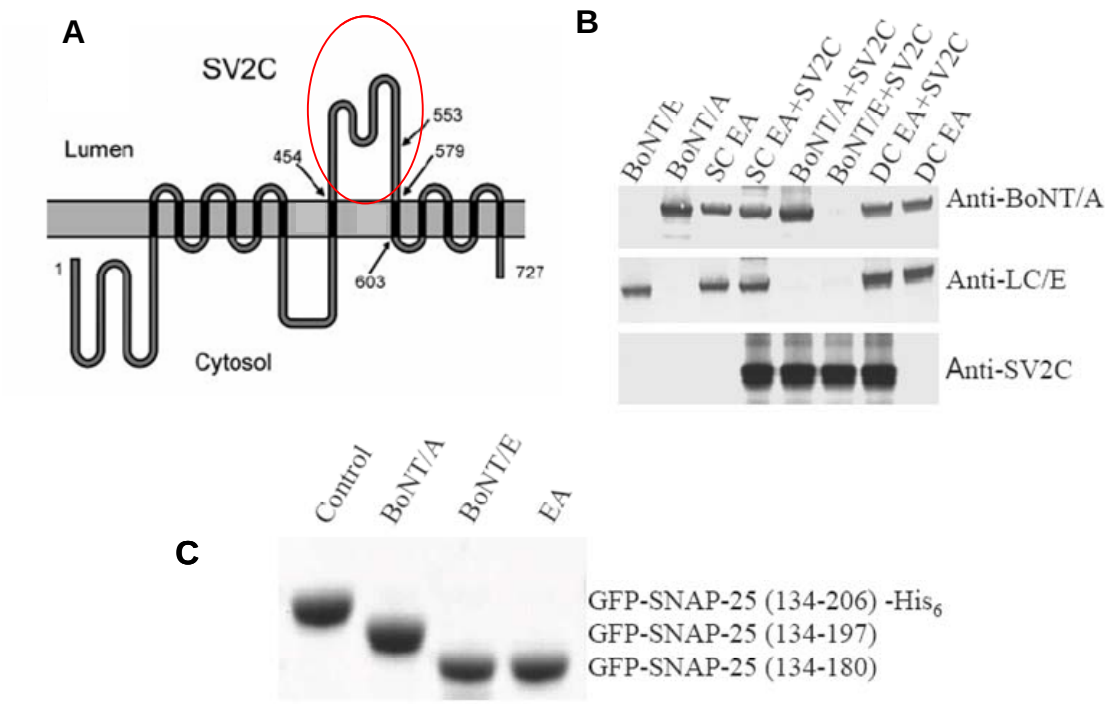

Fig. 5.4 Both SC and DC forms of EA bind to SV2C-L4 like BoNT/A but give /E-like cleavage products in vitro. *(A) SV2C structure with the fourth loop highlighted in red circle, cited from (Mahrhold et al., 2006); SV2C has 12 transmembrane domains and one large intravesicular domain, named loop 4. Numbers specify amino acid positions of the isoform SV2C. (B) GST-SV2C-L4 immobilised on glutathione–Sepharose beads was incubated with EA (SC or DC), BoNT/A or /E (DC) at 4°C for 4 hours; after extensive washing, the bound proteins were eluted in LDS sample buffer; < 5% of the total protein or 40 ng of marker toxins were analyzed by SDS-PAGE (see Chapter 2). Toxins and the fusion protein were subsequently detected by Western blotting with the antibodies indicated. (C) A model substrate [GFP-SNAP-25(134-206)-His_6; 13.5 µM] was incubated with 25 nM EA or its parental toxins for 30 minutes at 37°C (Wang et al., 2008); reactions were stopped by adding LDS-sample buffer and equal amounts of protein subjected to SDS-PAGE followed by Coomassie staining.*

5.2.5 EA cleaves SNAP-25 in cultured CGNs as well as BoNT/E and shows a faster rate of uptake than BoNT/A

5.2.5.1 EA efficiently binds, enters into rat cultured CGNs and cleaves SNAP-25

Cultured CGNs 7 DIV were incubated with native BoNT/A, /E or chimera EA for ~24 hours. These three toxins exhibited similar cleavage activity (Fig. 5.5 A) except /A reached saturation point at ~60% cleavage; this indicates EA is fully active (Fig. 5.5 B).

5.2.5.2 EA enters cultured neurones more rapidly than /A

The uptake of BoNT/A, /E or EA chimera was also studied in CGNs. Using conditions that stimulate synaptic vesicle recycling (Foran et al., 2003) in CGNs, which may promote the activity-dependent uptake of BoNTs as occurs at the neuromuscular junction (Dong et al., 2006), the potencies to BoNT/A, /E and EA chimera were increased but to different extents (Wang et al., 2008). However, the rates of cellular intoxication by BoNT/E and EA were clearly faster compared with BoNT/A (Fig. 5.6). Cleaved SNAP-25 was observed within 15 or 45 min of exposure to BoNT/E or chimera EA (Fig. 5.6 A); furthermore, in both cases, 50% of the total target had been cleaved within 160 min. In contrast, no product was detectable at 80 min in BoNT/A-treated cells, and <20% SNAP-25 proteolysis occurred after 160 min (Fig. 5.6). These findings indicate that the apparent relatively rapid uptake of BoNT/E in these different neuronal populations can be attributed to its H_N and/or LC. Moreover, the rate of uptake is not determined by acceptor binding domain, as EA and /A both bind to acceptor SV2 (Fig. 5.4) that is not used by /E (Mahrhold et al., 2006). It was reported in previous study that the protease rate of chimera EA is similar to /A but faster than /E (Wang et al., 2008). Thus, faster translocation to the cytosol seems to be the sole reason for the more rapid appearance of protease products.

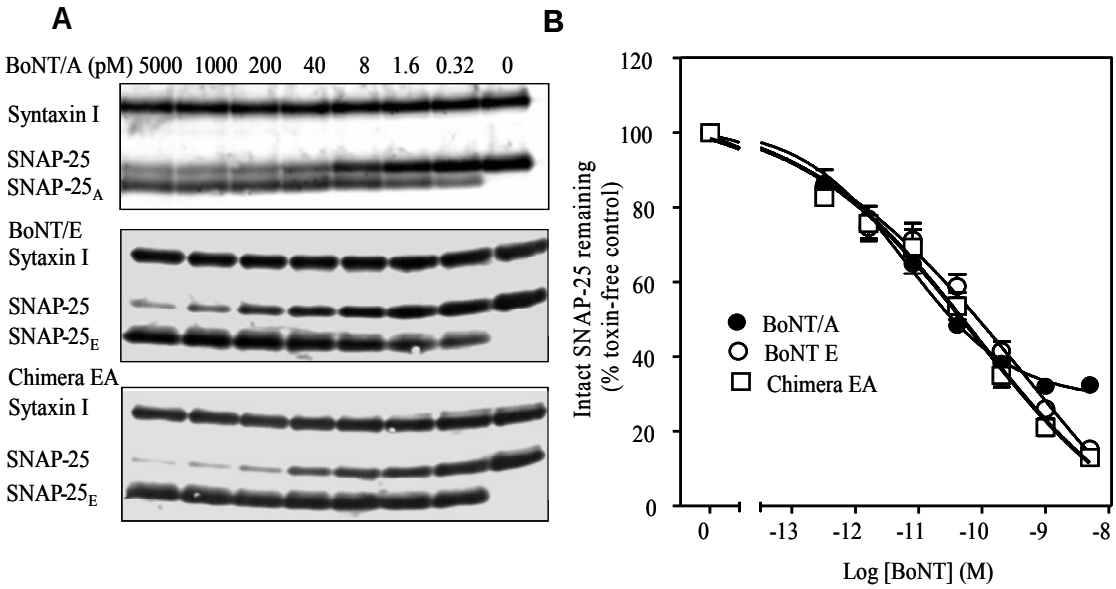

Fig. 5.5 EA efficiently cleaves SNAP-25 with similar potency as BoNT/E or /A in CGNs. *CGNs 7 DIV were incubated for 24 hours in culture medium with the specified concentrations of BoNT/A, /E or chimera EA. After removal of toxins by washing, cells were then solubilized in LDS-sample buffer and equal volumes of protein subjected to SDS-PAGE and Western blotting (A), with the specific antibodies indicated. (B) The extents of SNARE cleavage were quantified by densitometrically scanning and the proportion of substrate remaining calculated relative to an internal control, syntaxin I. Data plotted are means ± s.e.m.; n = 3.*

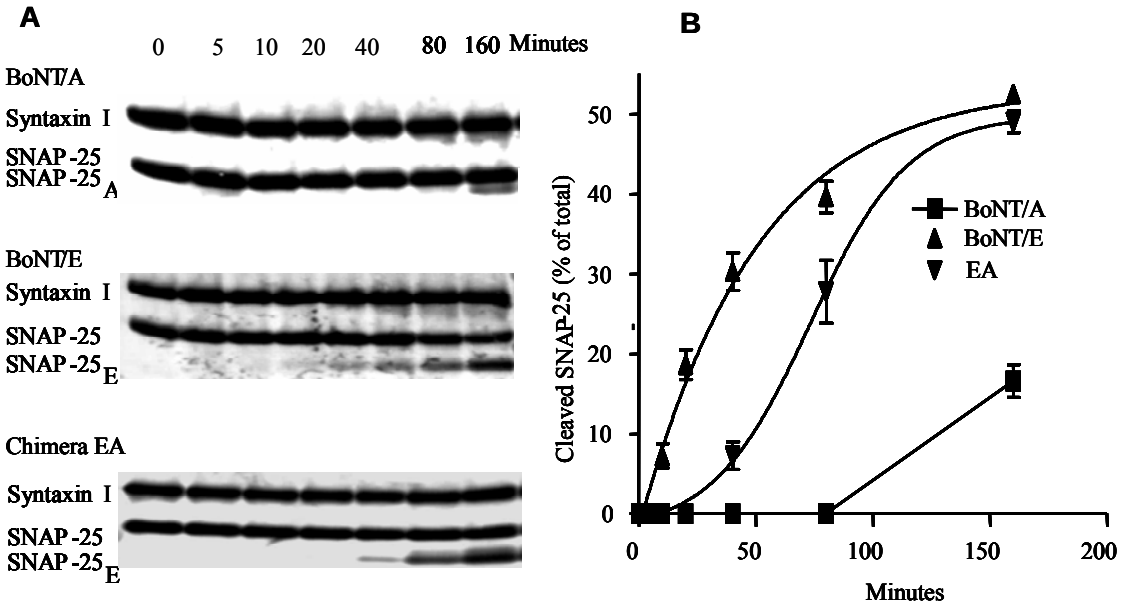

Fig. 5.6 EA enters cultured neurones more rapidly than /A. *CGNs 7 DIV were incubated with 500 pM toxins for 5 min in depolarization buffer (56 mM K^+) followed by washing with medium and incubation under the indicated conditions in culture medium. After removal of medium, cells were then solubilized in SDS-sample buffer and equal amounts of protein subjected to SDS-PAGE and Western blotting, with the specific antibodies indicated (A). The extents of SNARE cleavage were quantified by densitometrically scanning and the proportion of substrate remaining calculated relative to an internal control (syntaxin I) (B).*

5.2.6 EA, unlike /A, blocks synaptic vesicle fusion and CGRP release triggered by capsaicin in addition to K^+ depolarisation

The functional activity of EA relative to /A could be shown by monitoring its influence on the trafficking of exocytotic vesicles to the cell surface, using a proven immuno-cytochemical technique (Matteoli et al., 1992). Binding of a mAb (Syt-Ecto), specific for the intra-lumenal domain of the synaptic vesicle protein synaptotagmin I, to TGNs was stimulated greatly by either K^+-depolarisation (Fig. 5.7 A) or 1 μM capsaicin (Fig. 5.7 B). This indicated increased exposure of the epitope due to fusion of vesicles containing synaptotagmin I with the plasmalemma. Although pre-exposing TGNs to 100 nM BoNT/A blocked the enhancement of Syt-Ecto binding by K^+-depolarisation (Fig. 5.7 A), this did not prevent the increase in binding elicited by 1 μM capsaicin (Fig. 5.7 B), consistent with the toxin's feeble inhibition of CGRP release elicited by this stimulus (Fig. 5.1 A). In contrast, EA prevented both capsaicin-triggered exposure of the Syt-Ecto epitope as well as that elicited by depolarisation, revealing blockade of vesicle fusion regardless of the stimulus (Fig. 5.7 B).

The toxins' potencies for blocking CGRP release from TGNs relative to cleavage of SNAP-25 were assessed by exposing primary cultures to a range of concentrations, as described in Fig. 5.1. The cells were > 1000-fold more susceptible to chimera EA (Fig. 5.8) than BoNT/E (cf Fig. 5.1 C, D), based on their EC_{50} values for SNAP-25 cleavage being ~ 1 nM and >> 1 μM, respectively. Moreover, CGRP release was inhibited dose-dependently by EA (Fig. 5.8 B) whereas BoNT/E was impotent (cf. Fig. 5.1 D). Interestingly, after 12 hours incubation which proved to be optimal for SNAP-25 cleavage and CGRP release inhibition (data not shown), the concentration-dependency of EA for inhibition of CGRP-release (Fig. 5.8 B) elicited by bradykinin (EC_{50} = 0.8 nM) correlated very closely to the level of SNAP-25 cleavage, and K^+-evoked release showed intermediate susceptibility. Although blockade of the capsaicin-triggered response was the least sensitive (EC_{50} ~ 10 nM), it showed far greater sensitivity to EA than BoNT/A (cf Fig. 5.1 A).

Clearly, recombination of the most desirable features of BoNT/E and /A to create chimera EA produced a more effective and broad-range inhibitor of CGRP release from sensory TGNs. As BoNT/A and EA bind to the same acceptor and, by extrapolation, the same population of cells, it seems probable that the greater versatility

of EA can be attributed to a more effective disabling of SNAP-25 than is caused by BoNT/A.

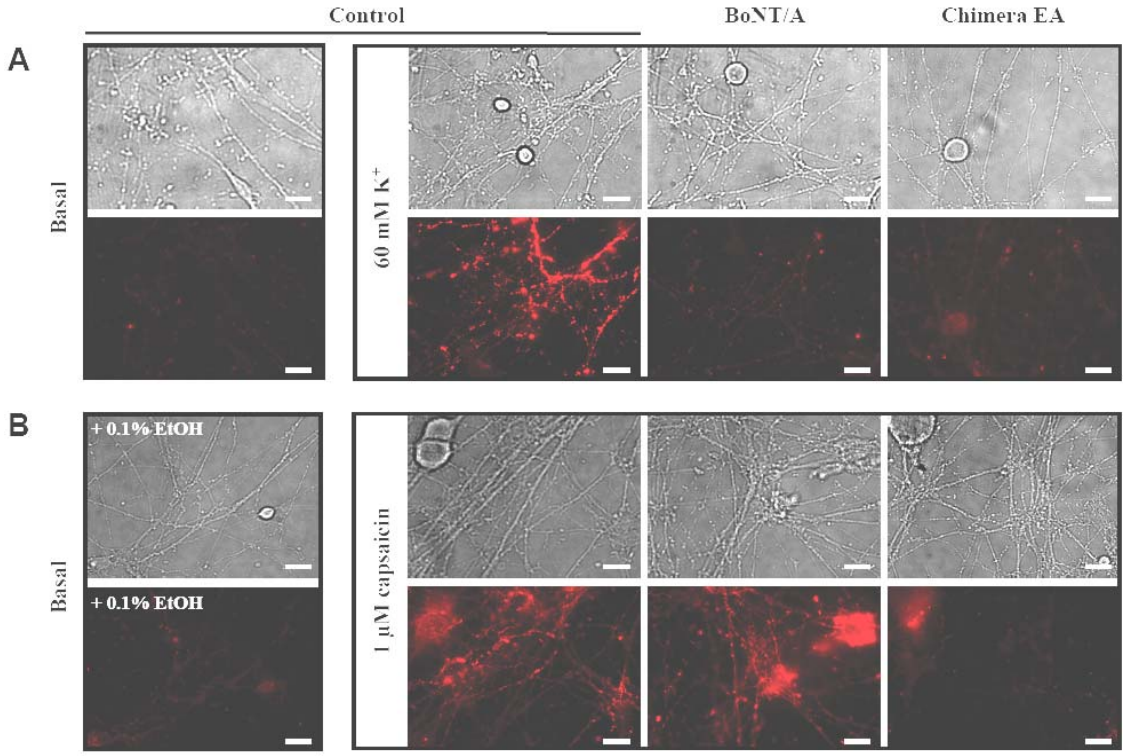

Fig. 5.7 EA and BoNT/A both inhibit K^+-evoked binding of synaptotagmin 1 antibody to sensory neurons whereas only EA blocked the capsaicin-stimulated interaction. *TGNs were grown on coverslips for 7 DIV, incubated with or without 100 nM EA or BoNT/A for 24 hours before washing, and exposure to Syt-Ecto antibody for 15 minutes in either basal or 60 mM K^+ (A) or 1 µM capsaicin (B). Cells were then fixed (see Chapter 2) and images of the same field recorded in phase contrast (top panels) or fluorescent mode (bottom panels). The increased fluorescent signal induced by K^+ stimulation was reduced to basal level by both toxins; in contrast, the elevated signal elicited by capsaicin remained unaffected by /A but significantly reduced by EA. In B, the vehicle (0.1% ethanol) for capsaicin was added to the basal medium. Scale bar = 20 µm.*

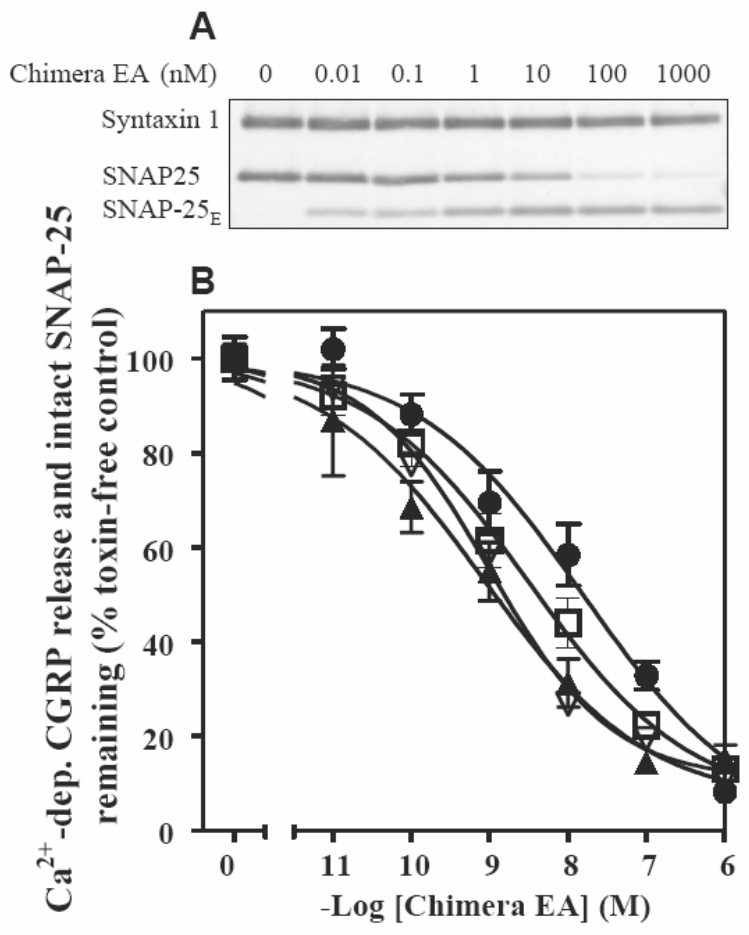

Fig. 5.8 EA enters /E-resistant TGNs, cleaves SNAP-25 and inhibits CGRP release evoked by all stimuli. *Cultured TGNs at 7 DIV were exposed to EA at 37°C in culture medium for 12 hours, and release of CGRP was assayed; Western blotting of the cells were performed and results calculated (as in Fig. 5.1) for cleavage of SNAP-25 (▽) by EA (A, B). (B) EA-induced inhibition of CGRP release evoked by 60 mM K^+ (□), 0.1 μM bradykinin (▲) or 1 μM capsaicin (●). Data plotted are means ± S.E.M.; n ≥ 4.*

5.2.7 The inhibitory ineffectiveness of BoNT/A compared to EA in TGNs accords with a differential stability of SNARE complexes formed by their SNAP-25 cleavage products

It has been reported that the 17 amino acids between the cleavage sites for BoNT/A and /E at the C-terminal of SNAP-25 are required for its high affinity binding to syntaxin (Bajohrs et al., 2004), although previous studies had found that N-terminal residues 2-82 are sufficient (Chapman et al., 1994; Hayashi et al., 1994). In view of these conflicting *in vitro* data, obtained with recombinant fusion proteins or tagged protein fragments, formation of SNARE complexes in sensory neurones *in situ* was examined for possible perturbations by BoNT/A or EA. For this purpose, neurones were solubilised with SDS and subjected to two-dimensional PAGE before detection of SNAREs by Western blotting (Lawrence and Dolly, 2002). This protocol exploits the stability of SNARE complexes, which resist dissociation in SDS at ambient temperature and can be electrophoretically separated from non-complexed SNAREs (Hayashi et al., 1994). Subsequent heating of the gel sections denatures the complexes and liberates their constituents, which can be resolved by a second electrophoresis step. In SDS extracts from non-intoxicated cells, the majority of each immunologically-detected SNARE (syntaxin, SNAP-25 and Sbr I) was not associated with any SDS-resistant complex (Fig. 5.9; note samples in lanes marked * were diluted before electrophoresis). This is shown by their migrations in PAGE being unchanged by boiling and matching the mobilities predicted by their molecular masses. However, some SNAP-25 was retarded in the primary gel, but not in the second gel of the boiled sample demonstrating that a minority of this protein is associated with SDS-resistant SNARE complexes. SNAP-25 was present in complexes of variable size from Mr = 52k to over 288k and, particularly, in the 104-288k range. Likewise, syntaxin was detected in SNARE complexes with Mr values between 52 and >288k; the 146-205k range showed the strongest intensity. In contrast, only a weak Sbr I immuno-signal could be detected, restricted to the Mr = 104-205k range. These observations suggest that some of the SNAP-25 and syntaxin in sensory neurones are associated tightly enough to resist dissociation by SDS. Sbr I (Fig. 5.9 A) appear to be minor components, indicative of the majority being binary SNAP-25:syntaxin complexes. However, it is not possible to calculate the precise ratio of each SNARE with the semi-quantitative technique used here. Stimulation of the TGNs with capsaicin produced only a moderate increase in the amounts of SDS-resistant complexes detected (Fig. 5.9 A) compared to

resting samples (data not shown). In cells exposed for 24 hours to 100 nM BoNT/A, the bulk of SNAP-25 was truncated, as shown by its increased mobility on PAGE (Fig. 5.9 A); notably, both cleaved and uncleaved SNAP-25 were detected in SDS-resistant complexes. Syntaxin was also found to be present together with a trace of Sbr I in these toxin-treated samples. The fraction of each SNARE associated with the complexes did not seem to be altered compared to non-intoxicated cells. Clearly, SNAP-25_A retains the ability to form SDS-resistant complexes with its SNARE partners. In contrast, only traces of SNAP-25_E were associated with complexes in the 74-146k range in TGNs treated with EA, despite most of the SNAP-25 having been cleaved (Fig. 5.9 A). In the EA- treated samples, the quantity of complexes was clearly reduced compared to toxin-free cells or those exposed to BoNT/A; minute amounts of uncleaved SNAP-25 and syntaxin were found in those complexes but Sbr I was undetectable. The inability of SNAP-25_E to form complexes in sensory TGNs, unlike SNAP-25_A, seems a likely explaination for the more extensive inhibition of exocytosis by EA than BoNT/A.

In separate series of experiments, the apparent scarcity of Sbr I in SDS-resistant SNARE complexes in TGNs was probed using BoNT/D because it cleaves Sbr I, II & III and inhibits evoked CGRP release (see Chapter 4). In cells exposed to this toxin, the amount of non-complexed Sbr I was reduced by 80% and Sbr I could not be detected in SDS-resistant complexes (Fig. 5.9 B). Nevertheless, the latter complexes containing syntaxin and SNAP-25 were not diminished compared to toxin-free controls, supporting the notion that such binary complexes lack Sbrs. In TGNs exposed simultaneously to both BoNT/A and /D, ~ 50% of the SNAP-25 and 80% of Sbr I were cleaved; notably, only intact SNAP-25 was found in complexes from these TGNs (only a trace of SNAP-25_A was detected), a striking contrast to its distribution in cells exposed to BoNT/A alone (Fig. 5.9 A). This suggests that Sbr I is required for stabilisation of complexes containing SNAP-25_A even though it cannot be detected in SDS-resistant complexes. One possible explanation is that Sbr I weakly associates with syntaxin:SNAP-25 (or SNAP-25_A) but is dissociated by SDS during cell solubilisation. If stable binding with syntaxin underlies the ability of SNAP-25_A to support CGRP release in TGNs, intact Sbr is essential for this to occur.

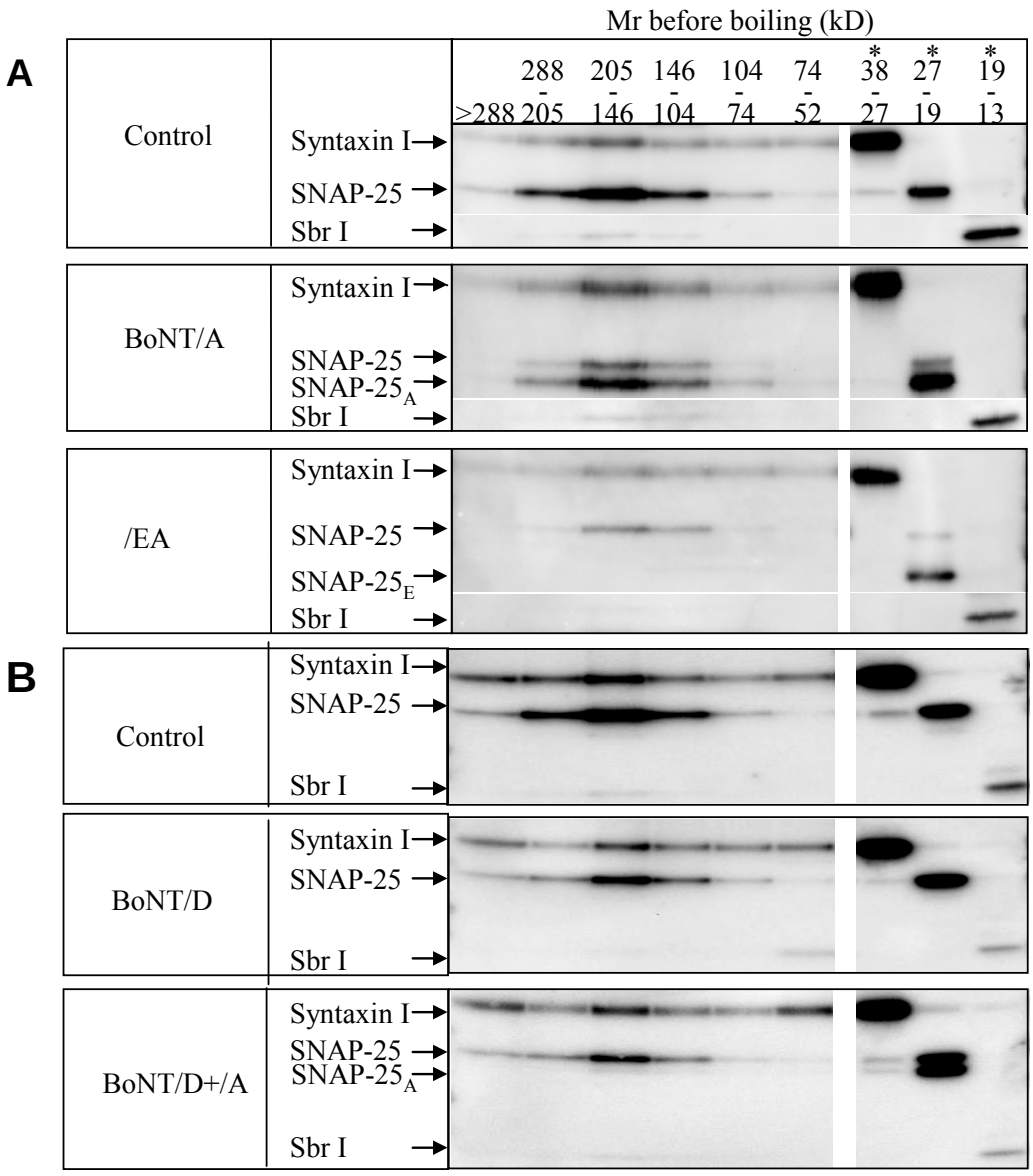

Fig. 5.9 The presence of BoNT/A-truncated SNAP-25 in SDS-resistant SNARE complexes requires intact Sbr. *TGNs at 7 DIV were incubated with or without (A) 100 nM BoNT/A or EA or (B) 100 nM BoNT/D or 100 nM BoNT/D plus BoNT/A in culture medium for 24 hours. After toxin removal, cells were stimulated with 1 µM capsaicin in the presence of 2.5 mM Ca^{2+} for 30 minutes, before lysis in 2xLDS sample buffer and SDS-PAGE (without boiling). Gel sections containing the separated proteins were excised according to migration distance and extracted by boiling in LDS sample buffer before re-electrophoresis and immunoblot analysis (see Chapter 2). Antibodies against syntaxin, SNAP-25 (recognizing intact and cleaved products) or Sbr I were used. Pictures shown are from a single experiment representative of results obtained on 3 independent occasions; ∗ 20% of sample volume was loaded was used in the lanes (A, B).*

5.2.8 BoNT/A and EA reduce the sensitivity to external Ca^{2+} of CGRP exocytosis triggered by K^+ from TGNs but only EA alters the Ca^{2+}-dependency of the response to capsaicin

SNAP-25 binds to synaptotagmin, a Ca^{2+}-sensor thought to be the regulator of vesicle fusion, through Ca^{2+}-independent and -stimulated interactions (Schiavo et al., 1997). The C-terminus of SNAP-25 has been implicated in the latter because its removal reduces the level of Ca^{2+}-dependent binding (Gerona et al., 2000). However, in the case of SNAP-25_A, the interaction is restored if $[Ca^{2+}]_i$ is elevated, suggesting that BoNT/A reduces the sensitivity of the Ca^{2+}-sensor. This finding has been used to explain the restoration of function to BoNT/A-intoxicated nerve terminals following treatments that open Ca^{2+}-channels and/or increase membrane permeability to Ca^{2+}. Applying this reasoning to the observed lack of blockade by BoNT/A of capsaicin-elicited responses from TGNs, stimulation with this agonist of VR1 may provoke greater elevation of $[Ca^{2+}]_i$ than K^+-depolarisation and, thereby, overcome the postulated reduction in Ca^{2+} sensitivity for triggering CGRP release. To test this hypothesis, the effects of BoNT/A or EA on the $[Ca^{2+}]$-dependency and amounts of CGRP release from TGNs were quantified in the absence and presence of capsaicin or a Ca^{2+}- ionophore, ionomycin.

Notably, dependencies on external $[Ca^{2+}]$ of the responses to K^+ and capsaicin were similar in control cells (Fig. 5.10 A, B), although there was a higher level of basal release in the presence of capsaicin; the EC_{50} values for external $[Ca^{2+}]$ were 0.6 and 0.9 mM, respectively, whilst EC_{MAX} was ~5 mM in both cases. CGRP release elicited by either stimulus (Fig. 5.10 A, B) was effectively inhibited by 100 nM EA at $[Ca^{2+}]$ up to 5 mM, with some lessening at higher concentrations; the Ca^{2+}-sensitivity was, apparently, reduced with respect to toxin-free control. In contrast, 100 nM BoNT/A poorly inhibited responses to capsaicin even at low external $[Ca^{2+}]$ but virtually abolished K^+-evoked CGRP release in 1 mM $[Ca^{2+}]$ or less; however, further increments in external $[Ca^{2+}]$ supported increasing levels of K^+-evoked CGRP release, with over 80 % of the maximal level seen at an extremely high $[Ca^{2+}]$ (Fig. 5.10 A). Assuming 100% recovery from inhibition could be achieved, the EC_{50} of Ca^{2+} for depolarisation-evoked release from BoNT/A-treated cells was ~15 mM, a ~30-fold reduction in sensitivity relative to that for toxin-free cells. On the other hand, BoNT/A did not alter the external Ca^{2+}-dependency of capsaicin-evoked CGRP release (EC_{50} ~1 mM) despite causing a partial decrement in the amount of exocytosis in response to

each [Ca^{2+}] (Fig. 5.10 B). Notably, the latter findings are difficult to reconcile with BoNT/A directly lowering sensitivity of the Ca^{2+}-sensing mechanism. To gain insights into this differential reversibility, the influence of altering $[Ca^{2+}]_i$ on the restoration of CGRP release from inhibition by toxins was investigated. TGNs treated with 100 nM BoNT/A or EA for 24 hours resulted in ~70-80 % inhibition of K^+-evoked CGRP release (Fig. 5.10 C). Although ionomycin (5 μM) gave a small (~10%) increase in CGRP release from toxin-free cells stimulated by K^+, it caused ~70% and ~20% recovery of exocytosis from cells pre-treated with BoNT/A or EA, respectively (Fig. 5.10 C). Notably, in Ca^{2+}-free medium, ionomycin and K^+ depolarisation failed to elicit any release from toxin-treated cells, indicating a requirement for extracellar Ca^{2+}. In contrast to K^+ depolarisation, ionomycin slightly decreased (~15%) the amount of CGRP release from toxin-free cells stimulated by capsaicin (Fig. 5.10 D); moreover, it did not rescue capsaicin-evoked CGRP release blocked by EA (Fig. 5.10 D; $p > 0.05$). When Ca^{2+} was omitted, neither capsaicin nor ionomycin could evoke release from TGNs pre-treated with BoNT/A or EA (Fig. 5.10 D). As differences in intracellular Ca^{2+} signalling could account for the observed discrepancy between the BoNT/A susceptibilities of responses to K^+-depolarisation and capsaicin, this was examined using TGNs pre-loaded with the membrane permeable Ca^{2+}-indicator dye, Fluo 4-AM.

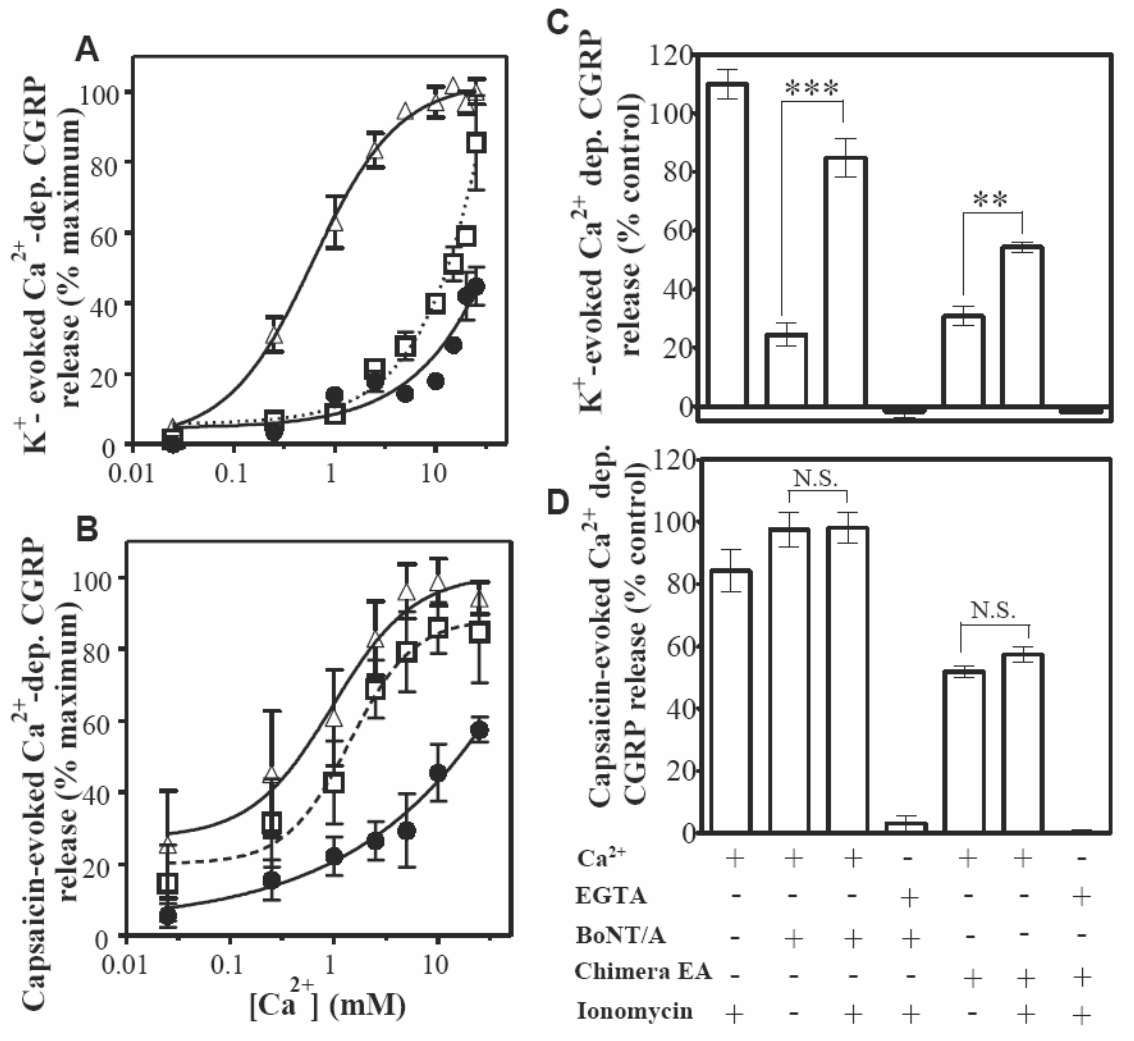

Fig. 5.10 Raising extracellular [Ca^{2+}] reveals differences in the effects of BoNT/A and EA on the Ca^{2+} dependency of release from capsaicin-stimulated cells whereas use of ionomycin showed that K^+-depolarization alone does not elevate $[Ca^{2+}]_i$ sufficiently to overcome inhibition by BoNT/A. *TGNs at 7 DIV were exposed to 100 nM BoNT/A (A, B □ or as indicated in C and D) or EA (A, B, ● or as indicated in C and D) at 37°C in culture medium for ~24 hours. CGRP release was evoked by 60 mM K^+ (A, C) or 1 µM capsaicin (B, D) in BR-HBS containing various [Ca^{2+}] (A, B), 2.5 mM Ca^{2+} in the presence and absence of 5 µM ionomycin, or in Ca^{2+}-free buffer with 2 mM EGTA as indicated (C, D). Vehicle for ionomycin (0.05% DMSO) was included. Exocytosis was normalized to the maximal release (in 25 mM Ca^{2+}) from toxin-free controls (A, B) and to the values from toxin- and ionomycin-free control cells (C, D). Data plotted are means ± S.E.M; n ≥ 3; Student's unpaired t-test: ***, p<0.001; **, p<0.01; N.S., p>0.05.*

5.2.9 Capsaicin elicits a more persistent increase in $[Ca^{2+}]_i$ than K^+ depolarisation

Fluorescence signals in cell bodies of randomly-selected TGNs, preloaded with Fluo 4-AM, was monitored before and during continuous exposure to 60 mM K^+, or 1 μM capsaicin; increased intensity indicates an elevation in $[Ca^{2+}]_i$. Notably, in toxin-free control cells, there was a sharp increase in $[Ca^{2+}]_i$ immediately after superfusion of 60 mM K^+, followed by decay to 50% of the peak within ~10 minutes (Fig. 5.11 A, B). A similarly sharp initial increase in $[Ca^{2+}]_i$ was elicited with 1 μM capsaicin in majority of the cells, presumably the VR1 positive neurons. Although the increment in intensity was lower than that evoked by K^+-depolarisation, the elevated fluorescence persisted longer in capsaicin-treated cells, with > 60% of the peak signal retained after 30 minutes (Fig. 5.11 A, B). Consistent with this, the level of $^{45}Ca^{2+}$ accumulation elicited by capsaicin was > 2-fold higher than that for 60 mM K^+ at each time point with a plateau not being reached even after 30 minutes; in contrast, nearly all the $^{45}Ca^{2+}$ uptake evoked by 60 mM K^+ occurred within 10 minutes (Fig. 5.11 E).

It is noteworthy that pre-treatment with 100 nM BoNT/A (Fig. 5.11 C) or EA (Fig. 5.11 D) did not alter the capsaicin-induced elevation of $[Ca^{2+}]_i$ which was more persistent than that caused by K^+ depolarisation. To ascertain if the prolonged increase in $[Ca^{2+}]_i$ by capsaicin influences exocytosis, the time course of CGRP release was monitored (Fig. 5.11 F). In toxin-free control cells, ~ 50% of the maximum response occurred within 2 minutes of capsaicin application, rising to ~90% at 8 minutes and reaching a plateau level within 15 minutes. Capsaicin-triggered CGRP release from BoNT/A-treated cells was notably lower at early time points ($p = 0.02$, $t = 2$ minutes; unpaired 2-tailed Student's t-test), even though the maximum amount finally released was only slightly lower than in the control ($p = 0.2$, $t = 32$ minutes). Calculation of the increments in release over time (Fig. 5.11 F inset) illustrated that exocytosis initially occurred more rapidly in the control than /A-treated TGNs but decelerated faster ($p = 0.02$, $t = 2$ minutes). These findings indicate that BoNT/A does not reduce the total amount of CGRP-containing vesicles that fuse since the same maximum levels were reached eventually (Fig. 5.11 F) but, rather, lower the apparent initial rate (Fig. 5.11 F inset). Thus, persistence of the Ca^{2+} signalling seems to be more important than $[Ca^{2+}]_i$ for alleviating inhibition by BoNT/A in these sensory neurons. EA decreased the level of exocytosis much further than BoNT/A, with only a fraction of the total release seen after 30 minutes (Fig. 5.11 F). Collectively, our results accord with the relative

stabilities of SNARE complexes containing Sbr I, syntaxin and full-length or BoNT-truncated SNAP-25. Removal of 26 C-terminal amino acids by EA prevents adoption of a stable SDS-resistant conformation and severely blocks CGRP release. In contrast, /A-truncated SNAP-25 is shortened by only 9 C-terminal residues and retains ability to form SDS-resistant complexes with its SNARE partners, but their stability is lower than complexes formed with uncleaved SNAP-25. Hence, BoNT/A inhibits release but, under certain circumstances, exocytosis can be recovered, albeit retarded relative to non-toxin controls; apparently, brief elevation of $[Ca^{2+}]_i$ is insufficient to elicit CGRP exocytosis but prolonged Ca^{2+}- signals can eventually elicit as much release as from toxin-free controls. These results are consistent with the notion that BoNT/A compromises the stability of pre-fusion SNARE complexes required for optimal rates of CGRP exocytosis.

Fig. 5.11 Capsaicin induces a less acute, but more prolonged, increase in $[Ca^{2+}]_i$ than K^+-depolarisation which negates the blockade by BoNT/A of its CGRP triggered release. *(A) Ratios of the fluorescent readings relative to basal value (f/f_0), taken every 10 sec over 30 minutes, are plotted for the control cells (A), BoNT/A- (C) or EA- treated (D) TGNs, recorded under continuous stimulation by 60 mM $[K^+]$ (red), or 1 μM capsaicin (green) in basal buffer. The data are also expressed as % of maximal signal (B) for the control cells. Individual cells were randomly selected for analysis from 2 independent preparations and the values were pooled to give the average ± S.E.M. at each time point; n = 45, 61 for control cells stimulated by 1 μM capsaicin or 60 mM K^+; 67, 46, BoNT/A-; 28, 52 for EA-treated cells. (E) The rates of ^{45}Ca uptake were measured for control cells in 3.5 mM K^+ (◇) and those exposed to 1 μM capsaicin (□) or 60 mM K^+ (△) after incubation for the indicated periods at room temperature with 24 μCi/ml ^{45}Ca. Following extensive washing, the cells were solubilized in 0.1% SDS buffer before counting in a β scintillation spectrometer. Capsaicin-induced ^{45}Ca uptake over 32 minutes into TGNs was ~4 pmol/well from one representative experiment. (F) CGRP release over time was monitored from control cells (△) or those treated for 24 hours with 100 nM BoNT/A (□) or EA (●), as described in Fig. 5.1. The rate of CGRP release (ΔCGRP/Δt) was calculated and plotted in the inset. All data plotted in (E) and (F) are means ± S.E.M., n ≥ 3.*

Fig. 5.11

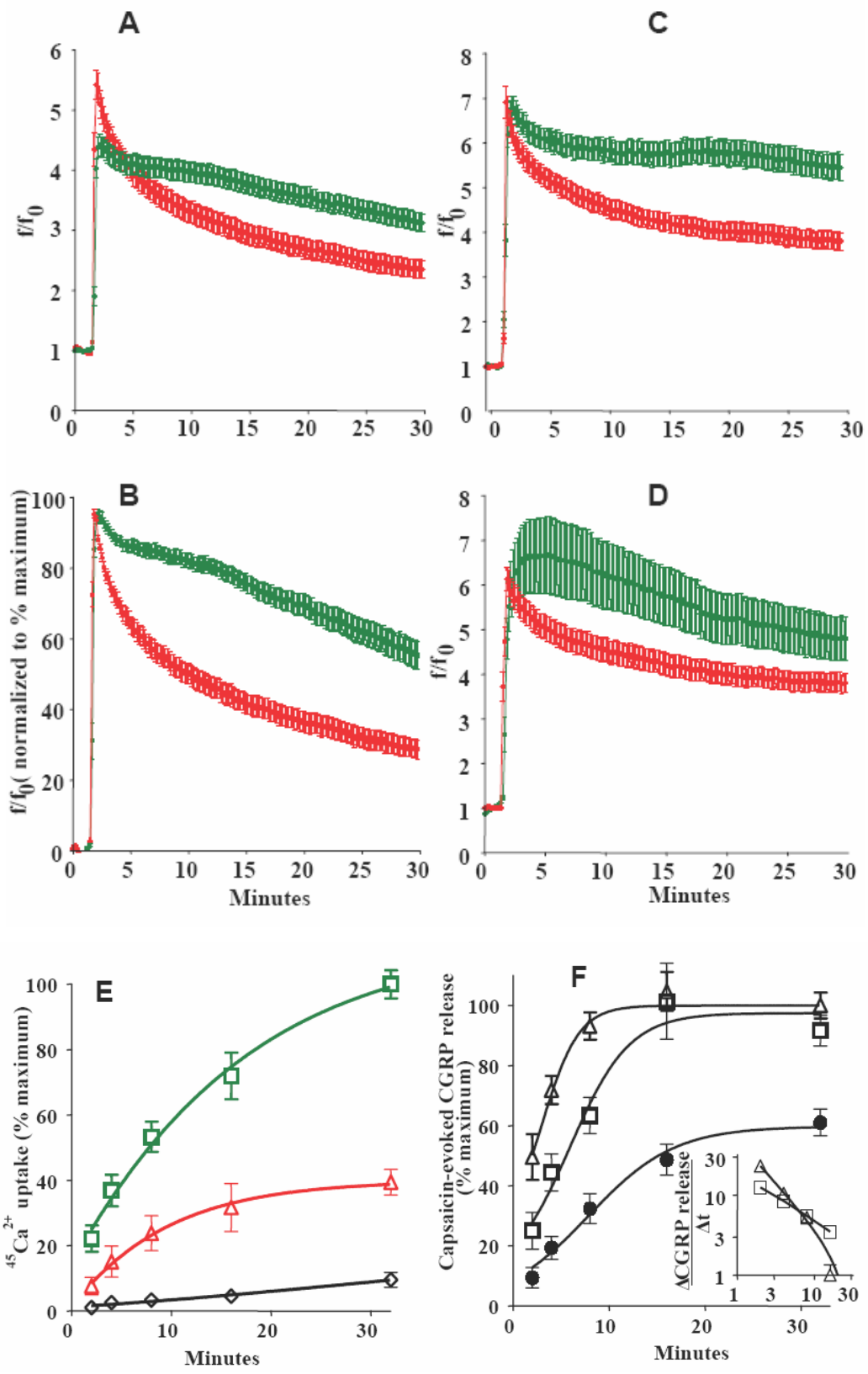
A
C
B
D
E
F
f/f0
f/f0(normalized to % maximum)
Minutes
45Ca2+ uptake (% maximum)
Capsaicin-evoked CGRP release (% maximum)
ΔCGRP release
Δt

5.3 Discussion

The usefulness of BoTOX for the treatment of pain symptoms was revealed by the reduced frequency and intensity of migraines seen in some sufferers who had received injections of BOTOX® (Binder et al., 2000). This accords with the attenuation by the toxin of capsaicin-induced pain in certain patient groups (Bach-Rojecky et al., 2005) and not others (Schulte-Mattler and Martinez-Castrillo, 2006; Tugnoli et al., 2007). In this context, it is noteworthy that capsaicin, a stimulant of sensory C-fibres, but not K^+-depolarisation can trigger secretion of pain mediators from BoNT/A-intoxicated sensory neurones *in vitro*. Although the exact mechanism for pain relief by BoNT/A remains to be deciphered, there is mounting evidence from animal and human studies for a direct action of the toxin on sensory neurons to abrogate the release of pain mediators [(Cui et al., 2004) and reviewed by (Aoki, 2005)]. Therefore, identifying features of other toxin forms with ability to completely block exocytosis from sensory neurones evoked by all stimuli is highly desirable because the resultant findings could help pinpoint the underlying mechanism; moreover, it would be advantageous to incorporate these into any new BoNT-derived analgesic. It was hoped that use of BoNT/E would achieve this objective due to its removal of 17 more residues than deleted by /A from the C-terminus of SNAP-25, and because of its higher potency and faster neuroparalytic action at motor terminals (Lawrence and Dolly, 2002; Simpson and DasGupta, 1983). Furthermore, the shorter lifetime of /E protease compared to type /A (Foran et al., 2003) could be advantageous for treatment of transient pain episodes [e.g. typical duration of pain in migraine is 1 to 3 days (Durham, 2006)], particularly in patients for whom such attacks are infrequent and prolonged inhibition may not be necessary. Disappointingly, in TGNs – a convenient model of sensory neurons – BoNT/E cleaved little SNAP-25 and gave no significant inhibition of CGRP release triggered by K^+ or capsaicin, highlighting a lack of its high-affinity acceptor (presently unknown) or a productive uptake system. Nevertheless, it is suggestive of H_C/E being useful for targetting to other neuron types in conditions where sensory inhibition needs to be avoided (eg. normalization of occular muscles).

Knowing that /A can access TGNs, it was predicted that H_C/A could mediate cell binding of H_NLC/E leading to intra-neuronal delivery of LC/E. Indeed, chimera EA was shown to bind to the /A acceptor SV2 (loop 4), enter the rat cultured CGNs almost as rapid as BoNT/E and faster than /A. Further investigation into a structural basis for the faster transport of BoNT/E protease relative to /A is fully warranted, considering

that development of the full therapeutic response to BoNT/A takes days to a week after injection (Ward and Barnes, 2007) and faster onset of paralysis would be a highly desirable property. Notably, chimera EA produces a more-broadly effective block of evoked CGRP exocytosis than BoNT/A, an important functional attribute. Moreover, this established a requirement for SNAP-25 in capsaicin-elicited peptide release from TGNs, as well as a C-terminal region of SNAP-25, the 17 amino acids between the scissile bonds for each toxin (residues 181-197), being critical. Deciphering a molecular basis for this difference in inhibition by EA and BoNT/A could give insights into the fundamentally important and ubiquitous mechanism of SNARE-driven membrane fusion; also, the outcomes should aid the designing of improved treatments for pain. The greater effectiveness of EA in blocking capsaicin-evoked exocytosis from TGNs correlates with the observed inability of /E cleaved SNAP-25 to form SDS-resistant complexes with syntaxin I. This constrasts with SNAP-25_A which can stably associate with syntaxin I; importantly, this was found to only occur in the presence of intact Sbr, a requirement not applicable to intact SNAP-25. In accord with these findings, *in vitro* studies have shown that BoNT/E more effectively reduces the stability of ternary SNARE complexes compared to /A (Hayashi et al., 1994), an effect attributed to the fact that only 3 of the 9 residues removed by BoNT/A are involved in the formation of coiled-coil α helical domains in the tenary SNARE complex whereas all of the extra 17 residues removed by BoNT/E are required (Sutton et al., 1998). It is noteworthy that syntaxin: SNAP-25 complexes represent an important intermediate that binds Sbr to form a meta-stable ternary complex before Ca^{2+} triggers a rapid 'zippering-up' that is thought to drive membrane fusion (Wojcik and Brose, 2007). One possible interpretation of the inhibitory effect seen with BoNT/A is that pre-fusion complexes are destabilised, as reflected by Sbr being needed for the complexes to acquire resistance to SDS. Such a perturbation could reduce the probability of vesicle fusion, leading to a reduced rate of CGRP release (Fig. 5.11 F). This deduction is fully consistent with the finding that, given sufficient time, almost as much CGRP was released from BoNT/A-treated cells as from controls (see later). However, the question remains as to why secretory responses to K^+-depolarisation (or bradykinin) are effectively blocked by BoNT/A if SNAP-25_A retains some functional capacity?

It is well established that the potent inhibition of neuromuscular transmission by BoNT/A can be attenuated by raising extracellular [Ca^{2+}] or by increasing the Ca^{2+}

permeability of the nerve terminal membrane (Cull-Candy et al., 1976). Herein, it was found that capsaicin-evoked CGRP release was insensitive to BoNT/A and inhibition of K^+-evoked CGRP release was overcome by either increasing the external [Ca^{2+}] or by including the Ca^{2+}-ionophore, ionomycin. Likewise, BoNT/A abolishes K^+-evoked transmitter release from synaptosomes or neuroendocrine cells, but such blockade is alleviated if the cell membrane is rendered permeable to Ca^{2+} with ionophores or pore-forming detergents (Ashton and Dolly, 1991; Lawrence et al., 1996). Hence, it has been postulated that BoNT/A blocks exocytosis by reducing the Ca^{2+}-affinity of the Ca^{2+}-sensor for exocytosis and, in support of this notion, it has been found that a higher [Ca^{2+}] is required to stimulate the binding of synaptotagmin (the putative Ca^{2+}-sensor) to SNAP-25_A than to uncleaved SNAP-25 *in vitro* (Gerona et al., 2000), although the significance of this interesting observation is unclear because ~100-fold higher [Ca^{2+}] was required in the binding than needed to trigger exocytosis (also see below). However, this latest study showed that BoNT/A causes little change in [Ca^{2+}]-sensitivity of capsaicin-evoked release from TGNs. Accordingly, BoNT/A is known to have minimal effect on the $[Ca^{2+}]_i$-dependency for catecholamine release from permeabilised neuroendocrine cells (Gerona et al., 2000; Lawrence and Dolly, 2002), wherein $[Ca^{2+}]_i$ can be tightly buffered by injection into nerve endings, and only slightly increases the $[Ca^{2+}]_i$ needed for vesicle fusion (Sakaba et al., 2005). Moreover, the Ca^{2+}-sensitivity for catecholamine secretion from neuroendocrine cells closely correlates with the cation requirements for inducing conformational changes in synaptotagmin 1 and SNAREs *in situ,* and the Ca^{2+}-sensitivities for all of these phenomena are unaffected by BoNT/A (Lawrence and Dolly, 2002). A reasonable conclusion from these arguments is that BoNT/A does not, in fact, reduce the [Ca^{2+}]-affinity of the exocytotic apparatus and, therefore, the success of capsaicin in triggering CGRP release from BoNT/A-intoxicated TGNs is unlikely to be due to higher levels of $[Ca^{2+}]_i$ being elicited than by stimuli that are unable to overcome inhibition by this toxin. Furthermore, K^+-depolarisation actually induced larger peak increases of fluorescence intensity in Fluo 4-AM loaded TGNs than exposure to capsaicin.

It is necessary, therefore, to consider other aspects of Ca^{2+}-signalling that may underlie differences in response to capsaicin and K^+-depolarisation. The spatial and temporal patterns of $[Ca^{2+}]_i$ signals are important factors that influence the amount and rate of exocytosis from secretory cells (Augustine and Neher, 1992). Fluo 4-AM revealed that capsaicin induced a more persistent increase in $[Ca^{2+}]_i$ than K^+, despite the initial peak

signal being somewhat lower in toxin free cells. Accordingly, over a 30 minutes period capsaicin stimulated > 2-fold more uptake of $^{45}Ca^{2+}$ than 60 mM [K^+] did not reach a plateau. Thus, capsaicin induces more persistent Ca^{2+} signals than K^+-depolarisation. Persistent elevation of $[Ca^{2+}]_i$ signals was shown herein to be critical for capsaicin and ionomycin (Durham and Russo, 2003) to elicit CGRP release from BoNT/A-intoxicated neurons, in accord with studies demonstrating that this toxin slows the rate of vesicle release and causes a delay before vesicles start fusing (Sakaba et al., 2005). Such functional data are consistent with the notion that BoNT/A may destabilise a pre-fusion SNARE complex (Fig. 5.9) required for the initial fast exocytotic burst (Wojcik and Brose, 2007; Xu et al., 1998). Spatial localisation of Ca^{2+} needs to be considered and the spatial pattern of Ca^{2+} signals is also likely to differ because capsaicin and K^+-depolarisation activate distince channels, ionomycin is a Ca^{2+}-selective ionophore that acts on both the plasma and intracellular membranes (Morgan and Jacob, 1994), and the high-concentration microdomains may be distant from secretory vesicles, especially large-dense core granules (Augustine and Neher, 1992) like those that contain CGRP.

Thus, the successful insertion of a different binding domain into BoNT/E: (i) endowed an ability to target to /E-insensitive neurons; (ii) produced a novel chimera capable of abolishing capsaicin- or ionomycin-elicited exocytosis of a pain mediator unlike /A whose inhibition is precluded by sustained elevation of $[Ca^{2+}]_i$ and (iii) revealed a basis for the ability of /EA, but not /A, to totally block capsaicin-induced CGRP release i.e. BoNT/A- but not /E-truncated SNAP-25 can participate in the formation of SDS-resistant SNARE complexes. This accords with observations on intact and truncated recombinant SNAREs (Hayashi et al., 1994) and findings that /A retards rather than prevents vesicle fusion in neurons (Sakaba et al., 2005).

6.0 Summary and recommendations for future work

6.1 The unique requirement of Sbr I for CGRP release from TGNs provides novel insights for designing new BoNT variants as anti-nociceptives

In this thesis, Sbr I was found to be essential for evoked Ca^{2+}-dependent CGRP release from TGNs (Chapter 4). For example, cleavage of Sbr II and III by BoNT/B and chimera BA in rat TGNs (I is resistant in this species) failed to block release of CGRP whereas it was inhibited in mouse neurons where Sbr I was also proteolysed. Knock-down of Sbr I expression in mouse and rat TGNs led to a substantial reduction of CGRP release (Chapter 4). This demonstrated requirement of Sbr I in peptide release from LDCVs in sensory neurons contrasts with the ability of Sbr II / III to suffice for exocytosis of several neurotransmitters from SCSVs or, indeed, for secretion from granules in chromaffin cells and PC-12 cells (Foran et al., 2003; Lomneth et al., 1991). Such an unique feature of a dependence on Sbr I for CGRP exocytosis from TGNs may be related to this occurring at sites remote from the active zones (Bernardini et al., 2004), enabling this pain mediator to reach blood vessels in the vicinity and activate its receptor thereon. In order to specifically target pain sensory neurons, novel BoNT forms which selectively cleave only Sbr I is fully warranted with the aid of insights gained from Sbr substrates, their recognition and cleavage (Chen et al., 2008; Sikorra et al., 2008). Modifications (mutations and/or deletions) of protease domains of Sbr-cleaving BoNTs, which are responsible for individual isoform recognition and/or cleavage, might achieve a toxin only cleaving Sbr I. Such a toxin should not affect other neuron types because the latter seem to utilize Sbr II and/or III (see Chapter 4 section 3). BoNT/D was demonstrated to be effective in blocking CGRP release elicited by all stimuli (Chapter 4), but the lack of its acceptor in human tissue makes it unsuitable for therapeutic purpose (Coffield et al., 1997). This could be resolved in future by engineering a new variant containing an acceptor binding domain shown to bind to TGNs with the protease of /D, known to cleave all the Sbr isoforms effectively blocking release of this pain peptide.

6.2 Proof of principle was gained for desired toxin targeting from a novel BoNT EA chimera blocking capsaicin-evoked exocytosis of CGRP from TGNs much more effectively than /A or /E

The ability of chimera EA to remove a further 17 residues from SNAP-25, in comparison to BoNT/A, yields a complete blockade of capsaicin-evoked CGRP release

rather than the negligible inhibition seen with /A (Chapter 5). EA is a more effective inhibitor of CGRP release from sensory neurones than either of its parents because it combines the superior /A property of cell binding via SV2 with the broader inhibitory capability of an /E protease that more effectively destabilises SNARE complexes. This demonstration of the successful substitution of the binding domain of /E with its counterpart from /A highlights the utility of protein engineering for retargetting BoNT/E to otherwise /E-insensitive cells. In a similar manner, the H_C of tetanus toxin has been used to retarget diptheria toxin to neurones (Francis et al., 2000). As highly purified EA is easily prepared with good yield and, importantly, high potency, this technology represents a marked improvement over sensory targetting by chemical conjugation of *Erythrina cristigalli* lectin to the /A LC-H_N fragment (Duggan et al., 2002). The latter suffers from the drawbacks of inconsistent chemical conjugation, complex manufacturing procedure, product heterogeneity and low specific activity. However, as the BoNT/A acceptor SV2 is widely expressed in the nervous system, BoNT LC-H_N fusions to polypeptide ligands for surface markers on specific neuronal system are now being developed for more specific targetting. A similar strategy has given encouraging results for targetting BoNT/C1 to lung epithilial cells with epidermal growth factor to inhibit mucus secretion (Foster et al., 2006). Further developments should incorporate the BoNT LC and translocation together with a specific acceptor binding moiety, a potential ligand for VR1, to selectively target nociceptive sensory neurons, the prime target of nociceptive C-fibres. The BoNT H_N in this hybrid would form a channel allowing the attached LC protease to translocate to the cytosol, cleave its substrate and block neuro-exocytosis of the pain mediators (Koriazova and Montal, 2003).

6.3 TGNs provide a natural BoNT/E acceptor null system for identify a putative /E acceptor

Discovery of a protein acceptor for each serotype of BoNTs is another attractive and challenging project [reviewed in (Verderio et al., 2006)], especially for BoNT/E whose acceptor is known to be distinct from BoNT/A (Dolly et al., 1994; Mahrhold et al., 2006). Lack of progress with investigations is in part due to a shortage of a suitable model system. The poor sensitivity of TGNs to BoNT/E (Chapter 5) is a novel feature, indicating a differential distribution of its unknown acceptor(s) in various neuronal systems. Thus, TGNs provide a natural null model for finding the specific /E acceptor,

in conjuncation with other highly susceptibable neurons i.e. CGNs (Chapter 5). With the aid of advanced substractive hybridization techniques, employing cDNA libraries encoding synaptic vesicle proteins derived from TGNs and CGNs might allow the putative protein acceptor for /E to be identified.

6.4 The dependency of inhibition by BoNT of capsaicin-evoked CGRP release from nociceptive neurons on the persistence of intracellular $[Ca^{2+}]_i$ warranted a more in-depth study

Chimera EA, but not BoNT/A, blocks capsaicin-elicited CGRP release (Chapter 5). The existence of the /A- but not EA- truncated SNAP-25 in SNARE complex is a reasonable explaination for the more extensive inhibition of capsaicin-elicited exocytosis by EA than BoNT/A. Capsaicin stimulation elicites a greater and more persistent increase in $[Ca^{2+}]_i$ than K^+-depolarisation. Elevated $[Ca^{2+}]_i$ was found to attenuate BoNT/A inhibition of CGRP release by slowing down the rate of vesicle release (Chapter 5); additionally, in moter nerve terminals, synaptosomes or neuroendocrine cell where $[Ca^{2+}]_i$ was elevated upon addition of Ca^{2+} ionophore or pore-forming detergents, BoNT/A blockade was alleviated (Ashton and Dolly, 1991; Lawrence et al., 1996; Simpson, 1978). As capsaicin and K^+-depolarisation activate distinct channels, and ionomycin is a Ca^{2+}-selective ionophore that acts on both the plasma and intracellular membranes (Morgan and Jacob, 1994), the spatial Ca^{2+} localisation and pattern of Ca^{2+} signals are likely to differ. Future in-depth studies to address the relationship between Ca^{2+} entry events and transmitter release are warranted, perhaps, using a combination of patch-clamp, photo-sensitive Ca^{2+} chelators, Ca^{2+} reporter dyes and amperometry of loaded oxidisable 'false transmitters', similar to that described for chromaffin cells, DRGs and other neuron types (Chow et al., 1994; Sakaba et al., 2005; Zhang and Zhou, 2002), Tracking fluorescent-conjugated SNAREs upon vesicle fusion by intra- or inter- molecular fluorescence resonance energy transfer (An and Almers, 2004) might also shed light on the mechanisms governing CGRP release and its blockade by various BoNTs.

In conclusion, this current study broadens the understanding of exocytosis of pain-related peptides from nociceptive neurons, it contributes successful examples of proof of principle of the toxin targeting approach and opens a brand new scope for

controlling SNARE-dependent exocytosis in a wide variety of secretory disorder diseases.

References

Aguado, F., Majo, G., Ruiz-Montasell, B., Llorens, J., Marsal, J. and Blasi, J. (1999). Syntaxin 1A and 1B display distinct distribution patterns in the rat peripheral nervous system. *Neuroscience* **88**, 437-46.

An, S. J. and Almers, W. (2004). Tracking SNARE complex formation in live endocrine cells. *Science* **306**, 1042-6.

Aoki, K. R. (2005). Review of a proposed mechanism for the antinociceptive action of botulinum toxin type A. *Neurotoxicology* **26**, 785-93.

Ashton, A. C. and Dolly, J. O. (1991). Microtubule-dissociating drugs and A23187 reveal differences in the inhibition of synaptosomal transmitter release by botulinum neurotoxins types A and B. *J Neurochem* **56**, 827-35.

Ashton, A. C. and Dolly, J. O. (1997). Microtubules and microfilaments participate in the inhibition of synaptosomal noradrenaline release by tetanus toxin. *J Neurochem* **68**, 649-58.

Augustine, G. J. and Neher, E. (1992). Calcium requirements for secretion in bovine chromaffin cells. *J Physiol* **450**, 247-71.

Baccaglini, P. I. and Hogan, P. G. (1983). Some rat sensory neurons in culture express characteristics of differentiated pain sensory cells. *Proc Natl Acad Sci U S A* **80**, 594-8.

Bach-Rojecky, L., Relja, M. and Lackovic, Z. (2005). Botulinum toxin type A in experimental neuropathic pain. *J Neural Transm* **112**, 215-9.

Bajjalieh, S. M., Frantz, G. D., Weimann, J. M., McConnell, S. K. and Scheller, R. H. (1994). Differential expression of synaptic vesicle protein 2 (SV2) isoforms. *J Neurosci* **14**, 5223-35.

Bajjalieh, S. M., Peterson, K., Linial, M. and Scheller, R. H. (1993). Brain contains two forms of synaptic vesicle protein 2. *Proc Natl Acad Sci U S A* **90**, 2150-4.

Bajohrs, M., Rickman, C., Binz, T. and Davletov, B. (2004). A molecular basis underlying differences in the toxicity of botulinum serotypes A and E. *EMBO Rep* **5**, 1090-5.

Bautista, D. and Julius, D. (2008). Fire in the hole: pore dilation of the capsaicin receptor TRPV1. *Nat Neurosci* **11**, 528-9.

Berg, E. A., Johnson, R. J., Leeman, S. E., Boyd, N., Kimerer, L. and Fine, R. E. (2000). Isolation and characterization of substance P-containing dense core vesicles from rabbit optic nerve and termini. *J Neurosci Res* **62**, 830-9.

Bergquist, F., Niazi, H. S. and Nissbrandt, H. (2002). Evidence for different exocytosis pathways in dendritic and terminal dopamine release in vivo. *Brain Res* **950**, 245-53.

Bernardini, N., Neuhuber, W., Reeh, P. W. and Sauer, S. K. (2004). Morphological evidence for functional capsaicin receptor expression and calcitonin gene-related peptide exocytosis in isolated peripheral nerve axons of the mouse. *Neuroscience* **126**, 585-90.

Binder, W. J., Brin, M. F., Blitzer, A., Schoenrock, L. D. and Pogoda, J. M. (2000). Botulinum toxin type A (BOTOX) for treatment of migraine headaches: an open-label study. *Otolaryngol Head Neck Surg* **123**, 669-76.

Binz, T., Blasi, J., Yamasaki, S., Baumeister, A., Link, E., Sudhof, T. C., Jahn, R. and Niemann, H. (1994). Proteolysis of SNAP-25 by types E and A botulinal neurotoxins. *J Biol Chem* **269**, 1617-20.

Bird, G. C., Han, J. S., Fu, Y., Adwanikar, H., Willis, W. D. and Neugebauer, V. (2006). Pain-related synaptic plasticity in spinal dorsal horn neurons: role of CGRP. *Mol Pain* **2**, 31.

Black, J. D. and Dolly, J. O. (1986). Interaction of 125I-labeled botulinum neurotoxins with nerve terminals. II. Autoradiographic evidence for its uptake into motor nerves by acceptor-mediated endocytosis. *J Cell Biol* **103**, 535-44.

Bloedel, J. R. and McCreery, D. B. (1975). Organization of peripheral and central pain pathways. *Surg Neurol* **4**, 65-81.

Blumenfeld, A. (2003). Botulinum toxin type A as an effective prophylactic treatment in primary headache disorders. *Headache* **43**, 853-60.

Brain, S. D. and Grant, A. D. (2004). Vascular actions of calcitonin gene-related peptide and adrenomedullin. *Physiol Rev* **84**, 903-34.

Breese, N. M., George, A. C., Pauers, L. E. and Stucky, C. L. (2005). Peripheral inflammation selectively increases TRPV1 function in IB4-positive sensory neurons from adult mouse. *Pain* **115**, 37-49.

Brungerb, M. A. B. a. A. T. (2005). New insights into clostridial neurotoxin–SNARE interactions *Trends in Molecular Medicine* **11**.

Burgen, A. S. V., Dickens, F. and Zatman, L.J., . (1949). The action of botulinum toxin on the neuro-muscular junction. *Journal of Physiology* **109**, 10–24.

Caterina, M. J., Leffler, A., Malmberg, A. B., Martin, W. J., Trafton, J., Petersen-Zeitz, K. R., Koltzenburg, M., Basbaum, A. I. and Julius, D. (2000). Impaired nociception and pain sensation in mice lacking the capsaicin receptor. *Science* **288**, 306-13.

Caterina, M. J., Schumacher, M. A., Tominaga, M., Rosen, T. A., Levine, J. D. and Julius, D. (1997). The capsaicin receptor: a heat-activated ion channel in the pain pathway. *Nature* **389**, 816-24.

Chai, Q., Arndt, J. W., Dong, M., Tepp, W. H., Johnson, E. A., Chapman, E. R. and Stevens, R. C. (2006). Structural basis of cell surface receptor recognition by botulinum neurotoxin B. *Nature* **444**, 1096-100.

Chapman, E. R., An, S., Barton, N. and Jahn, R. (1994). SNAP-25, a t-SNARE which binds to both syntaxin and synaptobrevin via domains that may form coiled coils. *J Biol Chem* **269**, 27427-32.

Chen, S., Hall, C. and Barbieri, J. T. (2008). Substrate recognition of VAMP-2 by botulinum neurotoxin B and tetanus neurotoxin. *J Biol Chem*.

Chow, R. H., Klingauf, J. and Neher, E. (1994). Time course of Ca2+ concentration triggering exocytosis in neuroendocrine cells. *Proc Natl Acad Sci U S A* **91**, 12765-9.

Chuang, H. H., Prescott, E. D., Kong, H., Shields, S., Jordt, S. E., Basbaum, A. I., Chao, M. V. and Julius, D. (2001). Bradykinin and nerve growth factor release the capsaicin receptor from PtdIns(4,5)P2-mediated inhibition. *Nature* **411**, 957-62.

Chung MK, G. A., Caterina MJ. (2008). TRPV1 shows dynamic ionic selectivity during agonist stimulation. *Nat Neurosci.* **11**.

Coffield, J. A., Bakry, N., Zhang, R. D., Carlson, J., Gomella, L. G. and Simpson, L. L. (1997). In vitro characterization of botulinum toxin types A, C and D action on human tissues: combined electrophysiologic, pharmacologic and molecular biologic approaches. *J Pharmacol Exp Ther* **280**, 1489-98.

Cortright, D. N. and Szallasi, A. (2004). Biochemical pharmacology of the vanilloid receptor TRPV1. An update. *Eur J Biochem* **271**, 1814-9.

Cui, M., Khanijou, S., Rubino, J. and Aoki, K. R. (2004). Subcutaneous administration of botulinum toxin A reduces formalin-induced pain. *Pain* **107**, 125-33.

Cull-Candy, S. G., Lundh, H. and Thesleff, S. (1976). Effects of botulinum toxin on neuromuscular transmission in the rat. *J Physiol* **260**, 177-203.

Davletov, B., Bajohrs, M. and Binz, T. (2005). Beyond BOTOX: advantages and limitations of individual botulinum neurotoxins. *Trends Neurosci* **28**, 446-52.

De Biasi, S. and Rustioni, A. (1988). Glutamate and substance P coexist in primary afferent terminals in the superficial laminae of spinal cord. *Proc Natl Acad Sci U S A* **85**, 7820-4.

Dolly, J. O. (2005). Molecular definition of neuronal targets for novel neurotherapeutics: SNAREs and Kv1 channels. *Neurotoxicology* **26**, 753-60.

Dolly, J. O., Black, J., Williams, R. S. and Melling, J. (1984). Acceptors for botulinum neurotoxin reside on motor nerve terminals and mediate its internalization. *Nature* **307**, 457-60.

Dolly, J. O., de Paiva, A., Foran, P., Lawrence, G., Daniels-Holgate, P. and Ashton, A. C. (1994). Probing the process of transmitter release with botulinum and tetanus neurotoxins. *Seminars in the Neurosciences* **6**, 149-158.

Dolly, J. O. and Lawrence, G. (2007). Mechanistic basis for the therapeutic effectiveness of botulinum toxin A on over-active cholinergic nerves. In *Clincial Uses of Botulinum Toxins*, (eds A. B. Ward and M. P. Barnes), pp. 9-25. Cambridge: Cambridge University Press.

Dong, M., Richards, D. A., Goodnough, M. C., Tepp, W. H., Johnson, E. A. and Chapman, E. R. (2003). Synaptotagmins I and II mediate entry of botulinum neurotoxin B into cells. *J Cell Biol* **162**, 1293-303.

Dong, M., Yeh, F., Tepp, W. H., Dean, C., Johnson, E. A., Janz, R. and Chapman, E. R. (2006). SV2 is the protein receptor for botulinum neurotoxin A. *Science* **312**, 592-6.

Doods, H., Arndt, K., Rudolf, K. and Just, S. (2007). CGRP antagonists: unravelling the role of CGRP in migraine. *Trends Pharmacol Sci* **28**, 580-7.

Duggan, M. J., Quinn, C. P., Chaddock, J. A., Purkiss, J. R., Alexander, F. C., Doward, S., Fooks, S. J., Friis, L. M., Hall, Y. H., Kirby, E. R. et al. (2002). Inhibition of release of neurotransmitters from rat dorsal root ganglia by a novel conjugate of a Clostridium botulinum toxin A endopeptidase fragment and Erythrina cristagalli lectin. *J Biol Chem* **277**, 34846-52.

Durham, P. L. (2006). Calcitonin gene-related peptide (CGRP) and migraine. *Headache* **46 Suppl 1**, S3-8.

Durham, P. L. and Cady, R. (2004). Regulation of calcitonin gene-related peptide secretion from trigeminal nerve cells by botulinum toxin type A: implications for migraine therapy. *Headache* **44**, 35-42; discussion 42-3.

Durham, P. L. and Russo, A. F. (1999). Regulation of calcitonin gene-related peptide secretion by a serotonergic antimigraine drug. *J Neurosci* **19**, 3423-9.

Durham, P. L. and Russo, A. F. (2003). Stimulation of the calcitonin gene-related peptide enhancer by mitogen-activated protein kinases and repression by an antimigraine drug in trigeminal ganglia neurons. *J Neurosci* **23**, 807-15.

Eckert, S. P., Taddese, A. and McCleskey, E. W. (1997). Isolation and culture of rat sensory neurons having distinct sensory modalities. *J Neurosci Methods* **77**, 183-90.

Edvinsson, L. (2004). Blockade of CGRP receptors in the intracranial vasculature: a new target in the treatment of headache. *Cephalalgia* **24**, 611-22.

Edvinsson, L. (2007). Novel migraine therapy with calcitonin gene-regulated peptide receptor antagonists. *Expert Opin Ther Targets* **11**, 1179-88.

Ermengem, E. v. (1897). Ueber einen neuen anaeroben Bacillus und seine Beziehungen zum Botulismus. *Zeitschrift fur Hyg und Infektionskr-ankheiten* **26**, 1–56.

Farinelli, I., Coloprisco, G., De Filippis, S. and Martelletti, P. (2006). Long-term benefits of botulinum toxin type A (BOTOX) in chronic daily headache: a five-year long experience. *J Headache Pain* **7**, 407-12.

Ferrer-Montiel, A., Garcia-Martinez, C., Morenilla-Palao, C., Garcia-Sanz, N., Fernandez-Carvajal, A., Fernandez-Ballester, G. and Planells-Cases, R. (2004). Molecular architecture of the vanilloid receptor. Insights for drug design. *Eur J Biochem* **271**, 1820-6.

Foran, P., Lawrence, G. and Dolly, J. O. (1995). Blockade by botulinum neurotoxin B of catecholamine release from adrenochromaffin cells correlates with its cleavage of synaptobrevin and a homologue present on the granules. *Biochemistry* **34**, 5494-503.

Foran, P. G., Mohammed, N., Lisk, G. O., Nagwaney, S., Lawrence, G. W., Johnson, E., Smith, L., Aoki, K. R. and Dolly, J. O. (2003). Evaluation of the therapeutic usefulness of botulinum neurotoxin B, C1, E, and F compared with the long lasting type A. Basis for distinct durations of inhibition of exocytosis in central neurons. *J Biol Chem* **278**, 1363-71.

Foster, K. A., Adams, E. J., Durose, L., Cruttwell, C. J., Marks, E., Shone, C. C., Chaddock, J. A., Cox, C. L., Heaton, C., Sutton, J. M. et al. (2006). Re-engineering the target specificity of Clostridial neurotoxins - a route to novel therapeutics. *Neurotox Res* **9**, 101-7.

Francis, J. W., Brown, R. H., Jr., Figueiredo, D., Remington, M. P., Castillo, O., Schwarzschild, M. A., Fishman, P. S., Murphy, J. R. and vanderSpek, J. C. (2000). Enhancement of diphtheria toxin potency by replacement of the receptor binding domain with tetanus toxin C-fragment: a potential vector for delivering heterologous proteins to neurons. *J Neurochem* **74**, 2528-36.

Freund, B. and Schwartz, M. (2003). Temporal relationship of muscle weakness and pain reduction in subjects treated with botulinum toxin A. *J Pain* **4**, 159-65.

Fusayasu, E., Kowa, H., Takeshima, T., Nakaso, K. and Nakashima, K. (2007). Increased plasma substance P and CGRP levels, and high ACE activity in migraineurs during headache-free periods. *Pain* **128**, 209-14.

Gazerani, P., Staahl, C., Drewes, A. M. and Arendt-Nielsen, L. (2006). The effects of Botulinum Toxin type A on capsaicin-evoked pain, flare, and secondary hyperalgesia in an experimental human model of trigeminal sensitization. *Pain* **122**, 315-25.

Gerona, R. R., Larsen, E. C., Kowalchyk, J. A. and Martin, T. F. (2000). The C terminus of SNAP25 is essential for Ca(2+)-dependent binding of synaptotagmin to SNARE complexes. *J Biol Chem* **275**, 6328-36.

Goadsby, P. J. and Edvinsson, L. (1993). The trigeminovascular system and migraine: studies characterizing cerebrovascular and neuropeptide changes seen in humans and cats. *Ann Neurol* **33**, 48-56.

Goadsby, P. J., Lipton, R. B. and Ferrari, M. D. (2002). Migraine--current understanding and treatment. *N Engl J Med* **346**, 257-70.

Guo, A., Vulchanova, L., Wang, J., Li, X. and Elde, R. (1999). Immunocytochemical localization of the vanilloid receptor 1 (VR1):

relationship to neuropeptides, the P2X3 purinoceptor and IB4 binding sites. *Eur J Neurosci* **11**, 946-58.

Gupta, V. K. (2005). Botulinum toxin type A therapy for chronic tension-type headache: fact versus fiction. *Pain* **116**, 166-7; author reply 167.

Hayashi, T., McMahon, H., Yamasaki, S., Binz, T., Hata, Y., Sudhof, T. C. and Niemann, H. (1994). Synaptic vesicle membrane fusion complex: action of clostridial neurotoxins on assembly. *EMBO Journal* **13**, 5051-61.

Hole, K. and Berge, O. G. (1981). Regulation of pain sensitivity in the central nervous system. *Cephalalgia* **1**, 51-9.

Hua, S. Y., Raciborska, D. A., Trimble, W. S. and Charlton, M. P. (1998). Different VAMP/synaptobrevin complexes for spontaneous and evoked transmitter release at the crayfish neuromuscular junction. *Journal of Neurophysiology* **80**, 3233-46.

Humeau, Y., Doussau, F., Grant, N. J. and Poulain, B. (2000). How botulinum and tetanus neurotoxins block neurotransmitter release. *Biochimie* **82**, 427-46.

Jankovic, J. (2004). Treatment of cervical dystonia with botulinum toxin. *Mov Disord* **19 Suppl 8**, S109-15.

Janz, R., Hofmann, K. and Sudhof, T. C. (1998). SVOP, an evolutionarily conserved synaptic vesicle protein, suggests novel transport functions of synaptic vesicles. *J Neurosci* **18**, 9269-81.

Janz, R. and Sudhof, T. C. (1999). SV2C is a synaptic vesicle protein with an unusually restricted localization: anatomy of a synaptic vesicle protein family. *Neuroscience* **94**, 1279-90.

Jin, R., Rummel, A., Binz, T. and Brunger, A. T. (2006). Botulinum neurotoxin B recognizes its protein receptor with high affinity and specificity. *Nature* **444**, 1092-5.

Kapoor, K., Saxena, P. (2004). Olcegepant. *Drugs Fut* **29**, 1088.

Karai, L. J., Russell, J. T., Iadarola, M. J. and Olah, Z. (2004). Vanilloid receptor 1 regulates multiple calcium compartments and contributes to Ca2+-induced Ca2+ release in sensory neurons. *J Biol Chem* **279**, 16377-87.

Kasai, M., Kumazawa, T. and Mizumura, K. (1998). Nerve growth factor increases sensitivity to bradykinin, mediated through B2 receptors, in capsaicin-sensitive small neurons cultured from rat dorsal root ganglia. *Neurosci Res* **32**, 231-9.

Keller, J. E., Cai, F. and Neale, E. A. (2004). Uptake of botulinum neurotoxin into cultured neurons. *Biochemistry* **43**, 526-32.

Keller, J. E. and Neale, E. A. (2001). The role of the synaptic protein snap-25 in the potency of botulinum neurotoxin type A. *J Biol Chem* **276**, 13476-82.

Kim, H., Lee, Y., Weiner, D., Kaye, R., Cahill, A. M. and Yudkoff, M. (2006). Botulinum toxin type a injections to salivary glands: combination with single event multilevel chemoneurolysis in 2 children with severe spastic quadriplegic cerebral palsy. *Arch Phys Med Rehabil* **87**, 141-4.

Koriazova, L. K. and Montal, M. (2003). Translocation of botulinum neurotoxin light chain protease through the heavy chain channel. *Nat Struct Biol* **10**, 13-8.

Kummer, W. (1992). Ultrastructure of calcitonin gene-related peptide-immunoreactive nerve fibres in guinea-pig peribronchial ganglia. *Regul Pept* **37**, 135-42.

Lacy, D. B., Tepp, W., Cohen, A. C., DasGupta, B. R. and Stevens, R. C. (1998). Crystal structure of botulinum neurotoxin type A and implications for toxicity. *Nat Struct Biol* **5**, 898-902.

Lawrence, G., Wang, J., Chion, C. K., Aoki, K. R. and Dolly, J. O. (2007). Two protein trafficking processes at motor nerve endings unveiled by botulinum neurotoxin E. *J Pharmacol Exp Ther* **320**, 410-8.

Lawrence, G. W. and Dolly, J. O. (2002). Multiple forms of SNARE complexes in exocytosis from chromaffin cells: effects of Ca(2+), MgATP and botulinum toxin type A. *J Cell Sci* **115**, 667-73.

Lawrence, G. W., Foran, P. and Dolly, J. O. (1996). Distinct exocytotic responses of intact and permeabilised chromaffin cells after cleavage of the 25-kDa synaptosomal-associated protein (SNAP-25) or synaptobrevin by botulinum toxin A or B. *Eur J Biochem* **236**, 877-86.

Levy, D., Jakubowski, M. and Burstein, R. (2004). Disruption of communication between peripheral and central trigeminovascular neurons mediates the antimigraine action of 5HT 1B/1D receptor agonists. *Proc Natl Acad Sci U S A* **101**, 4274-9.

Littleton, J. T., Bai, J., Vyas, B., Desai, R., Baltus, A. E., Garment, M. B., Carlson, S. D., Ganetzky, B. and Chapman, E. R. (2001). synaptotagmin mutants reveal essential functions for the C2B domain in Ca2+-triggered fusion and recycling of synaptic vesicles in vivo. *J Neurosci* **21**, 1421-33.

Liu, Y., Zhang, M., Broman, J. and Edvinsson, L. (2003). Central projections of sensory innervation of the rat superficial temporal artery. *Brain Res* **966**, 126-33.

Lomneth, R., Martin, T. F. and DasGupta, B. R. (1991). Botulinum neurotoxin light chain inhibits norepinephrine secretion in PC12 cells at an intracellular membranous or cytoskeletal site. *Journal of Neurochemistry* **57**, 1413-21.

Mahrhold, S., Rummel, A., Bigalke, H., Davletov, B. and Binz, T. (2006). The synaptic vesicle protein 2C mediates the uptake of botulinum neurotoxin A into phrenic nerves. *FEBS Letters* **580**, 2011-4.

Malin, S. A., Davis, B. M. and Molliver, D. C. (2007). Production of dissociated sensory neuron cultures and considerations for their use in studying neuronal function and plasticity. *Nat Protoc* **2**, 152-60.

Matteoli, M., Takei, K., Perin, M. S., Sudhof, T. C. and De Camilli, P. (1992). Exo-endocytotic recycling of synaptic vesicles in developing processes of cultured hippocampal neurons. *J Cell Biol* **117**, 849-61.

Mauskop, A. (2002). The use of botulinum toxin in the treatment of headaches. *Curr Pain Headache Rep* **6**, 320-3.

McCulloch, J., Uddman, R., Kingman, T. A. and Edvinsson, L. (1986). Calcitonin gene-related peptide: functional role in cerebrovascular regulation. *Proc Natl Acad Sci U S A* **83**, 5731-5.

McInnes, C. and Dolly, J. O. (1990). Ca2(+)-dependent noradrenaline release from permeabilised PC12 cells is blocked by botulinum neurotoxin A or its light chain. *FEBS Lett* **261**, 323-6.

Mehrotra, S., Gupta, S., Chan, K. Y., Villalon, C. M., Centurion, D., Saxena, P. R. and Maassenvandenbrink, A. (2008). Current and prospective pharmacological targets in relation to antimigraine action. *Naunyn Schmiedebergs Arch Pharmacol*.

Menezes, C., Rodrigues, B., Magalhaes, E. and Melo, A. (2007). Botulinum toxin type A in refractory chronic migraine: an open-label trial. *Arq Neuropsiquiatr* **65**, 596-8.

Mitsuhashi, M., Ohashi, Y., Shichijo, S., Christian, C., Sudduth-Klinger, J., Harrowe, G. and Payan, D. G. (1992). Multiple intracellular signaling pathways of the neuropeptide substance P receptor. *J Neurosci Res* **32**, 437-43.

Montecucco, C. and Schiavo, G. (1994). Mechanism of action of tetanus and botulinum neurotoxins. *Mol Microbiol* **13**, 1-8.

Morgan, A. J. and Jacob, R. (1994). Ionomycin enhances Ca2+ influx by stimulating store-regulated cation entry and not by a direct action at the plasma membrane. *Biochem J* **300 (Pt 3)**, 665-72.

Munson, C. M. C. M. (2007). Tag team action at the synapse. *EMBO reports* **8**, 834–838

Nystuen, A. M., Schwendinger, J. K., Sachs, A. J., Yang, A. W. and Haider, N. B. (2007). A null mutation in VAMP1/synaptobrevin is associated with neurological defects and prewean mortality in the lethal-wasting mouse mutant. *Neurogenetics* **8**, 1-10.

O'Connor, T. P. and van der Kooy, D. (1988). Enrichment of a vasoactive neuropeptide (calcitonin gene related peptide) in the trigeminal sensory projection to the intracranial arteries. *J Neurosci* **8**, 2468-76.

Olesen, J. and Lipton, R. B. (2004). Headache classification update 2004. *Curr Opin Neurol* **17**, 275-82.

Otto, H., Hanson, P. I. and Jahn, R. (1997). Assembly and disassembly of a ternary complex of synaptobrevin, syntaxin, and SNAP-25 in the membrane of synaptic vesicles. *Proceedings of the National Academy of Sciences of the United States of America* **94**, 6197-201.

Pellizzari, R., Rossetto, O., Schiavo, G. and Montecucco, C. (1999). Tetanus and botulinum neurotoxins: mechanism of action and therapeutic uses. *Philos Trans R Soc Lond B Biol Sci* **354**, 259-68.

Popoff, M. R., Marvaud, J. C. and Raffestin, S. (2001). [Mechanism of action and therapeutic uses of botulinum and tetanus neurotoxins]. *Ann Pharm Fr* **59**, 176-90.

Poyner, D. R., Sexton, P. M., Marshall, I., Smith, D. M., Quirion, R., Born, W., Muff, R., Fischer, J. A. and Foord, S. M. (2002). International Union of Pharmacology. XXXII. The mammalian calcitonin gene-related peptides, adrenomedullin, amylin, and calcitonin receptors. *Pharmacol Rev* **54**, 233-46.

Prado, M. A., Evans-Bain, B. and Dickerson, I. M. (2002). Receptor component protein (RCP): a member of a multi-protein complex required for G-protein-coupled signal transduction. *Biochem Soc Trans* **30**, 460-4.

Price, T. J., Louria, M. D., Candelario-Soto, D., Dussor, G. O., Jeske, N. A., Patwardhan, A. M., Diogenes, A., Trott, A. A., Hargreaves, K. M. and Flores, C. M. (2005). Treatment of trigeminal ganglion neurons in vitro with NGF, GDNF or BDNF: effects on neuronal survival, neurochemical properties and TRPV1-mediated neuropeptide secretion. *BMC Neurosci* **6**, 4.

Purkiss, J., Welch, M., Doward, S. and Foster, K. (2000). Capsaicin-stimulated release of substance P from cultured dorsal root ganglion neurons: involvement of two distinct mechanisms. *Biochem Pharmacol* **59**, 1403-6.

Rummel, A., Karnath, T., Henke, T., Bigalke, H. and Binz, T. (2004). Synaptotagmins I and II act as nerve cell receptors for botulinum neurotoxin G. *J Biol Chem* **279**, 30865-70.

Sakaba, T., Stein, A., Jahn, R. and Neher, E. (2005). Distinct kinetic changes in neurotransmitter release after SNARE protein cleavage. *Science* **309**, 491-4.

Salvatore, C. A., Hershey, J. C., Corcoran, H. A., Fay, J. F., Johnston, V. K., Moore, E. L., Mosser, S. D., Burgey, C. S., Paone, D. V., Shaw, A. W. et al. (2008). Pharmacological characterization of MK-0974 [N-[(3R,6S)-6-(2,3-difluorophenyl)-2-oxo-1-(2,2,2-trifluoroethyl)azepan-3- yl]-4-(2-oxo-2,3-dihydro-1H-imidazo[4,5-b]pyridin-1-yl)piperidine-1-carbox amide], a potent and orally active calcitonin gene-related peptide receptor antagonist for the treatment of migraine. *J Pharmacol Exp Ther* **324**, 416-21.

Schantz, E. (1994). Historical perspective. In: J Jankovic and M Hallet, Editors, Therapy With Botulinum Toxin, : Marcel Dekker Inc, New York, NY xxiii–xxvi.

Schiavo, G., Benfenati, F., Poulain, B., Rossetto, O., Polverino de Laureto, P., DasGupta, B. R. and Montecucco, C. (1992). Tetanus and botulinum-B neurotoxins block neurotransmitter release by proteolytic cleavage of synaptobrevin. *Nature* **359**, 832-5.

Schiavo, G., Matteoli, M. and Montecucco, C. (2000). Neurotoxins affecting neuroexocytosis. *Physiol Rev* **80**, 717-66.

Schiavo, G., Shone, C. C., Bennett, M. K., Scheller, R. H. and Montecucco, C. (1995). Botulinum neurotoxin type C cleaves a single Lys-Ala bond within the carboxyl-terminal region of syntaxins. *Journal of Biological Chemistry* **270**, 10566-70.

Schiavo, G., Stenbeck, G., Rothman, J. E. and Sollner, T. H. (1997). Binding of the synaptic vesicle v-SNARE, synaptotagmin, to the plasma membrane t-SNARE, SNAP-25, can explain docked vesicles at neurotoxin-treated synapses. *Proc Natl Acad Sci U S A* **94**, 997-1001.

Schoch, S., Deak, F., Konigstorfer, A., Mozhayeva, M., Sara, Y., Sudhof, T. C. and Kavalali, E. T. (2001). SNARE function analyzed in synaptobrevin/VAMP knockout mice. *Science* **294**, 1117-22.

Schulte-Mattler, W. J. and Martinez-Castrillo, J. C. (2006). Botulinum toxin therapy of migraine and tension-type headache: comparing different botulinum toxin preparations. *Eur J Neurol* **13 Suppl 1**, 51-4.

Sikorra, S., Henke, T., Galli, T. and Binz, T. (2008). Substrate recognition mechanism of VAMP/synaptobrevin cleaving clostridial neurotoxins. *J Biol Chem*.

Silberstein, S., Mathew, N., Saper, J. and Jenkins, S. (2000). Botulinum toxin type A as a migraine preventive treatment. For the BOTOX Migraine Clinical Research Group. *Headache* **40**, 445-50.

Silberstein, S. D. and Aoki, K. R. (2003). Botulinum toxin type A: myths, facts, and current research. *Headache* **43 Suppl 1**, S1.

Simpson, L. L. (1978). Pharmacological studies on the subcellular site of action of botulinum toxin type A. *J Pharmacol Exp Ther* **206**, 661-9.

Simpson, L. L. (1979). The action of botulinal toxin. *Rev Infect Dis* **1**, 656-62.

Simpson, L. L. (1980). Kinetic studies on the interaction between botulinum toxin type A and the cholinergic neuromuscular junction. *J Pharmacol Exp Ther* **212**, 16-21.

Simpson, L. L. (2004). Identification of the major steps in botulinum toxin action. *Annu Rev Pharmacol Toxicol* **44**, 167-93.

Simpson, L. L. and DasGupta, B. R. (1983). Botulinum neurotoxin type E: studies on mechanism of action and on structure-activity relationships. *J Pharmacol Exp Ther* **224**, 135-40.

Skofitsch, G. and Jacobowitz, D. M. (1985). Calcitonin gene-related peptide coexists with substance P in capsaicin sensitive neurons and sensory ganglia of the rat. *Peptides* **6**, 747-54.

Steranka, L. R., Manning, D. C., DeHaas, C. J., Ferkany, J. W., Borosky, S. A., Connor, J. R., Vavrek, R. J., Stewart, J. M. and Snyder, S. H. (1988). Bradykinin as a pain mediator: receptors are localized to sensory neurons, and antagonists have analgesic actions. *Proc Natl Acad Sci U S A* **85**, 3245-9.

Stevens, R. C., Evenson, M. L., Tepp, W. and DasGupta, B. R. (1991). Crystallization and preliminary X-ray analysis of botulinum neurotoxin type A. *J Mol Biol* **222**, 877-80.

Stucky, C. L., Rossi, J., Airaksinen, M. S. and Lewin, G. R. (2002). GFR alpha2/neurturin signalling regulates noxious heat transduction in isolectin B4-binding mouse sensory neurons. *J Physiol* **545**, 43-50.

Sutton, R. B., Fasshauer, D., Jahn, R. and Brunger, A. T. (1998). Crystal structure of a SNARE complex involved in synaptic exocytosis at 2.4 A resolution. *Nature* **395**, 347-53.

Suzuki, K., Iizuka, T. and Sakai, F. (2007). Botulinum toxin type A for migraine prophylaxis in the Japanese population: an open-label prospective trial. *Intern Med* **46**, 959-63.

Swaminathan, S. and Eswaramoorthy, S. (2000). Crystallization and preliminary X-ray analysis of Clostridium botulinum neurotoxin type B. *Acta Crystallogr D Biol Crystallogr* **56**, 1024-6.

Szallasi, A. and Blumberg, P. M. (1999). Vanilloid (Capsaicin) receptors and mechanisms. *Pharmacol Rev* **51**, 159-212.

Takamori, S., Holt, M., Stenius, K., Lemke, E. A., Gronborg, M., Riedel, D., Urlaub, H., Schenck, S., Brugger, B., Ringler, P. et al. (2006). Molecular anatomy of a trafficking organelle. *Cell* **127**, 831-46.

Tominaga, M., Caterina, M. J., Malmberg, A. B., Rosen, T. A., Gilbert, H., Skinner, K., Raumann, B. E., Basbaum, A. I. and Julius, D. (1998). The cloned capsaicin receptor integrates multiple pain-producing stimuli. *Neuron* **21**, 531-43.

Trimble, W. S., Gray, T. S., Elferink, L. A., Wilson, M. C. and Scheller, R. H. (1990). Distinct patterns of expression of two VAMP genes within the rat brain. *Journal of Neuroscience* **10**, 1380-7.

Trojanowski, J. Q., Walkenstein, N. and Lee, V. M. (1986). Expression of neurofilament subunits in neurons of the central and peripheral nervous system: an immunohistochemical study with monoclonal antibodies. *J Neurosci* **6**, 650-60.

Tsukamoto, K., Kohda, T., Mukamoto, M., Takeuchi, K., Ihara, H., Saito, M. and Kozaki, S. (2005). Binding of Clostridium botulinum type C and D neurotoxins to ganglioside and phospholipid. Novel insights into the receptor for clostridial neurotoxins. *J Biol Chem* **280**, 35164-71.

Tugnoli, V., Capone, J. G., Eleopra, R., Quatrale, R., Sensi, M., Gastaldo, E., Tola, M. R. and Geppetti, P. (2007). Botulinum toxin type A reduces capsaicin-evoked pain and neurogenic vasodilatation in human skin. *Pain* **130**, 76-83.

Verderio, C., Pozzi, D., Pravettoni, E., Inverardi, F., Schenk, U., Coco, S., Proux-Gillardeaux, V., Galli, T., Rossetto, O., Frassoni, C. et al. (2004). SNAP-25 modulation of calcium dynamics underlies differences in GABAergic and glutamatergic responsiveness to depolarization. *Neuron* **41**, 599-610.

Verderio, C., Rossetto, O., Grumelli, C., Frassoni, C., Montecucco, C. and Matteoli, M. (2006). Entering neurons: botulinum toxins and synaptic vesicle recycling. *EMBO Rep* **7**, 995-9.

Voller, B., Sycha, T., Gustorff, B., Schmetterer, L., Lehr, S., Eichler, H. G., Auff, E. and Schnider, P. (2003). A randomized, double-blind, placebo controlled study on analgesic effects of botulinum toxin A. *Neurology* **61**, 940-4.

Wang, J., Meng, J., Lawrence, G. W., Zurawski, T. H., Sasse, A., Bodeker, M. O., Gilmore, M. A., Fernandez-Salas, E., Francis, J., Steward, L. E. et al. (2008). Novel chimeras of botulinum neurotoxin /A and /E unveil contributions from the binding, translocation and protease domains to their functional characteristics. *J Biol Chem*.

Ward, A. B. and Barnes, M. P. (2007). Clinical Uses of Botulinum Toxins. Cambridge: Cambridge University Press.

Welch, M. J., Purkiss, J. R. and Foster, K. A. (2000). Sensitivity of embryonic rat dorsal root ganglia neurons to Clostridium botulinum neurotoxins. *Toxicon* **38**, 245-58.

Wojcik, S. M. and Brose, N. (2007). Regulation of membrane fusion in synaptic excitation-secretion coupling: speed and accuracy matter. *Neuron* **55**, 11-24.

Woolf, C. J. (2004). Pain: moving from symptom control toward mechanism-specific pharmacologic management. *Ann Intern Med* **140**, 441-51.

Woolf, C. J. and Ma, Q. (2007). Nociceptors--noxious stimulus detectors. *Neuron* **55**, 353-64.

Xu, T., Binz, T., Niemann, H. and Neher, E. (1998). Multiple kinetic components of exocytosis distinguished by neurotoxin sensitivity. *Nat Neurosci* **1**, 192-200.

Yamasaki, S., Baumeister, A., Binz, T., Blasi, J., Link, E., Cornille, F., Roques, B., Fykse, E. M., Sudhof, T. C., Jahn, R. et al. (1994). Cleavage of members of the synaptobrevin/VAMP family by types D and F botulinal neurotoxins and tetanus toxin. *J Biol Chem* **269**, 12764-72.

Zhang, C. and Zhou, Z. (2002). Ca(2+)-independent but voltage-dependent secretion in mammalian dorsal root ganglion neurons. *Nat Neurosci* **5**, 425-30.

Appendix
List of Suppliers

	Company	Country	Web
A			
	Abcam Ltd.	UK	www.abcam.com
	Amersham GE Healthcare	UK	http://www.amersham.com/
B			
	Biosciences	Ireland	www.biosciences.ie
C			
	Cayman Chemical (order through SPI-BIO)	France	www.spibio.com
	Chemicon Europe Ltd.	UK	www.chemicon.com
G			
	Gibco (order through Biosciences)	Ireland	www.biosciences.ie
I			
	Invitrogen (order through Biosciences)	Ireland	www.biosciences.ie
J			
	Jackson Immunoresearch Europe	UK	http://www.jireurope.com/home.asp
M			
	Millipore (order through AGB)	Ireland	www.agb.ie
	Molecular Probes (order through Biosciences)	Ireland	www.biosciences.ie
N			
	Neuromics Inc	USA	www.neuromics.com
P			
	Phoenix Europe GmbH	Germany	www.phoenixpeptide.com
	Pierce (order through Medical Supply Company Ltd.)	Ireland	www.medical-supply.ie
S			
	Santa Cruz (order through Fannin)	Ireland	http://www.fanninhealthcare.com/

Sigma-Aldrich	Ireland	www.sigmaaldrich.com/ireland
SPI-BIO	France	www.spibio.com
Sternberger Monoclonals Inc.	USA	www.sternbergermonoclonals.com
Synaptic Systems GmbH	Germany	www.sysy.com
T		
Tecan (order through Alpha Technologies)	Ireland	www.alphatech.ie
Trinity College Dublin, Bioresources Dept.	Ireland	www.tcd.ie/BioResources